Aalborg Universitet

AALBORG UNIVERSITY

Large Scale Demand Response of Thermostatic Loads

Totu, Luminita Cristiana

Publication date:
2015

Document Version
Accepted author manuscript, peer reviewed version

Link to publication from Aalborg University

Citation for published version (APA):
Totu, L. C. (2015). *Large Scale Demand Response of Thermostatic Loads*. Department of Electronic Systems, Aalborg University.

General rights
Copyright and moral rights for the publications made accessible in the public portal are retained by the authors and/or other copyright owners and it is a condition of accessing publications that users recognise and abide by the legal requirements associated with these rights.

- Users may download and print one copy of any publication from the public portal for the purpose of private study or research.
- You may not further distribute the material or use it for any profit-making activity or commercial gain
- You may freely distribute the URL identifying the publication in the public portal -

Take down policy
If you believe that this document breaches copyright please contact us at vbn@aub.aau.dk providing details, and we will remove access to the work immediately and investigate your claim.

Downloaded from vbn.aau.dk on: July 05, 2025

Large-Scale Demand Response of Thermostatic Loads

Ph.D. Thesis

Luminița Cristiana Totu

Submitted March 27, 2015

Thesis submitted:	March 27, 2015
PhD Supervisor:	Prof. Rafael Wisniewski Aalborg University
Assistant PhD Supervisor:	Associate Prof. John-Josef Leth Aalborg University
PhD Committee:	Prof. Roland P. Malhamé, Polytechnique Montréal Prof. Sean P. Meyn, University of Florida Associate Prof. Henrik Schiøler, Aalborg University
PhD Series:	Faculty of Engineering and Science Aalborg University

ISBN: 978-87-7152-069-9

© Copyright by Luminița Cristiana Totu

Preprint, 2015

Abstract

This study is concerned with large populations of residential thermostatic loads (e.g. refrigerators, air conditioning or heat pumps). The purpose is to gain control over the aggregate power consumption in order to provide balancing services for the electrical grid. Without affecting the temperature limits and other operational constraints, and by using only limited communication, it is possible to make use of the individual thermostat deadband flexibility to step-up or step-down the power consumption of the population as if it were a power plant. The individual thermostatic loads experience no loss of service or quality, and the electrical grid gains a fast power resource of hundreds of MW or more.

This study proposes and analyzes a mechanism that introduces random on/off and off/on switches in the normal thermostat operation of the units. This mechanism is called Switching Actuation. The control architecture is defined by parsimonious communication requirements that also ensure a high level data privacy, and it furthermore guarantees a robust and secure local operation. Mathematical models are put forward, and the effectiveness is shown by numerical simulations. A case of 10000 residential refrigerators is used throughout the work.

Synopsis

Denne undersøgelse omhandler store grupper af termostatiske belastninger (f.eks. køleskabe, klimaanlæg eller varmepumper). Formålet er at få styr på det samlede effektforbrug og at forsyne elnettet med balanceringstjenester. Uden at påvirke temperaturgrænserne og andre operationelle begrænsninger, og ved hjælp af kun begrænset kommunikation, er det muligt at udnytte den enkelte termostat fleksibilitet til at optrappe eller nedtrappe effektforbruget i den termostatiske gruppe, som om det var et kraftværk. De enkelte termostatiske belastninger oplever intet tab af tjeneste eller kvalitet, og elnettet får en hurtig effekt ressource på hundredvis af MW.

Denne undersøgelse foreslår og analyser en mekanisme, der introducerer tilfældige on/off og off/on skift i normal termostat drift af enhederne. Denne mekanisme kaldes Switching Aktivering. Kontrol arkitekturen er defineret ved sparsommelige kommunikationsbehov, der også har et højt kvalitetsniveau med hensyn til datasikkerhed. Desuden garanterer arkitekturen en robust og sikker lokalbetjening. Matematiske modeller er fremsat, og effektiviteten er vist ved numeriske simuleringer. Et case-studie af 10000 køleskabe anvendes gennem hele undersøgelsen.

Contents

Thesis Details

Thesis Title:	Large-Scale Demand Response of Thermostatic Loads
Ph.D. Student:	Luminița Cristiana Totu
Supervisors:	Prof. Rafael Wisniewski, Aalborg University
	Associate Prof. John-Josef Leth, Aalborg University

The main body of this thesis consist of the following papers.

[A] Luminița C. Totu, John Leth and Rafael Wisniewski, "Control for Large-Scale Demand Response of Thermostatic Loads", published in the proceedings of American Control Conference, 2013.

[B] Luminița C. Totu, Rafael Wisniewski, "Demand Response of Thermostatic Loads by Optimized Switching-Fraction Broadcast", published in the proceedings of 19^{th} IFAC World Congress, 2014.

[C] Luminița C. Totu, Rafael Wisniewski and John Leth, "Modeling Populations of Thermostatic Loads with Switching-Rate Actuation", published in the proceedings of 4^{th} Hybrid Autonomous Systems Workshop, 2014.

[D] Luminița C. Totu, Rafael Wisniewski and John Leth, "Demand Response of a TCL population using Switching-Rate Actuation", submitted to IEEE Transactions on Control Systems Technology, in 2014.

This thesis has been submitted for assessment in partial fulfillment of the PhD degree. The thesis is based on the submitted or published scientific papers which are listed above. Parts of the papers are used directly or indirectly in the extended summary of the thesis. As part of the assessment, co-author statements have been made available to the assessment committee and are also available at the Faculty. The thesis is not in its present form acceptable for open publication but only in limited and closed circulation as copyright may not be ensured.

Preface and Acknowledgements

This thesis is submitted as a collection of papers in partial fulfillment of the requirements for the degree of Doctor of Philosophy at the Section of Automation and Control, Department of Electronic Systems, Aalborg University, Denmark. The work has been carried out in the period from August 2011 to December 2014 under the supervision of Professor Rafael Wisniewski and Associate Professor John Joseph Leth, and has been supported by the Southern Denmark Growth Forum and the European Regional Development Fund, under the project "Smart & Cool".

I would like to thank everyone at the Section of Automation and Control, for an inspiring, resourceful and diverse research environment. Having also carried out my master studies here, I have has the opportunity to participate in many activities and on a variety of topics, from lectures to laboratory work, from conference organization and teaching related activities to study groups on advanced theoretical subjects, from navigation systems to Smart Grids. I am with no doubt a better professional for it.

I would especially like to thank my supervisor Rafael Wisniewski for his constant positive support during the PhD work, for giving freedom to research and for pulling me back before getting forever lost. I would like to thank my co-supervisor John Leth for his forthright and practical involvement, especially on getting started with the first paper, and to my smart and cool office and project colleagues, Morten Juelsgaard and Ehsan Shafiei for many interesting discussions. I would also like to thank the "Smart & Cool" project and participants for the working platform and the meetings.

As part of the project I have had the opportunity to visit the Automatic Control Laboratory at ETH Zürich, Switzerland. I would like to thank Professor John Lygeros for kindly accepting my academic stay, and to the entire group, both Automatic Control Lab and the Power Systems Lab, for a great working atmosphere. I would also like to specially thank Maryam Kamgarpour for the many discussions and her involved collaboration, it was of immense value to have a conversation partner fluent in the TCL jargon.

Last but not least, I would like to express my gratitude to my family and close ones for encouragement, patience and good advice in times of complain.

Luminița Cristiana Totu
Aalborg University, May 12, 2015

Acronyms

ADDRB Automated Direct Demand Response via Broadcast

COP Coefficient of Performance

DD Dynamic Demand

DR Demand Response

DSM Demand Side Management

GSHS Generalized Stochastic Hybrid System

HVAC Heating Ventilation and Air-Conditioning

HVDC High-Voltage Direct Current

ms mean-square

ODE Ordinary Differential Equation

PDE Partial Differential Equation

SDE Stochastic Differential Equation

SHS Stochastic Hybrid System

TCL Themostatically Controlled Load

Part I

Introduction

Presentations

This chapter presents the context, the problem and the approach.

1 Context and Motivation

1.1 Energy Balancing

For the most part, the electricity grid operates like a closed circuit that needs to be in balance between power supply and demand (and line losses) at all times. If the total consumption becomes larger than the generation, the grid frequency starts to decrease from its nominal value. In the opposite case, if the generation exceeds the consumption, the grid frequency starts to increase. In both cases, if the imbalance is not quickly compensated, the grid is destabilized and subsystems start to collapse one by one: generator units trip out, switches and transformers servicing the distribution grid are disconnected, and the power is out.

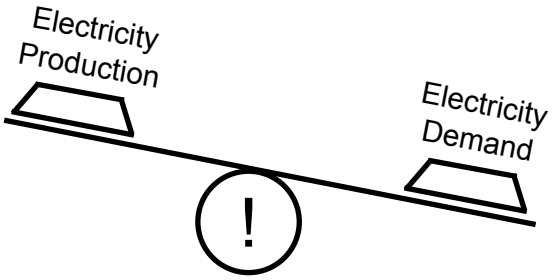

Fig. 1: Electricity is a just-in-time product, and needs to be in a very close balance between production and consumption at all times.

To assure the balance between the electrical supply and demand, a complex mechanism is in place with operations running at different time-scales. While the details differ between grid systems from different regions or countries, the overall balancing structure is essentially the same.

With a view on the long time-scale, large consuming entities, such big industries, need to secure supply months or years in advance. Electricity purchase agreements need to be made with the grid authority and/or with specific generators, to drive the required infrastructure and investments.

On a medium time-scale, the grid authority makes predictions about the consumption, and schedules accordingly the generation plan for the next day(s). The generation schedule is dispatched between the different generator units using a cost minimization principle and taking into account the constraints of the transmission network. This can be done either centrally or by means of a market system. Regarding consumption predictions, these are made using historical data and taking into account aspects such as the season and the day of the week, weather forecasts and a variety of other factors, and are, in general, quite accurate.

In the shorter time scale, a service hierarchy with three main levels is in operation at all times.

On a time scale of a few seconds, which can be considered as real-time, the inherent turbine inertia of the synchronous generator units and the automatic response (droop speed control, [23, Chapter 11.1]) of specifically assigned generators unit counteract imbalances by using measurements of the grid frequency. This mechanism is active at all times, smooths out small deviations, caused for example by normal demand fluctuations, and is referred to as primary or frequency control.

To compensate for imbalances that persist over the time scale of the primary control, the grid authority secures a quantity of additional or reserve power that can respond fast (e.g. within 30 seconds) and is reliable to commands. This makes it possible to compensates for larger imbalances such as unexpected generator unit outages or unusual demand fluctuations. Generator units running on fossil fuels are typical providers because of their predictable and controllable characteristics. To provide this service, they run under-capacity, an inefficient set-point, or in "spinning" mode i.e., producing but not connected to the grid. Additionally, very large consumers can also provide reserve services by agreeing to cut a part of their consumption at notice. Reserve services need to be accounted on both the positive and negative direction, such that balance can be restored for situation of both underproduction (overconsumption) and overproduction (underconsumption). An important aspect is that the provisioning of secondary reserves has both stand-by and activation costs.

Finally, the grid authority also secures tertiary energy reserves. These have a slower response, but longer activation time, and are used to relieve units providing the secondary reserve in the case of prolonged system imbalances.

Introductory literature about the balancing services, together with a number of other services required for maintaining the integrity, stability and power quality in an electrical grid can be found, for example, in the beginning sections of [18](focus on the European region), [20](US) and [15](Denmark).

1.2 Wind and Solar Generation

In many countries, sustainable generation of electrical energy using wind and solar based technologies is increasing [16]. While the overall wind and solar power generation potential has the size needed to cover a significant percentage of the electrical demand, see e.g. [24], large-scale integration in the power system is challenging. The variable characteristic of these generators produces a balancing effort that cannot be efficiently met by traditional solutions [5].

When looking at the medium time-scale, wind and solar generation are often desirable because the marginal costs are low and operation is effectively pollution

free. These type of generators are also becoming competitive in terms of investment costs compared to traditional generator technologies, and together with environment considerations, this makes them an increasingly attractive option also at the planning stage. However, one of the main disadvantages of the wind and solar generation is in relation to the short time balancing problem.

Wind and solar generation have a stochastic and partially uncontrollable characteristic. While averages over long time scales are predictable, on the shorter time scale the generation output can exhibit rapid and large deviations from the scheduled plan. This increases the real-time balancing effort, both in terms of frequency and reserves, and can lead to the paradoxical situation of requiring more fossil-fuels generators to provide stand-by capacity.

New generators are challenging the electricity grid in other ways too. Other imputed drawbacks are the lack of inherent inertia and the dispersed characteristic, both challenges for the traditional power system architecture.

1.3 Energy Storage

An obvious solution to the energy balancing problem is the use of energy storages. There are many different technologies, suitable for different time-scale operations. The main examples are pumped hydroelectric stations, mechanical flywheels, different type of chemical batteries, hydrogen and compressed air solutions, capacitors and superconductive magnetic solutions, and, not least, different forms of thermal storage. However, none of these solutions distinguishes itself as a clear winner for large-scale adoption. Some of the disadvantages include very high investment and operation costs, safety concerns, or low efficiency. In the near future, the more likely scenario is that of a limited adoption of storage facilities, combined with a Smart Grid approach.

1.4 Smart Grid

A new investment cycle is approaching for most of the electrical infrastructure in the world. Taking into account the forecasted needs for the next 30-40 years, as well as the new climate context and pollution policies, the renewal process requires more than simply replacing and rescaling of the system components. Transformations of the electrical power system are needed, and they can be classified in three categories: changes on the generation side, changes in the transmission and distribution network, and changes on the consumption side.

Many power systems have already begun such transformation process. High levels of wind generation are seen in the Danish grid (close to 39% of the total electrical energy consumption 2014), and small, distributed photovoltaic generation has significantly increased in the German grid. On the consumption side, advanced household metering infrastructure is being installed in various countries (among the forerunners are Italy, UK, Denmark, USA) allowing users to better monitor their electricity consumption, and incentivizing an efficient and economical use. On the distribution and transmission levels, system upgrades including deployment of phasor measurement units and construction of HVDC connection lines are improving the interconnectivity between national and regional power systems. These can all be seen as the beginning of the Smart Grid [17, 36].

> "Smart Grid" is an umbrella term for a number of developing solutions (technological, but also socio-economical) that would make use of real-time information exchange, distributed storages, systems interconnectivity and intelligent solutions to transform the electrical grid. Smart Grids can facilitate the integration of more variable and geographically dispersed generators, can improve the overall efficiency of the electrical system by reducing the current needs for expensive energy reserves, and can optimize infrastructure investments. These solutions are enabled by the advancements in the information and communication technology, and by automation and control.

One of the main points of the Smart Grid agenda is the creation of mechanisms for a cost-effective and agile way of handling the real-time balancing operations. The European Smart Grid Strategic Research Agenda [40, 41] emphasizes that

> *"as many technologies as possible should serve the goal of a better electricity load-generation balancing"*,

and lists energy storage solutions, construction of long distance interconnection links, and enabling the flexibility of electricity consumption as challenges and priorities for the near future. The latter category provides the main context and motivation for this work, and will be elaborated in the next section.

1.5 Demand Side Management (DSM)

In the traditional grid the consumption side is, for the most part, a passive actor. As discussed, at the planning level the supply is dispatched to meet the forecasted demand, and in real-time operation the supply takes the main responsibility for energy and power balance. The Smart Grid is pushing for developments on the demand-side, with the aim of making the consumption side an active element of the grid. DSM measures can be classified in four categories,

- efficiency measures,
- classical incentives and contracts,
- Demand Response (DR), and
- Dynamic Demand (DD).

The first two categories can be seen as conventional, while the last two categories are novel.

Efficiency measures have the aim of reducing the amount of energy needed to obtain the same amount of product and services. Even small improvements can lead to significant overall benefits. For example, many countries have implemented programs for phasing out incandescent light bulbs. In the European Union, it is estimated that a total roll out of more efficient lighting alternatives will save about 40 TWh of energy per year, which is the equivalent to the total electrical energy consumption of a country such as Romania [14]. Efficiency measures are not directly addressing the energy balancing problem, but are an indirect contributor, for example by reducing (or stopping the increase) of the amount of energy that needs to be secured for reserves.

Classical incentives and contracts refer to demand-side measures that have been in use for a good number of years (or decades), and are not a novelty. Time-of-day (or time-of-use) pricing, enabled by analog meters with time switches (preprogrammed or with remote activation via e.g. radio), has been in use for both the residential and the industrial sectors in many countries. It can be used to reshape the daily consumption pattern and to reduce the peak load, helping the energy balancing problem at the planning stage. Interruptible contracts offer pricing benefits in exchange for allowing the grid some amount of direct control over consuming devices. For example, US Florida residential customers have the possibility of enrolling air-conditioning, water heaters and pool pumps to an automatic control program that can turn appliances off for a limited period of time and for a maximum of 3-4 times a year [31]. Furthermore, large industries can offer secondary reserve services by bidding or contracting their availability to drop a large amount of consumption in specified time slots. Activation takes place only when needed by the grid, according to a manual or automated communication protocol. Interruptible contracts and consumption-side reserves help the grid balancing operations in the shorter time scale.

As shown by classical incentives and interruptible contracts, the passive role of the consumption-side is not intrinsic, and one of the main challenges of the Smart Grid agenda is to enable a higher degree of consumption flexibility. The idea is to encourage consumption when variable generation is high, and conversely, to reduce consumption when variable generation is low. Adapting the consumption to the variability of the generation has obvious advantages, and the overall objective is not necessarily to consume *less*, but to consume *smarter*.

1.6 Demand Response (DR) and Dynamic Demand (DD)

> DSM solutions in which consumption is responsive to real-time signals are called DR programs.

The DR concept is relatively new, and is motivated by the low cost, availability and practical size of communication and computation platforms. There is a good amount of white papers and theoretical work on different DR strategies, and demonstrations are also starting to be reported in the literature. There are however no large-scale deployment programs.

In this work, time-of-day pricing is not seen as a DR program, because tariffs are fixed in advance and do not reflect the real-time state of the variable generation or the balancing needs of the grid. Furthermore, the aforementioned interruptible contracts are also not seen as DR programs. This is because an important assumption of the contract is that the grid will not make frequent use of the control option, while DR programs have an "at all times" or continuous availability characteristic. Furthermore, an important principle of DR programs is nondisruptivness. DR programs should not significantly interfere with the main products or services that power consuming devices are providing. This is also the implied meaning of the word "flexibility".

"Demand response is clearly the killer application for the smart grid".

Jon Wellinghoff, Federal Energy Regulatory Commission, 2009

DR strategies can be classified according to different criteria. One of the most important classification is according to the response type. DR programs can be *direct* or *indirect*.

In direct programs, the entity issuing the DR signal has decision making capabilities over the consuming device(s). The DR signal is closely related to the physical operation of the device(s), for example a turn on/turn off command, a setpoint, or similar. In direct DR programs the response of the consumption to a particular signal is predictable.

In indirect programs, the entity issuing the DR signal does not have decision making capabilities over the consuming device. The DR signal has the characteristics of an incentive or invitation, for example a price in explicit monetary units, or in levels: high, normal or low. In indirect DR programs the response to a particular signal is generally less predictable, and multiple negotiations or iterations might be needed to obtain a desired outcome.

Another classification of DR programs is based on the sector criteria, allowing to distinguish between the specific requirements in the context of industrial, residential, or commercial (tertiary) sectors.

> DD is a specific or restricted form of DR, where the external coordinating signal is the grid frequency.

DD programs require individual consuming devices to be able to measure the grid frequency directly and with good accuracy, and prescribe the response protocol or algorithm that the device should execute based on the measurement result. DD is thus a form of frequency control. DD was first proposed in in the late '70s [37], but the method never caught momentum for deployment. In the context of new grid challenges, DD interest has restarted [6, 38, 45].

2 Demand Response of Thermostatic Loads

2.1 Themostatically Controlled Loads (TCLs)

> TCLs are relatively small, residential and commercial appliances that perform a cooling and/or heating task, and that have an on-off power consumption characteristic driven by a thermostat.

In the context of power system operation and Smart Grid technologies, residential TCLs such as refrigerators, air-conditioners, heat-pumps and water-boilers, and commercial TCLs such as vending machines are a promising resource of demand response services [13].

A TCL device has three main components: a power active component, a thermally active component, and thermal loads or compartments. For example, the power consumption of a domestic refrigerator is driven by the compressor component, the thermally active component is the vapor-compression cycle, and the fresh-food and freezer compartments, together with the stored items, are the thermal loads. A more

detailed description of the main components in a domestic refrigerator is made in App. Z, as this type of TCL is the case study of choice in this work.

TCLs are natural candidates for DR programs because of their inherent power consumption flexibility.

> An electrical load or appliance is (power) flexible if it is able to fulfill its nominal operational objectives under more than one power consumption pattern or profile.

Fig. 2 shows two different power consumption patterns that both fulfill the thermal requirements of normal service: the classical thermostat operation, and a modified operation where switch-on and switch-off actions occur before the thermostat limits are reached, in a seemingly random pattern that could be motivated by external grid conditions. It is however difficult to see from Fig. 2 alone how the modified operation can help the grid. To explain this, it is important to look at the power consumption behavior of a large group of TCLs.

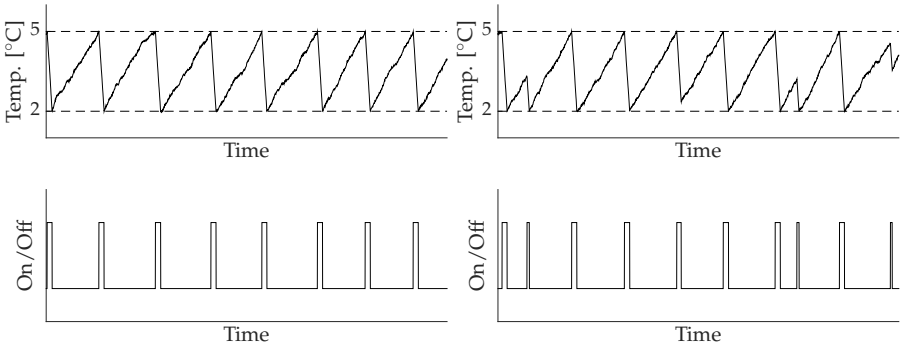

Fig. 2: Two different power consumption patterns. A normal thermostat operation is shown in the left graphs, where on/off switches occur at the upper and lower limits of the temperature band. On the right graphs, switches can also occur when the temperature is inside the thermostat band.

Since an individual TCL has a very small energy storage capacity relative to the scale of the power system operation, any relevant DR strategy requires the participation of a very large number of TCLs. Under normal conditions, the power consumption of a TCL population, which is the aggregation of individual on/off power consumptions, is a relatively flat profile. This is because the switch-on and switch-off actions of the TCLs are not synchronized within the population. In particular, the baseline level b should be close in value to the product between the average duty-cycle $\bar{d}$, the average power rating $\bar{p}$, and the number of loads n,

$$b \approx \bar{d}\bar{p}n, \tag{1}$$

where the duty-cycle is defined as the fraction of time a unit is "on" in normal operation. By purposely modifying the switch-on and switch-off times of the individual TCLs, it becomes possible to obtain useful power responses at the population level, see Fig. 3.

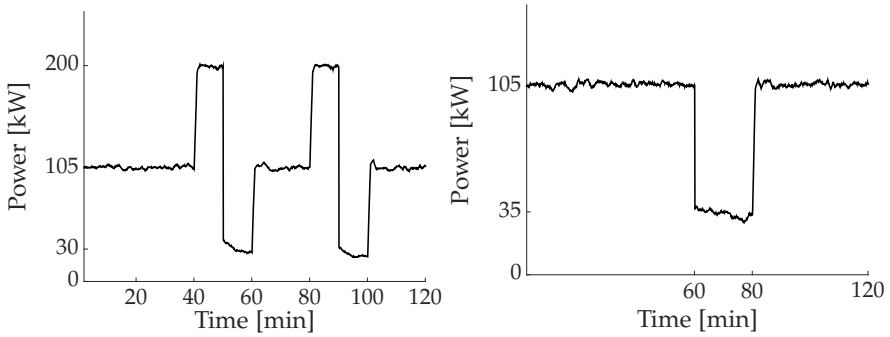

Fig. 3: Aggregated power consumption of a simulated fleet of 10000 refrigerators, manipulated around the baseline level of approximately 100 kW, two examples.

The aggregated response shown in Fig. 3 is similar to a coherent, individual response from a large energy asset such as a pumped storage unit, or a big industry performing a load shifting action. TCLs can thus provide useful balancing services, albeit only in the short and medium time scales (frequency, primary and secondary reserves). Because of this, TCLs can be said to have electrical storage capacity or load shifting capabilities (the ability to consume in advance or to postpone consumption).

But there are also some important differences. Firstly, the energy needs of a TCL are more constrained than those of more typical storage systems such as electrical batteries or hydro-pumping storage stations, and the energy levels are fluctuation on a much fast time-scale compared to other thermal storages such as district water-heating reservoir tanks or industrial cold storages.

At the same time, it is perhaps relevant to point out that TCLs do not have true electrical energy storage properties. In the "on" part of the individual TCLs operation cycle, electrical energy is used to pump heat into-to (in the case of a heating TCL) or out-of (in the case of a cooling TCL) the thermal load compartments. It can be said that the organized electron movement in the power supply cable is used to change the average characteristic of the unorganized movement of molecules in the thermal load compartments. But the energy transformation cannot be reversed: TCLs are not equipped to transform the molecular kinetic energy back to electricity. The bidirectionality of energy transformation, even though losses and other limitations must be accounted for, is a highly desirable characteristic of storage systems. Examples of a bidirectional storages are batteries, hydro-pumping stations, or high temperature, closed thermal storage systems equipped with turbine generators [44].

Furthermore, it can be seen that TCLs do not have typical load shifting capabilities. A washing machine, for example, can be connected to a Smart Grid plug and instructed to perform a service cycle with a flexible start time, but no later than a hard deadline. Within the hard deadline constraint, it can be considered that all starting times (or waiting times) are equally good from the perspective of the service cycle to be accomplished, and the grid has full liberty to choose. A similar flexibility example is the charging process for an electrical vehicle battery. The power consumption flexibility of a TCL is however more restrictive, and inherently more complex because of the temperature dependence that cannot be directly expressed in time coordinates.

Using terminology from [35], energy storage systems and load shifting systems can be modeled as *bucket*, *battery* and *bakery* resources. The TCL requires a new type of model, one that could be called a *leaky bucket*. While aggregation formulations have been successfully investigated for *bucket*, *bakery* and *battery* models, it is not clear how to aggregate *leaky bucket* models.

An important question about DR of TCLs is whether or not their cumulated capacity is significant enough for balancing operations? This work is not directly concerned with planning studies, however, a simple back-of-the-envelope calculation for Denmark, gives a positive response. Table 1 summarizes data from Danish statistical sources [1, 2] and shows the baseline consumption of different residential TCLs. These numbers are comparable with the average amount of traded energy reserves in 2012 in Western Denmark[1], approximately 58 MW for primary reserves, and approximately 180 MW for secondary reserves [11].At the same time, the DR potential of TCLs is also supported by other works, for example [13], [25] or [39], where the latter makes a rough estimation of 20 GW TCL power available for reserves in the USA. A detailed analysis of the grid balancing relevance and capacity size of TCLs is made in [30] for the California state.

Table 1: Statistical data on residential TCLs in Denmark

	El. consumption [GWh/year]	Average power [MW]
Fridges	525	59.85
Freezers	296	33.74
TOTAL		93.59 MW
Electric water heaters	497	56.65
Electric radiators	687	78.31
Heat-pumps	(no data)	(no data)
TOTAL		134.96 MW

2.2 Automated Direct Demand Response via Broadcast (ADDRB)

The main technical challenges of DR for TCLs are related to the large number of individual units and the distributed structure. Realistic solutions must keep computational complexity in check and use communication flows that are feasible under cost and privacy criteria. As such, this work focuses on solutions that are aligned with the following three principles. Similar principles have been discussed in other works, e.g. [21]:

[P1] Actuation takes place via broadcast communication. The network requirements for the actuation channel are reduced and the communication is fast, since the same signal is sent to all units.

[P2] Actual physical decisions (switch-on and switch-off actions) take place at the individual unit level and account for the local conditions. This guarantees a robust, nondisruptive local operation.

[1]The Danish electrical system is divided between two control zones, the Western and the Eastern part.

[P3] Measurements at the unit level area are used sparsely and anonymously. This is to ensure that network requirements for the measurement channel are not excessive, and that the overall solution is privacy friendly.

Together, these three principles will be called Automated Direct Demand Response via Broadcast (ADDRB), see Fig. 4. It is highlighted that this is a *direct* type of demand response, although it maintains the lightweight communication requirements of the *indirect* type.

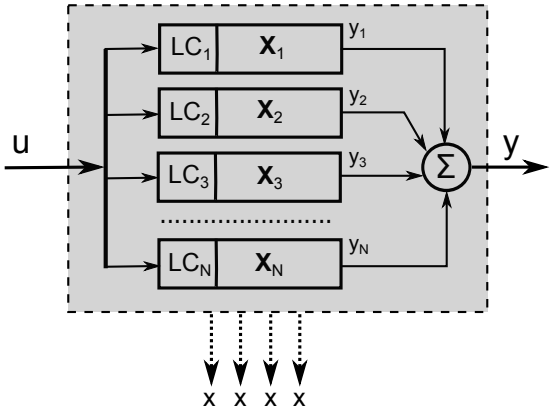

Fig. 4: Schematic overview of the ADDRB approach. The command u is the same for all the units in the population, and attempts to manipulate an aggregated property y, the power consumption. Information about the system is gathered anonymously and only partially from the individual units $\mathbf{X}_i$, $i \in \{1, \ldots, N\}$ and sparsely in time.

It is mentioned that the ADDRB architecture could be studied and applied to other types of loads, for example electrical vehicle batteries or non-thermostatic household appliances such as washing machines and driers.

3 State of the Art for DR of TCLs

3.1 Cold Load Pickup

The systematic study of large groups of thermostatic loads started in the power system and in the control literature in the '80s with the works of Ihara and Schweppe [19] and Malhame and Chong [28]. The interest was on modeling the oscillatory effects in the power consumption after a planned (direct load control) or unplanned interruption (black-out).

In normal operation, a population of thermostatic units operates in a desynchronized manner, where some units are on and consuming power, and others are off. The overall power consumption has an approximate flat profile (a baseline, like in the beginning part of power trajectories from Fig. 3), because as some of the units turn on, some will also turn off. However, after a period of interruption in the power supply, at restoration, a large percentage of units will start at the same time. This leads to a period of synchronized operation, where units turn both *on* and *off* at approximately the same time, leading to big variations and oscillation in the overall power

consumption, see Fig. 5. The period of synchronized operation can be significant, until different sources of randomness have time to accumulate and desynchronize the power consumption cycles.

> In the power system literature, the oscillatory rebound effect in the power consumption of a TCL population, as a result of a synchronization process (usually a power interruption), is known as Cold Load Pickup. Despite the name, it is relevant for both cooling and heating TCLs.

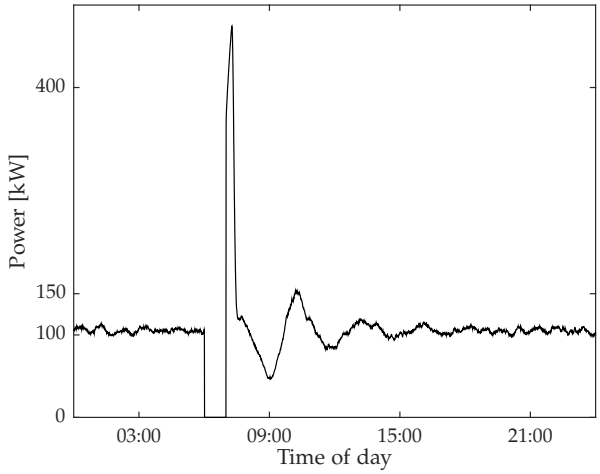

Fig. 5: A simultaneous interruption in the power supply of the TCL population leads to a Cold Load Pickup phenomenon. In the simulated trajectory, an one hour blackout occurs between 06:00 and 07:00 am. At least two significant peaks and one valley can be seen in the transient period following the blackout.

The works [19], [28] and [27] put forward an analysis of the phenomenon by using a bottom-up and physically-based modeling strategy, and capture the oscillatory behavior in both a qualitative and quantitative way. Each TCL unit is modeled in a simplified manner, focusing only on the main features of the dynamical behavior, the thermal dynamics as seen at by the thermostat mechanism, the on/off switching and, optionally, stochastic disturbances.

These works then define probability quantities in connection with the temperature and on/off mode states of an individual TCL. Working in the probability space gives a way to directly aggregate individual units into a population model, under a statistical independence assumption that is not restrictive. The aggregation is done by using probability quantities as approximations for population fractions (percentages).

Making use of the bottom-up modeling approach, [32], [33] and [43] further contribute with a focus on numerical simulations.

Overall, the works enumerated in this section put at the disposal of the grid tools to predict and better plan load shedding and restoration procedures. This is especially relevant for densely populated areas, with a high contribution of heat and cooling loads, in the winter and summer time respectively.

3.2 DR Actuation of TCLs

After three decades, TCLs come again into focus. Enabled by the low cost of computing and communication hardware, automated DR strategies can be developed. For example, advanced thermostats able to communicate with the grid are being installed at customer sites in the USA [4] as a part of various direct load control programs. Furthermore, smart thermostats are becoming commercially available from a variety of producers, for different customer segments, from private home users to HVAC system developers and other commercial entities [3]. These smart thermostats provide additional services (remote activation, preprogrammed profiles, auto-detection of open windows, etc.), which can interest both the users and the grid. This context motivates the development of control algorithms that can engage the power consumption flexibility of TCLs at a large-scale, and beyond the simplistic load-shedding paradigm.

The following overview of the TCL DR literature is focused on presenting three actuation strategies that fulfill the ADDRB principles, namely

- the Setpoint Actuation,
- the Toggle Control,
- and the Switching Actuations: the Switching-Fraction and the Switching-Rate.

An actuation strategy creates an input or control channel into/for the the TCL population. Signals can then be sent over the input channel to manipulate the state and power output of the TCL population. Relevant signals can be created by a control algorithm that uses a model of the TCL population system and measurements.

In 2009, Callaway [12] analyzes a method for influencing the power consumption of a TCL population by using a common command signal to offsets the thermostat setpoint of all units. The effect of this type of actuation is sketched in Fig. 6, showing how the entire thermostat band of a TCL is shifted by the external signal, which can be expressed in absolute or relative units.

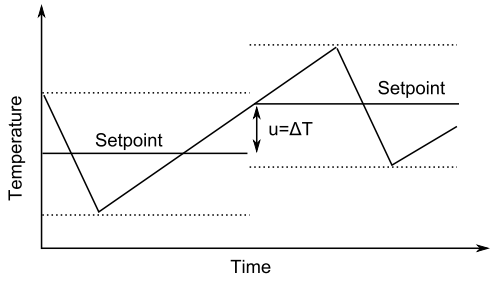

Fig. 6: A change in the thermostat set-point value. The width of the thermostat band remains constant.

> The Setpoint Actuation is a method for manipulating the aggregated power consumption of a TCL population by simultaneously shifting the thermostat bands of all units with the same (absolute or relative) amount, either in the positive or in the negative direction.

The probabilistic modeling from [28] is then used as an analysis framework, and a linear input-output dynamic model is developed. The input is the thermostatic offset, and the output is aggregated power consumption. The input-output model is used in a control scheme that actively compensate for wind fluctuation with a TCL population in a simulation scenario.

Control methods for the Setpoint Actuation are further developed by other works. In [34], a control scheme based on a different linear input-output model is proposed. In addition, because the thermostat mechanism is normally based on a low-resolution temperature sensor, a demultiplex strategy is used to extend the Setpoint Actuation by grouping TCLs into clusters. The clusters receive different, coarse-resolution setpoint changes, but in a such a way that the overall effect approximates a common, fine-resolution setpoint change. In [7] and [8], the probabilistic modeling framework is again used, this time to develop a more advanced, bilinear model of the input-output dynamic model for the Setpoint Actuation. Based on this model, a nonlinear sliding mode controller is designed. In [42], the authors add error boundaries to the probabilistic model and set-up an Kalman estimation scheme.

Toggle-Control is proposed in [22, 29]. This method is based on partitioning the thermostat temperature interval $[T_{\min}, T_{\max}]$ into a relatively large number N of bins (or cells). The command u sent to the TCL population consists of two vectors, say p and $\bar{p}$, each with N-elements. For p, each element $p_i \in [0, 1]$ represents a switch-on probability, while for $\bar{p}$, each element $\bar{p}_i \in [0, 1]$ represents a switch-off probability. Upon receiving the command, each unit in the population reacts in a probabilistic manner. A power mode switch action is decided or not, according to a Bernoulli trial with a success probability associated with its current temperature (and with the switch direction). This actuation logic is sketched in Fig. 8.

> Toggle Control is a method for manipulating the aggregated power consumption of a TCL population by having units switch-on and/or switch-off according to independent, temperature-parametrized probabilities. A vector of switch-on and switch-off probabilities, in which elements are associated with specific temperature intervals or bins, are communicated to each unit in the TCL population. Units react as soon as they receive the signal, and thus the units with successful random trials switch simultaneously (except for communication out-of-phase effects).

Given a large enough population, this randomized actuation gives a predictable and consistent result at the aggregate level. This actuation is advantageous because, given the state of the population as a *histogram of the temperatures and on/off power mode* in the population, the result of a particular actuation is intuitive, and easy to calculate and predict, see Fig. 8, by moving indicated fractions of the bar quantities between the on and off bins with the same temperature.

However there are some disadvantages. The broadcast signal has a large footprint as it consists of one rational number for each of the bins, and the issue of the thermostat's low-resolution appears again. In principle, the TCLs need to be equipped with high resolution temperature sensors to be able to distinguish between the narrow temperature bins.

The Switching-Fraction actuation proposed in [46, 47] and by this work in Pa-

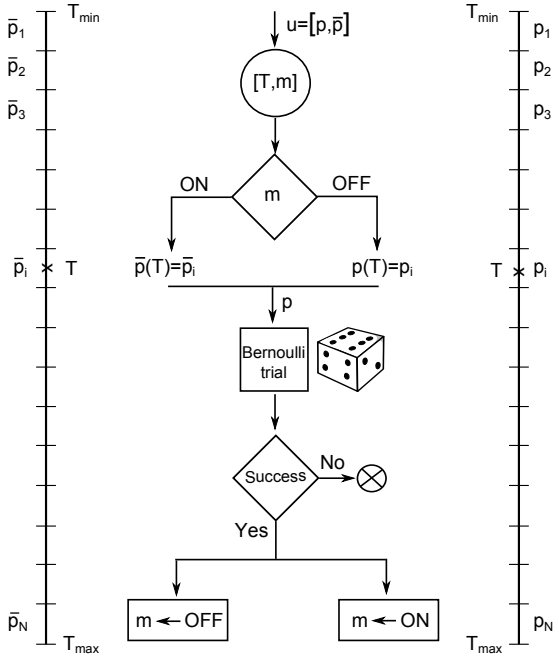

Fig. 7: Overview of the Toggle Control logic at the unit level.

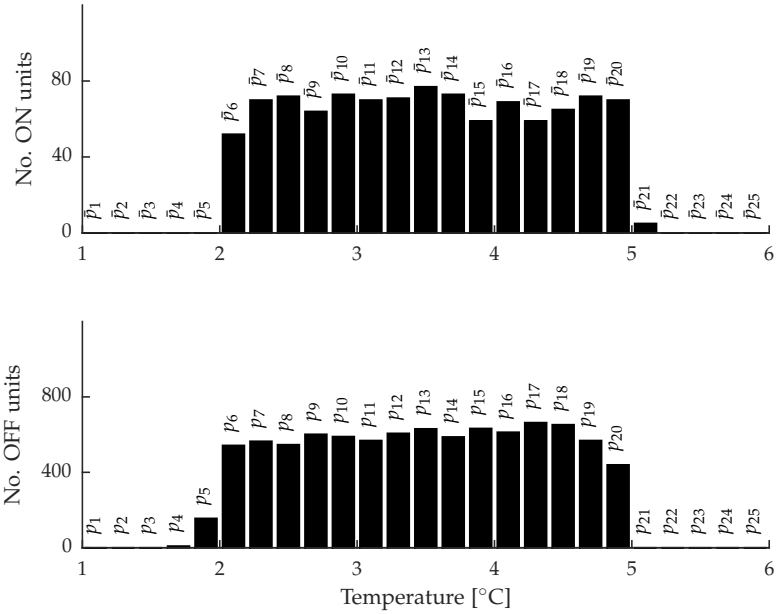

Fig. 8: Overview of the Toggle Control actuation at the population level.

pers A and B, can be seen as a particular form of Toggle Control where the communicated probability values are the same for all the histogram bins with the same power mode, $p_1 = p_2 = p_3 = \ldots$, and $\bar{p}_1 = \bar{p}_2 = \bar{p}_3 = \ldots$, see Fig. 9. The switching signal thus has only two components: one targeting units "on" with a "switch-off" probability, and one targeting units "off" with a "switch-on" probability. This resolves the main disadvantages of the toggle actuation, but creates a situation of underactuation in the modeling. As a result, control algorithms are more challenging to design.

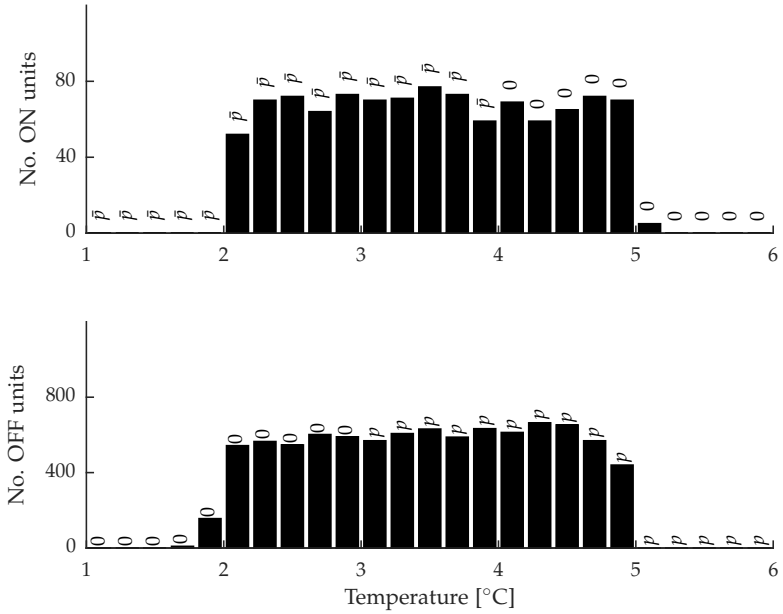

Fig. 9: Overview of the Switching-Fraction actuation at the population level. Temperature safezones (addressed later in this work) are included in these graphs, by setting switch probabilities to zero.

> The Switching-Fraction actuation is a method for manipulating the aggregated power consumption of a TCL population by having units switch-on according to a probability $p \in [0,1]$, and/or switch-off according to a probability $\bar{p} \in [0,1]$. Units react as soon as they receive the signal, and thus the units with successful random trials switch simultaneously (except for communication out-of-phase effects).

A further form of Switching Actuation, the Switching-Rate, has been proposed in Papers C and D. Instead of probabilities, switching-rates are communicated to the units in the TCL population. This results in switching actions that are not simultaneous but distributed in time, and is explained in more detail in the next chapters. The Switching-Rate mechanism can be seen as similar to the DD random strategy from [6], but the way it is integrated in the thermostat logic (hard limits are maintained) and modeling elements (using the entire state distribution to characterize the population, as opposed to only the temperature mean and variance) are different.

It is important to point out that both the Toggle Control and the Switching Actuations take place within the inherent flexibility of the thermostat, meaning that - unlike the thermostat setpoint shift/offset control - the minimum and maximum temperature limits are not crossed during operation.

Other approaches to actuation exist in the literature. For example, [39] proposes an open-loop actuation strategy, where predefined power responses can be triggered without rebound oscillatory effects. The main idea is to avoid actions that create "bulges and dents" (partial synchronization) in the underlying temperature distributions within the population, as these will propagate as a traveling wave and only slowly decay. Three such safe protocols are proposed, some of them maintaining the original thermostat band and others using a shift operation. This approach requires a digital logic equipped with some memory functions and, as part of the protocol, units can be requested to perform actions based on their individual temperature and mode state at the beginning of the actuation cycle. Overall the approach presents advantages, such as one way communication, and a predefined strategy for dangerous synchronizations, but can also be seen as less agile in using the available power flexibility. Another desynchronzation algorithm is given in [10], this specific strategy complements the thermostat setpoint actuation.

Recently, in [26] proposes and analyzes an actuation that symmetrically narrows the deadband within the original thermostat limits.

A new direction for approaching the distributed, large-scale demand response problems is through mean-field games. Similar to the ADDRB architecture, the setup of a mean-field game consists of single shared signal needs to reach all individuals within the population. The individuals then solve an optimization problem, in a fully decentralized way. The objective of the individual optimization includes local terms, a cross coupling term related to the shared signal (the population goal), and a prediction of the behavior of the "rest of the crowd" to the current conditions. The individual unit needs information about the population ("rest of the crowd"), but only in an offline manner. For mean-field approaches to DR and DD of TCLs are presented in [9, 21]. Different from the mean-field formulation, in the ADDRB setup presented in this work the population knowledge is present only at a central level, and a more *direct* command is sent to the individual units.

4 Content Outline

The Smart Grid context and the background for DR of TCLs have been presented. An overview of the main modeling and computational tools used in this work follows, including examples and comments for the TCL case. The the main contributions of the work are then summarized, and concluding remarks are presented together with a list of open issues. The main body of the work consists of four chapters organized as scientific articles, Papers A, B, C and D. Papers A and B concern the Switching-Fraction actuation, while papers C and D present the Switching-Rate actuation, including motivation, modeling and control results. There are two appendices, one on TCL duty-cycle calculations and one on modeling aspects for domestic refrigerators.

References

[1] Elmodelbolig statistics. `http://statistic.electric-demand.dk/`.

[2] Energistatistik, 2012.

[3] Navigant research leaderboard report: Smart thermostats, *Executive Report*, 2013.

[4] American recovery and reinvestment act smart grid highlight: Jumpstarting a modern grid, oct 2014.

[5] International Energy Agency. *The Power of Transformation Wind, Sun and the Economics of Flexible Power Systems,* Executive Summary. 2014.

[6] David Angeli and P-A Kountouriotis. A stochastic approach to "dynamic-demand" refrigerator control. *Control Systems Technology, IEEE Transactions on*, 20(3):581–592, 2012.

[7] Saeid Bashash and Hosam K Fathy. Modeling and control insights into demand-side energy management through setpoint control of thermostatic loads. In *American Control Conference (ACC), 2011*, pages 4546–4553. IEEE, 2011.

[8] Saeid Bashash and Hosam K Fathy. Modeling and control of aggregate air conditioning loads for robust renewable power management. *Control Systems Technology, IEEE Transactions on*, 21(4):1318–1327, 2013.

[9] Dario Bauso. A game-theoretic approach to dynamic demand response management. *arXiv preprint arXiv:1410.6840*, 2014.

[10] Jan Bendtsen and Srinivas Sridharan. Efficient desynchronization of thermostatically controlled loads. *arXiv preprint arXiv:1302.2384*, 2013.

[11] Benjamin Biegel, Mikkel Westenholz, Lars Henrik Hansen, Jakob Stoustrup, Palle Andersen, and Silas Harbo. Integration of flexible consumers in the ancillary service markets. *Energy*, 67:479–489, 2014.

[12] Duncan S Callaway. Tapping the energy storage potential in electric loads to deliver load following and regulation, with application to wind energy. *Energy Conversion and Management*, 50(5):1389–1400, 2009.

[13] Duncan S Callaway and Ian A Hiskens. Achieving controllability of electric loads. *Proceedings of the IEEE*, 99(1):184–199, 2011.

[14] European Commission Press Release Database. Memo on phasing out conventional incandescent bulbs, 2009.

[15] Energinet.dk. Ancillary services to be delivered in denmark. tender conditions, 2012.

[16] Renewable Energy Policy Network for the 21st Century. Global status report, 2014.

[17] Litos Strategic Communication for the U.S. Department of Energy. The smart grid: An introduction, 2008.

[18] Eurelectric Thermal Working Group et al. Ancillary services. unbundling electricity products–an emerging market, 2004.

[19] Satoru Ihara and Fred C Schweppe. Physically based modeling of cold load pickup. *Power Apparatus and Systems, IEEE Transactions on*, (9):4142–4150, 1981.

[20] Brendan Kirby. Ancillary services: Technical and commercial insights. *Retrieved October*, 4:2012, 2007.

[21] Arman C Kizilkale and Roland P Malhame. Collective target tracking mean field control for markovian jump-driven models of electric water heating loads. In *IFAC World Congress*, 2014.

[22] Stephan Koch, Johanna L Mathieu, and Duncan S Callaway. Modeling and control of aggregated heterogeneous thermostatically controlled loads for ancillary services. In *Proc. PSCC*, pages 1–7, 2011.

[23] Prabha Kundur, Neal J Balu, and Mark G Lauby. *Power system stability and control*, volume 7. McGraw-hill New York, 1994.

[24] Anthony Lopez, Billy Roberts, Donna Heimiller, Nate Blair, and Gian Porro. Us renewable energy technical potentials: a gis-based analysis. *Contract*, 303:275–3000, 2012.

[25] Ning Lu and Srinivas Katipamula. Control strategies of thermostatically controlled appliances in a competitive electricity market. In *Power Engineering Society General Meeting, 2005. IEEE*, pages 202–207. IEEE, 2005.

[26] Nariman Mahdavi, Cristian Perfumo, and Julio H Braslavsky. Towards load control of populations of air conditioners with guaranteed comfort margins. In *World Congress*, volume 19, pages 9930–9935, 2014.

[27] Roland Malhamé. A jump-driven markovian electric load model. *Advances in Applied Probability*, pages 564–586, 1990.

[28] Roland Malhame and Chee-Yee Chong. Electric load model synthesis by diffusion approximation of a high-order hybrid-state stochastic system. *Automatic Control, IEEE Transactions on*, 30(9):854–860, 1985.

[29] Johanna L Mathieu and Duncan S Callaway. State estimation and control of heterogeneous thermostatically controlled loads for load following. In *System Science (HICSS), 2012 45th Hawaii International Conference on*, pages 2002–2011. IEEE, 2012.

[30] Johanna L Mathieu, Mark EH Dyson, and Duncan S Callaway. Resource and revenue potential of california residential load participation in ancillary services. *Energy Policy*, 80:76–87, 2015.

[31] Sean Meyn, Prabir Barooah, Ana Busic, and Jordan Ehren. Ancillary service to the grid from deferrable loads: the case for intelligent pool pumps in florida. In *Decision and Control (CDC), 2013 IEEE 52nd Annual Conference on*, pages 6946–6953. IEEE, 2013.

[32] RE Mortensen and KP Haggerty. A stochastic computer model for heating and cooling loads. *Power Systems, IEEE Transactions on*, 3(3):1213–1219, 1988.

[33] RE Mortensen and KP Haggerty. Dynamics of heating and cooling loads: models, simulation, and actual utility data. *Power Systems, IEEE Transactions on*, 5(1):243–249, 1990.

[34] Cristian Perfumo, Ernesto Kofman, Julio H Braslavsky, and John K Ward. Load management: Model-based control of aggregate power for populations of thermostatically controlled loads. *Energy Conversion and Management*, 55:36–48, 2012.

[35] MK Petersen, K Edlund, LH Hansen, J Bendtsen, and J Stoustrup. A taxonomy for modeling flexibility and a computationally efficient algorithm for dispatch in smart grids. In *American Control Conference (ACC)*, pages 1150–1156, 2013.

[36] European SmartGrids Technology Platform. Vision and strategy for european electricity networks of the future, 2006.

[37] FC Schweppe. Frequency adaptive, power-energy re-scheduler (1979). *United States Patent*, 4317049.

[38] Joe A Short, David G Infield, and Leon L Freris. Stabilization of grid frequency through dynamic demand control. *Power Systems, IEEE Transactions on*, 22(3):1284–1293, 2007.

[39] Nikolai A Sinitsyn, Soumya Kundu, and Scott Backhaus. Safe protocols for generating power pulses with heterogeneous populations of thermostatically controlled loads. *Energy Conversion and Management*, 67:297–308, 2013.

[40] European Technology Platform SmartGrids. Strategic research agenda for europes's electricity networks of the future, 2007.

[41] European Technology Platform SmartGrids. Smart grids strategic research agenda for research, development and demonstration needs towards 2035, March 2012.

[42] Sadegh Esmaeil Zadeh Soudjani, Sebastian Gerwinn, Christian Ellen, Martin Fränzle, and Alessandro Abate. Formal synthesis and validation of inhomogeneous thermostatically controlled loads. In *Quantitative Evaluation of Systems*, pages 57–73. Springer, 2014.

[43] Canbolat Ucak and Ramazan Caglar. The effects of load parameter dispersion and direct load control actions on aggregated load. In *Power System Technology, 1998. Proceedings. POWERCON'98. 1998 International Conference on*, volume 1, pages 280–284. IEEE, 1998.

[44] Sanne Wittrup. Siemens vil lagre stroem i kaempe sandbunker, ingenioeren, November 2014.

[45] Zhao Xu, Jacob Ostergaard, and Mikael Togeby. Demand as frequency controlled reserve. *Power Systems, IEEE Transactions on*, 26(3):1062–1071, 2011.

[46] Wei Zhang, Karanjit Kalsi, Jason Fuller, Marcelo Elizondo, and David Chassin. Aggregate model for heterogeneous thermostatically controlled loads with demand response. In *Power and Energy Society General Meeting, 2012 IEEE*, pages 1–8. IEEE, 2012.

[47] Wei Zhang, Jianming Lian, Chin-Yao Chang, and K. Kalsi. Aggregated modeling and control of air conditioning loads for demand response. *Power Systems, IEEE Transactions on*, 28(4):4655–4664, Nov 2013.

Methodology

The chapter provides an overview of the main theoretical and computational tools used in this work, and includes examples and comments related to the TCL case.

5 Stochastic Hybrid System (SHS)

5.1 Dynamical Systems

A dynamical system is a mathematical representation that captures the essential characteristics of a natural or technological process in terms of describing the evolution in time of key properties/states/variables. The mathematical representation can explain, predict and help the understanding of the process. Additionally, it is essential when attempting to control the process.

Dynamical systems consists of

- a set of quantifiable properties/states/variables, and
- a set of rules describing how the states evolve/change in time.

The states of the system are chosen or processed to be in a numerical form, and can be classified as continuous- or discrete-valued. For example, the temperature in a particular point of a room is essentially a continuously-valued variable, meaning that it can take any numerical real value within some interval. On the other hand, the output of a digital thermometer is a discrete-valued variable because of the limited resolution and the output nature of the digital equipment. States that are categorical or ordinal in nature are processed into discrete-valued numerical data.

The dynamic rules can also take different forms. They can be deterministic, non-deterministic or stochastic, and can use a time-based or an event-based description.

For systems with a deterministic dynamical rule, given the initial or the current state, only a single future outcome is possible. In the case of non-deterministic systems, there can be more than one possible evolution path. Stochastic systems have associated probabilities for each of the possible evolution paths.

The difference between a time-driven dynamic and an event-based dynamic is understood in the following way: in the case of a time-based dynamic rule, the evolution of the state is directly related to a time variable[2], and in the case of an event-driven dynamic rule, the evolution of a state is not directly related to time, but to the occurrence or arrival of an event. Although there might be a timing mechanism behind the

[2]The time variable can be either continuously- or discrete-valued

description of the event, this is not necessary or may not be explicit. Time-based dynamics are naturally related to continuous-valued states, while event-based dynamics are naturally related to discrete-valued states, see also [7](Ch.1.3). Systems with an interaction between the time-driven and event-driven dynamics, and with a coupling of continuous- and discrete-valued states, are called hybrid systems.

The sections below will introduce hybrid systems, Markov chains, Stochastic Differential Equations (SDEs), and Stochastic Hybrid Systems (SHSs). SHSs are the tool of choice for describing Themostatically Controlled Loads (TCLs) in this work.

5.2 Hybrid Systems

The main characteristic of Hybrid Systems is the interaction of the time-driven and event-driven dynamics. Time-driven dynamics are related to continuously-valued states and are typically described by differential or difference equations. Event-driven dynamics are related to discrete-valued states and are typically described by automata[3]. There are different classes of hybrid systems, see e.g. [8], and this section will introduce the broad class of hybrid automata.

5.2.1 Automata

An automaton is a mechanism for describing logical and discrete behaviors. It is also known as a state machine, or as a state (transition) diagram, which is the graphical representation of the automaton.

Definition (Automaton). A typical automaton consists of the following elements (adapted from [7](Ch.2.2)):

- a set of discrete states or modes, $\mathcal{Q} = \{q_1, q_2, \ldots\}$;
- a set of events $\mathcal{E} = \{e_1, e_2, \ldots\}$;

  The events can be thought of as external inputs, resulting from the interaction of the process with the environment or with another process[4], or as internal events inherent to the system.
- a transition function, which can be of two types:
  - deterministic transition function ϕ_d that associates a start-state and an event with an end-state,

    $$\phi_d : \mathcal{Q} \times \mathcal{E} \to \mathcal{Q},\ \phi_d(q, e) \in \mathcal{Q},$$

    where ϕ_d does not need to be defined on its entire domain (a partial function);

    This can be further clarified by introducing a helper function Γ, called an active event function, that describes which events are defined, pos-

[3] Both time-driven dynamics and the event-driven dynamics can also be represented by other formalisms, for example partial differential equations or a mixed system of dynamic and algebraic equations, and respectively, Petri nets or other discrete mathematical modeling languages.

sible or allowed from each state,

$$\Gamma : \mathcal{Q} \to 2^{\mathcal{E}},\ \Gamma(q) \subseteq \mathcal{E}.$$

It is mentioned that the empty set $\varnothing$ and the $\mathcal{E}$ set itself are members of the power set $2^{\mathcal{E}}$, which is the set of all subsets of $\mathcal{E}$. Within the definition, it is possible to have different events leading to the same end-state, or an end-state that is the same as the start state;

– non-deterministic transition function ϕ_n that associates a start state and an event with a set of possible end-states,

$$\phi_n : \mathcal{Q} \times \mathcal{E} \to 2^{\mathcal{Q}},\ \phi_n(q, e) \subseteq \mathcal{Q};$$

The active event function can be identically defined as above.

Alternatively, transitions can be specified as a set $\mathcal{T} \subseteq \mathcal{Q} \times \mathcal{E} \times \mathcal{Q}$, where each element consists of a start state, an event, and an end state. In this case, the difference between a deterministic and a non-deterministic automaton can be made by inspecting the transition set $\mathcal{T}$ for the existence of multiple elements with the same start-state and event pair.

Another observation is that non-determinism is caused when starting from the same state, multiple end-destinations are possible using the *same* event. The situation of different end-states by different events is not non-determinism within this definition.

- an initial state $q_0 \in \mathcal{Q}$, or a set of possible initial states $q_0 \subseteq \mathcal{Q}$ (a non-deterministic feature);
- (optionally) a set of marked states, $\mathcal{Q}_m \subseteq \mathcal{Q}$.

The definition of the automaton prescribes the logical rules and allowed order of events or transitions for the evolution of the system, but no timing information.

TCL example. Using the automaton modeling, the logic of a thermostat can be represented as in Fig. 10. There are two discrete states, $\mathcal{Q} = \{q_0 \equiv \text{OFF},\ q_1 \equiv \text{ON}\}$ and two events $\mathcal{E} = \{e_0 \equiv \text{TURNOFF},\ e_1 \equiv \text{TURNON}\}$. The transition function (or set) are deterministic. From the OFF state, only the TURNON event is allowed (possible), and from the state ON only the TURNOFF event is allowed. The trajectory (execution, or solution) of such a system thus consists of alternating ON-OFF state sequences, and the acceptable ordered event list is, similarly, an alternating sequence of TURNON and TURNOFF events. The initial state determines the first element in these sequences.

The thermostat on/off logic is one of the simplest forms of automata, and not truly and interesting object in this framework. The operations and tools of automaton framework, such as model verification and the development of supervisory control,

[4]There exist frameworks for defining automata with outputs, not discussed here. This would then allow a complete input/output design.

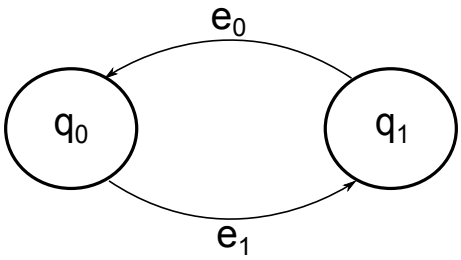

Fig. 10: Simple automata with two discrete states, and two events.

are inconsequential for this example. At the same time, the automaton framework is incomplete to model the thermostat logic. The next step is to extend the automaton framework and combine the event-based dynamics with a simple form of time-driven dynamics.

5.2.2 Timed Automata

Timed automata are a modeling framework for extending the logical descriptions with clock or timing content. Clocks are the simplest form of time-driven dynamic. A clock is a continuous variable $c(t)$, $c : \mathbb{R}_+ \to \mathbb{R}_+$, with a time-driven evolution given by the ordinary differential equation

$$\frac{dc(t)}{dt} = 1. \tag{2}$$

A timed automaton based on clocks [2] will be presented next. The following elements will be added to the logical automaton,

- a number of clock variables $c_k(t)$, where k is the index;
- guards or timing conditions that are prerequisites for transitions, these will be defined in terms of the clock variables;
- invariant conditions that describe a type of transition forcing, again defined in terms of the clock variables;
- clock reset actions consisting of the assignment $c_k(t) = 0$, taking place at the moment of the (instantaneous) transition.

Definition (Timed Automaton). A timed automaton with guards and invariants consists of the following elements (adapted from [7](Ch.5.6)):

- a set of discrete states or modes, $\mathcal{Q} = \{q_1, q_2, \ldots\}$;
- a set of events $\mathcal{E} = \{e_1, e_2, \ldots\}$;
- a set of clocks $\mathcal{C} = \{c_1, c_2, \ldots\}$;
- a set of transitions $\mathcal{T} \subseteq \mathcal{Q} \times \mathcal{E} \times \mathcal{Q}$, where each transition element consists of a start state, an event, and an end state;

- guard conditions associated with each transition $\{g_j,\ \forall j \in \mathcal{T}\}$, taking values in a class of allowed clock constraints $g_j \in \mathbb{C}(\mathcal{C}) \cup \{\varnothing\}$;

  The set of admissible constraints $\mathbb{C}(\mathcal{C})$ consists of inequality relations involving the clock variables and a constant (rational) value. A transition is not enabled unless the associated guard condition (if not equal to the empty-set) is evaluated in to be true in clock-time logic.

  Depending on the transition set $\mathcal{T}$ and the guard conditions $\{g_j\}$, the automaton can be deterministic or non-deterministic. A non-deterministic automaton has timed transitions with the same start-state, event pair, and with guard conditions that are not mutually exclusive in the clock-timed logic, leading to different end-states.

- a subset of clock variables associated with each transition, $\{\mathcal{C}_j \subset \mathcal{C}, \forall j \in \mathcal{T}\}$, to be reset the moment of the (instantaneous) transition j;

- state invariant conditions defined via a partial function $I : \mathcal{Q} \to \mathbb{C}(\mathcal{C})$;

  If an invariant condition is present for a state, the automaton can only remain in the respective state as long as the condition is fulfilled. Before the invariant condition expires, a transition must take place from the set of available choices given by $\mathcal{T}$.

- an initial mode $q(0) = q_0$, and initial clock values, usually zero, $c_k(0) = 0,\ \forall k$.

The definition of the clock variables introduced the concept of time as a positive real number. The discrete state can now be considered as a function of time, $q(t)$, $q : \mathbb{R}_+ \to \mathcal{Q}$. Furthermore, the time just before a transition is denoted by t^-, and the time just after a transition is denoted by t^+. This is necessary to consider because the transitions are instantaneous. If a clock variable c_k is first reset by the transition taking place at time t, its value right before the transition $c_i(t^-) = \lim_{s \nearrow t} c_k(s) = t$ and right after the transition is $c_k(t^+) = \lim_{s \searrow t} c_k(s) = 0$. A typical convention is to consider the trajectory of the clock variables as càdlàg, i.e., right continuous with left limits, $c_k(t) = c_k(t^+)$. Similarly, $q(t)$ is càdlàg variable, and a transition from mode i to mode j at time t is equivalent to $q(t^-) = i$, $q(t) = q(t^+) = j$.

TCL example. Using the timed automaton modeling framework, the thermostat example can be extended. For example, minimum on-time and minimum off-time conditions can be modeled as guards, see Fig 11. These conditions ensure that frequent switching behavior is avoided. It would be desirable to also define state invariant conditions. For example, taking the case of a cooling function, it would be desirable to have the thermostat leave the OFF state before the temperature becomes too high, and similarly, have the thermostat leave the ON state before the temperature becomes too cold. The problem with introducing such conditions is that the temperature is a not a clock variable. Within the formal-

ism of timed automata with guards and invariants, forced transitions can only be specified using an approximate timing design. For example, it can be assumed that for a good operation under some known conditions, the OFF time should not be longer than 60 minutes, and the ON time should not be longer than 25 minutes.

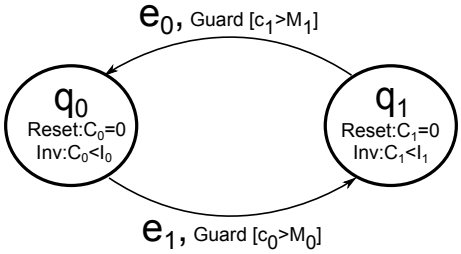

Fig. 11: Timed automata with two clocks, c_0 and c_1, guard and invariant conditions. Values M_0, M_1, I_0, I_1 are parameters.

5.2.3 Hybrid Automata

To introduce temperature conditions into the thermostat example, the automaton definition needs to be further extended. The required step is to replace the clock variables with continuous-valued variables, $x_k(t) : \mathbb{R}_+ \to \mathbb{R}$, with more general time-driven dynamics. Furthermore, the reset actions and guard conditions will also be more general.

Definition (Hybrid Automaton). A hybrid automaton can be defined in the following way (adapted from [7](Ch.5.7)):

- a set of discrete-states or modes, $\mathcal{Q} = \{q_1, q_2, \ldots\}$;
- a set of events $\mathcal{E} = \{e_1, e_2, \ldots\}$;
- a continuously-valued vector state-variable $X \in \mathcal{X} \subseteq \mathbb{R}^n$;
- a continuously-valued vector input-variable $U \in \mathcal{U} \subseteq \mathbb{R}^m$;
- dynamics of the continuous variable defined by a vector field

  $$F : \mathcal{Q} \times \mathcal{X} \to \mathbb{R}^n, \ \frac{dX(t)}{dt} = F(q(t), X(t));$$

  It is furthermore possible to consider the case of dynamics with external inputs.
- a transition set $\mathcal{T} \subseteq \mathcal{Q} \times \mathcal{E} \times \mathcal{Q}$, consisting of a discrete start-state, and event, and a discrete end-state;

- guard conditions associated with each transition, expressed as a sub-domain of $\mathcal{X}$, $G_j \subseteq \mathcal{X}, \forall j \in \mathcal{T}$;

  A transition j is active/allowed at time t only if the continuous state $X(t) \in G_j$.

- functions R_j associated with each transition $j \in \mathcal{T}$, $R_j : \mathcal{X} \times \mathcal{U} \rightarrow \mathcal{X}$, which define the reset or jump of the continuous state at the moment of the transition;

  The dependence of the discrete states and of the event is included by the transition index j.

- state-invariant or domain conditions for each mode $i \in \mathcal{Q}$, $I_i \subseteq \mathcal{X}$;

  The system can remain in the discrete mode i only as long as the continuous variable fulfills $X(t) \in I_i$.

- an initial discrete-state $q(0) = q_0$, and an initial continuous-state $X(0) = X_0$.

TCL example. The thermostat logic can be described by the hybrid automaton in Fig. 12.

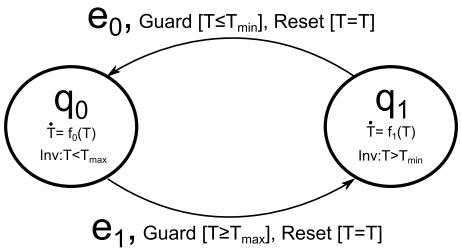

Fig. 12: Hybrid automata description of a thermostat mechanism.

It is mentioned that there are other hybrid system/automata definitions in the literature. For example, [18] uses the notion of edges instead of events. This is because the focus is on the state transitions themselves and not on the event trigger semantic. Therefore, state transitions are identified only by the start-state and the end-state, and there can be at most one edge between two states. Another example is the general hybrid dynamical system definition [4], where in each discrete-mode an explicitly distinguished continuous dynamical system is considered (with its own domain, input space, and dynamic), and mode transitions are divided between an autonomous (uncontrollable) set and a controllable set. And while the description in this section has started from the discrete theory side with the automaton object, e.g. [12] puts forward a modeling approach starting from mathematical analysis to formally discuss the concept of solutions of a hybrid system and their properties. In all cases, there are correspondences and (at least partial) equivalences between the different hybrid

system frameworks.

Finally, it is mentioned that there are two classes of problems or questions that can be posed on hybrid systems/automata. The first class of problems are specific to the Computer Science field, such as formal model verification and reachability analysis. A state is called reachable if there exist a valid system evolution trajectory starting from a given initial state or set of initial states. A valid trajectory fulfills all guard and invariant conditions, and follows the transition set. Reachability questions are essential for model verification. For example, safety analysis can be performed by building an appropriate model and checking the reachability of the unsafe state(s). Since the answer will obviously depend on the underlying system, the reachability problem is asking whether an analysis can be performed algorithmically. This question is answered negatively for the class of hybrid automata, meaning that it is computationally infeasible to check reachability questions in general. However, there exist subclasses of hybrid automata for which algorithmic reachability analysis is feasible, such as Rectangular Hybrid Automata [14]. The second class of problems that can be posed for hybrid system/automata are specific to System and Control Theory. Stability analysis [18] is such an example. Control problems are difficult, but a variety of techniques are available. These include purely discrete methods (supervisory control), game theoretic approaches, and optimal approaches.

5.3 Continuous-Time Markov Chains

Markov chains are dynamic processes with a discrete-valued domain, event-based dynamic, and a stochastic timing mechanism associated with the events. The events are not considered as external inputs, but are part of the internal description of the system.

Definition (Markov Chain). A Markov chain consists of:

- a set of discrete states or modes, $\mathcal{Q} = \{q_1, q_2, \ldots\}$;
- a set $\mathcal{T}$ of edges or state-transitions, each consisting of an ordered pair of states, $\mathcal{T} \subseteq \mathcal{Q} \times \mathcal{Q}$;

  Each transition can optionally be associated/labeled with an event symbol. However, it is not the events themselves but the state transitions that are the main working object. In the Markov chain framework it is not distinguished between events that cause the same transition. Furthermore, the start-state and the end-state in a transition pair must be different.
- a non-negative transition rate (or intensity) associated with each edge $(i, j) \in \mathcal{T}$. For time-homogeneous Markov chains the rate is a positive constant $\lambda_{ij} > 0$, while for time-inhomogeneous Markov chains, the rate is a non-negative function of time $\lambda_{ij} : \mathbb{R}_+ \to \mathbb{R}_+$;

  Rates with value 0 can be associated to pairs $(i, j) \notin \mathcal{T}$, $i \neq j$, and similarly $\lambda_{ij}(t) = 0$ means that at time t the transition (i, j) is not allowed/cannot happen.

- an initial state which is specified in the form of a random variable q_0 with the probability mass π_0,

$$\pi_0 : \mathcal{Q} \to [0,1],\ \pi_0(i) = \Pr(q_0 = i),\ \sum_{i \in \mathcal{Q}} \pi_0(i) = 1.$$

The rest of this section will present the Markov (or memoryless) property, clarify the stochastic transition mechanism, and introduce the Forward and Backward propagation equations of the process. These topics are reviewed without presenting measure theory foundations and general probabilistic theory and concepts.

A stochastic process can be seen as a collection of random variables indexed by time. Markov chains are by definition stochastic processes, taking values on a discrete domain $\mathcal{Q}$, that satisfy the Markov property. This property alone gives a lot of structure to the resulting process. In the following, the time index is taken to be continuous, $t \in [0, +\infty)$, and the stochastic process is denoted $\{q(t)\}$, where $q(t)$ is the state of the Markov chain system at time t.

If for any ordered sequence of time points $t_k > t_{k-1} \ldots > t_1$, and any sequence of values $(i_k, \ldots, i_1)$, each in $\mathcal{Q}$, the equality

$$\Pr\big[q(t_k) = i_k \mid q(t_{k-1}) = i_{k-1}, \ldots, q(t_1) = i_1\big] = \Pr\big[q(t_k) = i_k \mid q(t_{k-1}) = i_{k-1}\big] \quad (3)$$

holds, then $\{q(t)\}$ is Markovian. The property expresses the fact that the evolution in time of the process only depends on the present and not also on the past, or that the dynamics never look back past the current state.

The Markov property leads to exponentially distributed state holding times.

State holding times are random variables Y_i describing how long the process remains in the same state $i \in \mathcal{Q}$. Because the process $\{q(t)\}$ is memoryless, the state transitions cannot depend on past information, and thus they cannot depend on the amount of time the process has been in a particular state. The state transitions must therefore have the same chance of happening for case when the state holding time is small as for when the state holding time is longer. This translates into the following condition,

$$\Pr\big[Y_i > s + t \big| Y_i > t\big] = \Pr\big[Y_i > s\big], \quad (4)$$

and, using conditional probability definition/axiom $\Pr\big[a \wedge b\big] = \Pr\big[a \mid b\big]\Pr\big[b\big]$ leads to

$$\begin{aligned} \Pr\big[Y_i > s + t \wedge Y_i > t\big] &= \Pr\big[Y_i > s\big]\Pr\big[Y_i > t\big] \Leftrightarrow \\ \Leftrightarrow \Pr\big[Y_i > s + t\big] &= \Pr\big[Y_i > s\big]\Pr\big[Y_i > t\big]\,. \end{aligned} \quad (5)$$

Because $\Pr\big[Y_i > y\big]$ is a tail distribution (or complementary cumulative distribution), it must also decrease monotonically, and have the boundary conditions $\Pr\big[Y_i > 0\big] = 1$ and $\lim_{y \to \infty} \Pr\big[Y_i > y\big] = 0$. The following exponential function satisfies these conditions,

$$\Pr\big[Y_i > y\big] = \exp(-\Lambda_i y),\ \Lambda > 0 \quad (6)$$

and furthermore, it can be shown that it is the only relevant function that does so. Parameter Λ is called the rate.

Markov time-inhomogeneous processes have the memoryless property, the process does not depend on its history, but the stochastic properties vary/are changing in time. As such, the state holding time Y_i still fulfills a memoryless property, but needs to be specified together with the start moment of the timing,

$$\Pr\big[Y_i(t_0) > s + t \big| Y_i(t_0) > t\big] = \Pr\big[Y_i(t_0 + t) > s\big]. \tag{7}$$

This leads to the following form of exponential distribution,

$$\Pr\big[Y_i(t_0) > y\big] = \exp\big(-\int_{t_0}^{t_0+y} \Lambda_i(\tau) d\tau\big), \tag{8}$$

where the rate parameter Λ can be time varying.

When the state holding time Y_i expires, a new state is randomly chosen from the set of allowed/defined transitions. If $\mathcal{Q}_i \subseteq \mathcal{Q}$ is the set of possible end-states from $i \in \mathcal{Q}$, as prescribed by $\mathcal{T}$, then to each j element in $\mathcal{Q}_i$ there corresponds a transition probability $\rho_{ij} \in [0, 1]$, such that $\sum\limits_j \rho_{ij} = 1$.

When defining the elements of a Markov chain, in the beginning of the section, neither state-holding rates nor transition probabilities were used, but rather transition rates λ_{ij}. There is an equivalent relation between these elements.

The state-transition mechanism can be though of in the following way. From the start-state i, a number of random state-transition events $j \in \mathcal{Q}_i$ can take place. It can be said that these are independent, and that the waiting times until their occurrence/arrival have the memoryless property, thus being exponentially distributed with rates λ_{ij}. Let Z_{ij} denote the random waiting time for the event that leads to end-state j,

$$\Pr\big[Z_{ij} > t\big] = \exp(-\lambda_{ij} t). \tag{9}$$

The state-holding is the minimum of the Z_{ij} variables,

$$\begin{aligned}\Pr\big[Y_i > t\big] &= \Pr\big[Z_{ij_1} > t \wedge Z_{ij_2} > t \wedge \dots\big] = \prod_{j \in \mathcal{Q}_i} \Pr\big[Z_{ij} > t\big] \\ &= \prod_{j \in \mathcal{Q}_i} \exp(-\lambda_{ij} t) = \exp\big(-\sum_{j \in \mathcal{Q}_i} \lambda_{ij} t\big)\end{aligned} \tag{10}$$

Thus the state-holding rate is $\Lambda_i = \sum\limits_{j \in \mathcal{Q}_i} \lambda_{ij}$. The transition probabilities can also be expressed in terms of λ_{ij}, namely, $\rho_{ij} = \frac{\lambda_{ij}}{\Lambda_i}$, see [7](Ch.6.8.2). For time-inhomogeneous processes, the state holding rate is time-varying, $\Lambda_i(t) = \sum\limits_{j \in \mathcal{Q}_i} \lambda_{ij}(t)$.

In general, a stochastic process is completely specified only if the all the joint probabilities are known. The Markov property leads to the joint probabilities being expressed as

$$\begin{aligned}&\Pr\big[q(t_k) = i_k \wedge q(t_{k-1}) = i_{k-1} \wedge \dots \wedge q(t_1) = i_1\big] = \Pr\big[q(t_k) = i_k \big| q(t_{k-1}) = i_{k-1}\big] \cdot \\ &\Pr\big[q(t_{k-1}) = i_{k-1} \big| q(t_{k-2}) = i_{k-2}\big] \cdot \dots \cdot \Pr\big[q(t_2) = i_2 \big| q(t_1) = i_1\big] \cdot \Pr\big[q(t_1) = i_1\big],\end{aligned} \tag{11}$$

where the conditional probability definition/axiom was used. This means that joint probabilities are completely determined by arguably simpler objects, namely the transition functions $p_{ij}(s, t) \triangleq \Pr\big[q(t) = j \;\big|\; q(s) = i\big]$ (and an initial condition).

In the following, the relation between the transition functions $p_{ij}(s,t)$ and the transition rates λ_{ij} is clarified, in order to conclude that the elements listed at the beginning of the section are sufficient to completely specify the Markov chain stochastic process.

In the transition function $p_{ij}(s,t)$, the interval $[s,t]$ can be decomposed by taking a time point $s < u < t$ and by using the law of total probability and the Markov property. This leads to the following important relation,

$$\begin{aligned} p_{ij}(s,t) &\triangleq \Pr\big[q(t) = j \mid q(s) = i\big] = \\ &= \sum_{r\in Q} \Pr\big[q(t) = j \mid q(u) = r, q(s) = i\big] \cdot \Pr\big[q(u) = r \mid q(s) = i\big] = \\ &= \sum_{r\in Q} \Pr\big[q(t) = j \mid q(u) = r\big] \cdot \Pr\big[q(u) = r \,\big|q(s) = i\big] = \sum_{r\in Q} p_{rj}(u,t)p_{ir}(s,u), \end{aligned} \quad (12)$$

which is known as the Chapman-Kolmogorov equation. This equation can be written in a matrix form, by organizing the transition functions $P(s,t) = \{p_{ij}(s,t)\}$ such that elements with the same i index are on the same row and the elements with the same j are on the same column,

$$P(s,t) = P(s,u)P(u,t),\ s \le u \le t. \quad (13)$$

The relation can be further manipulated to obtain two differential forms.

First, using time indexes $s \le t \le t + \Delta t$ the Forward differential form is obtained,

$$\begin{aligned} P(s,t+\Delta t) &= P(s,t)P(t,t+\Delta t) \;\Big|\; - P(s,t) \\ P(s,t+\Delta t) - P(s,t) &= P(s,t)(P(t,t+\Delta t) - I) \;\Big|\; \frac{1}{\Delta t} \\ \frac{P(s,t+\Delta t) - P(s,t)}{\Delta t} &= P(s,t)\frac{P(t,t+\Delta t) - I}{\Delta t} \;\Big|\; \lim_{\Delta t\to 0} \\ \frac{\partial P(s,t)}{\partial t} &= P(s,t)A(t), \end{aligned} \quad (14)$$

where $P(s,t)$ has been assumed to be differentiable in the second parameter and the limit $\frac{P(t,t+\Delta t)-I}{\Delta t} \triangleq A(t)$ has been assumed to exist. The well-behaved nature of the $P(s,t)$ and $A(t)$ elements can be argued from the exponential form discussed above, and the complete mathematical discussion pertains to the core of Markov theory. Matrix $A(t)$ is called the *generator* or the *infinitesimal generator* of the Markov process.

Secondly, using time indexes $s \le s + \Delta s \le t$ and the fact that $\lim_{\Delta s\to s} P(s,s+\Delta s) = P(s,s) = I$, the Backward differential form is obtained,

$$\begin{aligned} P(s,t) &= P(s,s+\Delta s)P(s+\Delta s,t) \;\Big|\; - P(s,s+\Delta s)P(s,t) \\ (I - P(s,s+\Delta s))P(s,t) &= P(s,s+\Delta s)(P(s+\Delta s,t) - P(s,t)) \;\Big|\; \frac{1}{\Delta s} \\ -\frac{P(s,s+\Delta s) - I}{\Delta s}P(s,t) &= P(s,s+\Delta s)\frac{P(s+\Delta s,t) - P(s,t)}{\Delta s} \;\Big|\; \lim_{\Delta s\to 0} \\ \frac{\partial P(s,t)}{\partial s} &= -A(s)P(s,t). \end{aligned} \quad (15)$$

The transition functions $P(s,t)$, together with the initial condition $P(s,s) = I$, can be determined uniquely from the differential forms if matrix $A(t)$ is known. Therefore, full knowledge of the transition functions is contained in $A(t)$.

In the case of a homogeneous Markov chain, $P(s,t) = P(t-s)$, $P(0) = I$, and $A(t) = A$, resulting in the following differential forms

$$\dot{P}(t) = P(t)A,\ \dot{P}(t) = -AP(t)\ , \tag{16}$$

which has the solution $P(t) = e^{At} = I + A + \frac{1}{2}A^2 + \ldots$. In the case of the inhomogeneous chain, an $P(s,t)$ can be represented using the product-integral, see. e.g. [15] and references therein.

The last item to clarify is the relation between the generator matrix $A(t)$ and the transition probabilities λ_{ij} as introduced above. The initial state probability has been introduced in the Markov chain definition as π_0. Notation π_t will denote the state probability mass vector at time t (as a row vector). Using the transition functions and the law of total probability, it can be seen that

$$\pi_t = \pi_0 P(0,t), \tag{17}$$

and using the Forward differential form, it can be obtained that

$$\frac{d\pi_t}{dt} = \pi_t A(t), \tag{18}$$

also know as the master equation of the Markov chain. Element wise, the master equation expresses the following relation,

$$\begin{aligned}
&\Pr\big[q(t+h) = i\big] - \Pr\big[q(t) = i\big] = h \sum_{j \in Q} \Pr\big[q(t) = j\big] \cdot A_{ji}(t), \text{ as } h \to 0 \Rightarrow \\
&\Pr\big[q(t+h) = i\big] = \Pr\big[q(t) = i\big] \cdot \big(1 + hA_{ii}(t)\big) + h \sum_{j \in Q - \{i\}} \Pr\big[q(t) = j\big] \cdot A_{ji}(t), \\
&\qquad\qquad\qquad\qquad\qquad\qquad\qquad\qquad\qquad\qquad \text{as } h \to 0.
\end{aligned} \tag{19}$$

It can be seen that this description matches the infinitesimal understanding of the transition rates λ_{ij}. These have been introduced as the parameters for the exponential random state-transition waiting times, Z_{ij}, $i \neq j$.

$$\Pr\big[q(t+h) = j \;\big|\; q(t) = i\big] = \Pr\big[Z_{ij} < h\big] = 1 - \exp(-\lambda_{ij}h) = \lambda_{ij}h + o(h) \tag{20a}$$

$$\Pr\big[q(t+h) = i \;\big|\; q(t) = i\big] = \Pr\big[\min_{j \neq i} Z_{ij} > h\big] = \exp(-\Lambda_i h) = 1 - \Lambda_i h + o(h) \tag{20b}$$

Thus the elements of the generator matrix $A(t)$ are the transition rates, $a_{ij} = \lambda_{ij}$, $i \neq j$, and $a_{ii} = -\Lambda_i = -\sum_{j \neq i} \lambda_{ij}$.

An observation is that the structural properties of a transition rate matrix are therefore,

- square dimension;
- positive non-diagonal elements;
- columns that sum to 1.

Markov chains can be studied for both transient and steady-state analysis (more results for time homogeneous processes), and furthermore a decision/control theory exists. In this case, the transition rates are not fixed, but can be seen as a function of the external inputs.

> *TCL example.* In the thermostat example, a Markov chain behavior appears when the Switching-Rate actuation is considered. The switching actuation consists of the probabilistic transition rates behavior, over the simple discrete state space of the thermostat, with $\mathcal{Q} = \{q_0 = \text{OFF}, q_1 = \text{ON}\}$. The rates (or intensities) $\lambda_{01} \triangleq \lambda_1$ and $\lambda_{10} \triangleq \lambda_0$ are externally prescribed, and thus influence the state occupancy/probability trajectory π_t.

5.4 Stochastic Differential Equations (SDEs)

5.4.1 Diffusion Processes

Stochastic processes with the Markov memoryless property can also take values in a continuous set/space $\mathcal{X} \in \mathbb{R}^n$. When working on a discrete space, one of the main probabilistic objects was the transition function $\Pr\big[q(t) = j \;\big|\; q(s) = i\big],\ s < t,\ i, j \in \mathcal{Q}$. For continuously-valued stochastic processes, the pointwise probabilities are all essentially zero, and therefore the working object for transitions is instead

$$\Pr\big[X(t) \in \mathcal{A} \;\big|\; X(s) = x\big],\ s < t,\ \mathcal{A} \subset \mathcal{X},\ x \in \mathcal{X}.$$

More rigorously, the set $\mathcal{A}$ has to be part of a σ-algebra defined on $\mathcal{X}$, generally the Borel algebra $\mathcal{B}(\mathcal{X})$.

The Markov property (eq. (3) for Markov chains) can be expressed as

$$\begin{aligned}\Pr\big[X(t_k) \in \mathcal{A} \;\big|\; X(t_{k-1}) = x_{k-1}, X(t_{k-2}) = x_{k-2}, X(t_1) = x_1\big] = \\ = \Pr\big[X(t_k) \in \mathcal{A} \;\big|\; X(t_{k-1}) = x_{k-1}\big].\end{aligned} \tag{21}$$

The Chapman-Kolmogorov equation, as a result of the total probability law and of the Markov property, is written for $s < u < t$ as

$$\Pr\big[X(t) \in \mathcal{A} \;\big|\; X(s) = x\big] = \int_{\mathcal{X}} \Pr\big[X(t) \in \mathcal{A} \;\big|\; X(u) = y\big] \cdot \Pr\big[X(u) \in dy \;\big|\; X(s) = x\big] dy\,. \tag{22}$$

Furthermore, if the transition function admits a transition density function,

$$\Pr\big[X(t) \in \mathcal{A} \;\big|\; X(s) = x\big] = \int_{\mathcal{A}} f(z, t, x, s) dy, \tag{23}$$

the Chapman-Kolmogorov equation can be written as

$$f(z, t, x, s) = \int_{\mathcal{C}} f(z, t, y, u) f(y, u, x, s) dy. \tag{24}$$

In a step that is correspondingly similar to the presentation of Markov chains, the Chapman-Kolmogorov equation for transition densities can be manipulated to yield two differential forms: a Forward and a Backward equation. To derive these

differential forms more assumptions and analytic conditions on the Markov process and its transition functions are required, see e.g. [11](Ch.3). The subclass of Markov processes called diffusion processes is characterized by the following properties,

$$\lim_{t \searrow s} \frac{1}{t-s} \int_{|y-x|>\epsilon} f(y,t,x,s)dy = 0, \tag{25a}$$

$$\lim_{t \searrow s} \frac{1}{t-s} \int_{|y-x|<\epsilon} (y-x) f(y,t,x,s)dy = A(x,s), \tag{25b}$$

$$\lim_{t \searrow s} \frac{1}{t-s} \int_{|y-x|<\epsilon} (y-x)^2 f(y,t,x,s)dy = B(x,s)\ , \tag{25c}$$

for all $\epsilon > 0,\ s > 0$. These conditions force the underlying Markov process to have continuous sample paths. The term $A(x,s)$ is called the drift, and the term $B(x,s) \geq 0$ is the diffusion coefficient. For multidimensional diffusion processes the notation $(y-x)^2$ is understood as $(y-x)(y-x)^T$, and $B(x,s) > 0$ is a positive definite matrix. If the diffusion coefficient is non-zero, the sample paths of the process are nowhere differentiable.

For the class of diffusion processes, the Forward and Backward differential equations take the following form:

$$\frac{\partial f(z,t,x,s)}{\partial t} + \sum_i \frac{\partial}{\partial z_i}\Big(A_i(z,t) f(z,t,x,s)\Big) = \frac{1}{2}\sum_i\sum_j \frac{\partial^2}{\partial z_i \partial z_j}\Big(B_{ij}(z,t) f(z,t,x,s)\Big), \tag{26}$$

$$\frac{\partial f(z,t,x,s)}{\partial s} = -\sum_i A_i(x,s)\frac{\partial f(z,t,x,s)}{\partial x_i} - \frac{1}{2}\sum_i\sum_j B_{ij}(x,s)\frac{\partial^2 f(z,t,x,s)}{\partial x_i \partial x_j}, \tag{27}$$

where i and j are component indexes for an $n-$dimensional process. The Forward equation for diffusion processes is also called the Fokker-Planck, Fokker-Planck-Kolmogorov, or Forward-Kolmogorov. A more general differential form can be obtained for processes with jump discontinuities, see e.g. [11](Ch.3).

> *TCL example.* The temperature dynamics of a TCL will be described by diffusion processes. The drift part will be given by a simplified physical law, used to capture the systematic knowledge of the temperature variations from cold to hot and from hot to cold, and the diffusion coefficient will account for random variations around the systematic trajectory. The Forward differential equations of the thermal dynamics will be the main tool used to describe a population of TCLs. Additionally, App. Y shows how the Backward differential equation can be used to calculate duty-cycle elements for a TCL with stochastic dynamics, and how the duty-cycle elements are different from the case of deterministic dynamics. This is an application of first-passage/first-hitting times type of problems.

5.4.2 Itô Stochastic Integration

Diffusion processes are often represented and studied with the tools of Itô stochastic calculus. For this reason, the main concepts of Itô stochastic calculus will be introduced next.

The building block for randomness with continuous sample paths is the Weiner process.

Definition (Weiner process). A one-dimensional Weiner stochastic process $W(t)$ is defined by the following properties:

- $W(0) = 0$;
- W_t has continuous sample paths;
- the increment random variables $\Delta W(t_1, t_2) = W(t_2) - W(t_1)$ and $\Delta W(t_3, t_4) = W(t_4) - W(t_3)$ are independent for any t_1, t_2, t_3, t_4 such that $0 \leq t_1 < t_2 \leq t_3 < t_4$ (increment variables over non-overlapping time intervals);
- the increment process $\Delta W_t(h) = W(t+h) - W(t)$ is independent of t, i.e. stationary, and thus $\Delta W_t(h) = \Delta W(h) = W(h) - W(0)$;
- the increment process $\Delta W(h)$ has a Gaussian distribution with mean zero and standard deviation $\sqrt{h}$, i.e.

$$\Pr\big[\Delta W(h) < x\big] = \frac{1}{2}\left[1 + \frac{2}{\sqrt{\pi}} \int_0^{\frac{x}{\sqrt{2h}}} e^{-y^2} dy\right]$$
$$\Pr\big[x < \Delta W(h) < x + dx\big] = dx \frac{1}{\sqrt{2\pi h}} \exp\left(-\frac{x^2}{2h}\right).$$

These properties can be shown to be coherent, meaning that they do not exclude each other. Furthermore, they completely and consistently describe a Markov stochastic process with transition function

$$\Pr\big[X(s+h) \in \mathcal{A} \big| X(s) = x\big] = \int_{\mathcal{A}} \underbrace{\frac{1}{\sqrt{2\pi h}} \exp\left(-\frac{(y-x)^2}{2h}\right) dy}_{f(y, t+h|x,t)}. \tag{28}$$

The Gaussian property (the exponential form) is a consequence of imposing the Markov property.

An important remark is that the transition density $f(y, t+h, x, t)$ of the Weiner process is the solution of the differential Forward and Backward equations (26) and (27) with $n = 1$, drift term $A = 0$ and diffusion coefficient $B = 1$. A multidimensional Weiner process $\bar{W}(t) \in \mathbb{R}^m$ is understood as a stacked version of m independent Weiner processes. In this case the drift term is $A = 0_{m \times 1}$ and the diffusion coefficient $B = I_m$.

The next step is to introduce the concept of stochastic integration, see e.g. [11](ch.4), [13](ch.2) or [21](ch.1.4) and the references within.

In the deterministic setting the integral of a function over a domain is seen as the limit of a sum over an ever finer partition of the integration domain. In the one-dimensional case, given a domain $[a, b]$ and a function $f : [a, b] \to \mathbb{R}$, the Riemann

integral $\int_a^b f(x)dx$ is introduced as:

$$\int_a^b f(x)dx \triangleq \lim_{|x^{[a,b]}|\to 0} \sum_{i=0}^{N} f(\bar{x}_i)(x_{i+1} - x_i), \tag{29}$$

where $x^{[a,b]}$ is a partition of the interval $[a,b]$, $x^{[a,b]} = (x_0 = a < x_1 < x_2 \ldots < x_N < x_{N+1} = b)$, notation $|x^{[a,b]}|$ is used for $\max_{i\in\{0,N\}}(x_{i+1} - x_i)$, and $\bar{x}_i \in [x_i, x_{i+1})$. Furthermore, the Riemann-Stieltjes integral of a function f (the integrand) with respect to another function g (the integrator), $\int_a^b f(x)dg(x)$, where both f and g are defined over [a,b], is

$$\int_a^b f(x)dg(x) \triangleq \lim_{|x^{[a,b]}|\to 0} \sum_{i=0}^{N} f(\bar{x}_i)\left(g(x_{i+1}) - g(x_i)\right). \tag{30}$$

Similarly, stochastic integration is introduced by clarifying the meaning of $\int_a^b X(s)ds$ and $\int_a^b X(s)dY(s)$, where $X(s)$ and $Y(s)$ are not deterministic functions, but stochastic processes. The same principle of sums over ever finer partitions remains at the core of the definition. However the analysis of conditions under which the convergence of this sums is consistent brings more details in the formulation.

First, the convergence concept itself needs to be clarified for sequences of random variables. The mean-square (ms) limit convergence is used,

$$X_N \overset{\text{ms}}{\to} X \;\equiv\; \lim_{N\to\infty} E(|X_N - X|^2) = 0,$$

where X_n is the sequence of random variables.

Furthermore, in the deterministic case, the convergence of the partition sums is independent of the choice of the points $\bar{x}_i$ within in the interval $[x_i, x_{i+1}]$. This is not the case for the stochastic integrals. In the Itô formulation, $\bar{x}_i = x_i$.

Definition (Itô stochastic integral). In broad strokes, the Itô stochastic integral is

$$\int_s^t X(u)dY(u) \overset{\Delta}{=} \text{ms}\lim \sum_{i=0}^{N} X(u_i)\big(Y(u_{i+1}) - Y(u_i)\big), \tag{31}$$

where $u^{[s,t]} = (s = u_0 < u_1 < \ldots < u_N < u_{N+1} = t)$ is the ever finer partition of the integration interval $[s,t]$.

Among the properties of the stochastic integrals, linearity and additivity over subintervals are maintained, similar to the case of the deterministic integral. Some

examples of stochastic integrals are:

$$\int_0^t dW(u) = \text{ms}\lim \sum_{i=0}^{N} \big(W(u_{i+1}) - W(u_i)\big) = W(t) - W(0) = W(t) \tag{32a}$$

$$\int_0^t dG(W(u)) = \text{ms}\lim \sum_{i=0}^{N} \big(G(W(u_{i+1})) - G(W(u_i))\big) = G(W(t)) - G(0) \tag{32b}$$

$$\int_0^t W(u)dW(u) = \text{ms}\lim \sum_{i=0}^{N} W(u_i)\big(W(u_{i+1}) - W(u_i)\big) = \frac{1}{2}W^2(t) - \frac{t}{2} \tag{32c}$$

$$\int_0^t (dW(u))^2 = \text{ms}\lim \sum_{i=0}^{N} \big(W(u_{i+1}) - W(u_i)\big)^2 = t \tag{32d}$$

$$\int_0^t (dW(u))^{>2} = \text{ms}\lim \sum_{i=0}^{N} \big(W(u_{i+1}) - W(u_i)\big)^{>2} = 0 \tag{32e}$$

$$\int_0^t du dW(u) = \text{ms}\lim \sum_{i=0}^{N} \big(u_{i+1} - u_i\big)\big(W(u_{i+1}) - W(u_i)\big) = 0. \tag{32f}$$

SDEs are a symbolic representation for the following expression composed of stochastic integrals,

$$\begin{aligned} dX(t) = a(X(t),t)dt + b(X(t),t)dY(t),\ X(0) \equiv \\ \equiv X(t) = X(0) + \int_0^t a(X(u),u)du + \int_0^t b(X(u),u)dY(u) \end{aligned} \tag{33}$$

The multi-dimensional form is straightforward,

$$\begin{aligned} dX(t) = A(X(t),t)dt + \bar{B}(X(t),t)d\bar{Y}(t),\ X(0) \equiv \\ \equiv X(t) = X(0) + \int_0^t A(X(u),u)du + \int_0^t \bar{B}(X(u),u)d\bar{Y}(u), \end{aligned} \tag{34}$$

where $X(t) \in \mathbb{R}^n$, and $\bar{W}(t) \in \mathbb{R}^m$.

Of interest for this work is only the case when the integrator random process $Y(t)$ is the Brownian motion, these leading to diffusion processes in the Markov sense discussed above. A physical interpretation of these SDEs is that they describe dynamics with a deterministic drift component $a(x,t)$ and a noisy component with variance $b^2(x,t)$. The noise (white noise) is used to describe the infinitesimal behavior of the Weiner process increment $dW(t)$, that is a random, irregular and rapidly fluctuating contribution. For the multidimensional case, the diffusion coefficient used in the differential Forward and Backward equations (26) and (27) is given by $B = \bar{B}\bar{B}^T$.

An important tool in SDE calculus is the chain rule of derivation. This allows to find solutions of complex equations building from simple results. The stochastic calculus chain rule, also known as Itô rule or lemma, is different from the deterministic case. Let a diffusion process $x(t)$ be described by the general SDE

$$dX(t) = a(X(t),t)dt + b(X(t),t)dW(t), \tag{35}$$

and $f(y,t)$ a differentiable function (twice in y, once in t). The differential expression of $G(t) = f(X(t),t)$, namely $dG(t)$, is then given by:

$$dG(t) = \left(\frac{\partial f}{\partial t}(X(t),t) + a(X(t),t)\frac{\partial f}{\partial y}(X(t),t) + \frac{1}{2}b^2(X(t),t)\frac{\partial^2 f}{\partial y^2}(X(t),t) \right) dt + \\ + b(X(t),t)\frac{\partial f}{\partial y}(X(t),t)dW(t) \ . \tag{36}$$

The multidimensional Itô lemma written for

$$dX(t) = A(X(t),t)dt + \bar{B}(X(t),t)d\bar{W}(t), \tag{37}$$

is

$$dG(t) = \left(\frac{\partial f}{\partial t}(X(t),t) + \sum_i A_i(X(t),t)\frac{\partial f}{\partial y_i}(X(t),t) + \right. \\ \left. + \frac{1}{2}\sum_i \sum_j B_{ij}(X(t),t)\frac{\partial^2 f}{\partial y_i \partial y_j}(X(t),t) \right) dt + \sum_i \sum_j \bar{B}_{ij}(X(t),t)\frac{\partial f}{\partial y_i}(X(t),t)dW_j(t), \tag{38}$$

where $B(X,t) = \bar{B}(X(t),t)\bar{B}^T(X(t),t)$.

5.4.3 Ornstein-Uhlenbeck Process

A one-dimensional Ornstein-Uhlenbeck process is described by the following SDE,

$$dX(t) = (-aX(t) + b)dt + \sigma dW(t), \ a > 0, \sigma > 0. \tag{39}$$

This is a one-dimensional SDE, with an affine drift term and a constant diffusion coefficient. It has the explicit solution

$$X(t) = \frac{b}{a} + \exp(-at)\left(X_0 - \frac{b}{a} \right) + \sigma \int_0^t \exp\big(-a(t-u) \big) dW(u) \ , \tag{40}$$

which can be checked using the Itô lemma (36). The explicit solution can be processed to characterize the mean and variance of the process over time as

$$\mathrm{E}\big[x(t)\big] = \frac{b}{a} + \exp(-at)(\mathrm{E}[X_0] - \frac{b}{a}), \tag{41}$$

same as for the ODE equivalent, and

$$\mathrm{Var}\big[X(t)\big] = \exp(-2at)\mathrm{Var}[X_0] + \sigma^2 \int_0^t \exp(-2a(t-u))du = \\ = \exp(-2at)(\mathrm{Var}[X_0] - \frac{\sigma^2}{2a}) + \frac{\sigma^2}{2a}. \tag{42}$$

Furthermore, the time correlation is characterized by

$$\mathrm{E}\big[X(t_1)X(t_2)\big] = \exp(-a(t_1+t_2))\left(\mathrm{Var}[X_0] - \frac{\sigma^2}{2a} \right) + \frac{\sigma^2}{2a}\exp(-a|t_1 - t_2|). \tag{43}$$

These expressions have the following stationary forms,

$$\lim_{t\to\infty} \mathrm{E}\big[X(t)\big] = \frac{b}{a}, \tag{44}$$

$$\lim_{t\to\infty} \mathrm{Var}\big[X(t)\big] = \frac{\sigma^2}{2a}, \tag{45}$$

$$\lim_{t_1,t_2\to\infty} \mathrm{E}\big[X(t_1)X(t_2)\big] = \frac{\sigma^2}{2a}\exp(-a|t_1 - t_2|)\,. \tag{46}$$

The above have been introduced as results of SDE calculus, but a parallel analysis can be carried out using the corresponding Forward differential (Fokker-Planck) equation describing the evolution in time of the probability density function,

$$\frac{\partial f(x,t,x_0,0)}{\partial t} = -\frac{\partial}{\partial x}\Big((-ax+b)f(x,t,x_0,t)\Big) + \frac{\sigma^2}{2}\frac{\partial^2 f(x,t,x_0,0)}{\partial x^2}, \tag{47}$$

and the tools of partial differential calculus.

TCL example. The temperature dynamics of a TCL are modeled as

$$dT(t) = \begin{cases} \big(-aT(t)+b_0\big)dt + \sigma dW(t), & \text{when the power cycle is off} \\ \big(-aT(t)+b_1\big)dt + \sigma dW(t), & \text{when the power cycle is on}\,, \end{cases} \tag{48}$$

where $a = \frac{\mathrm{UA}}{C}$, $b_0 = \frac{\mathrm{UA}}{C}T_{\mathrm{amb}}$, $b_1 = \frac{\mathrm{UA}}{C}T_{\mathrm{amb}} - \frac{\mathrm{COP}\cdot W}{C}$, with UA, C, T_{amb}, COP, and W standing in for physical coefficients, all positive. It can be seen that each branch of the dynamic is an Ornstein-Uhlenbeck process. However this is not enough to evaluate the overall solution or properties, since the stochastic dynamic is interconnected with the logic of the power cycle on/off actions.

5.5 Stochastic Hybrid System (SHS)

The TCL dynamical behavior has both hybrid and probabilistic characteristics. This work considers that both these traits are essential and need to be included in the mathematical representation. This leads to the investigation of the Stochastic Hybrid System (SHS), a framework that promises modeling, analysis and control tools. At the same time, the framework is both relatively new and has a broad scope, leading to results that are incomplete or restricted to particular cases and computational tools that are modest [19]. The notion of General Stochastic Hybrid System (GSHS) [5, 6] is introduced next.

Generalized Stochastic Hybrid Systems (GSHSs) allow for continuous dynamics described by SDEs, discrete dynamics with both probabilistic transitions characterized by rates (similar to the case of Markov chain transitions), forced transitions (similar to the invariant concept of hybrid systems), and probabilistic resets of the continuous-state as a result of the discrete transitions.

Definition (Generalized Stochastic Hybrid System (GSHS)). A GSHS has the following elements:

- a domain for the discrete-state or mode, $\mathcal{Q} = \{q_1, q_2, \ldots\}$;
- a set of (open) domains for the continuous-state, $\mathcal{X}^q \subseteq \mathbb{R}^n$, one for each discrete mode;
- the hybrid domain is composed of the union of the pairs of discrete-state and the associated continuous domain $\mathcal{H} = (q_1 \times \mathcal{X}^{q_1}) \cup (q_2 \times \mathcal{X}^{q_2}) \cup \ldots$;
- for each mode $q \in Q$, the evolution of the continuous state $X^q(t) \in \mathcal{X}^q$ is driven by an SDE

$$dX^q(t) = A^q(X^q(t))dt + \bar{B}^q(X^q(t))d\bar{W}(t),$$

  where $A^q : \mathcal{X}^q \to \mathbb{R}^n$ is the drift vector field, $\bar{W}(t)$ is an m dimensional Weiner process, and $\bar{B}^q : \mathcal{X}^q \to \mathbb{R}^{n\times m}$;
- spontaneous transitions, described by two elements:
  - state-dependent transition rate functions $\lambda_{ij} : \mathcal{X}^{q_i} \to \mathbb{R}_+$;
  - probability law (measure) for the continuous-state reset that takes place at the same time as the discrete transition, $R^{\lambda}_{ij} : \mathcal{X}^{q_i} \times \mathcal{B}(\mathcal{X}^{q_j}) \to [0, 1]$;

  The rate mechanism is similar to the time-inhomogeneous Markov chain dynamic. The holding time in discrete-state state i, given that the system entered this state at time t, the random variable $Y_i(t)$, is characterized by

$$\Pr\big[Y_i(t) > y\big] = \exp\left(-\int_t^{t+y} \sum_j \lambda_{ij}(X(\tau))d\tau\right),$$

  and the transition probabilities to a new mode j are also implicitly defined by the transition rates λ_{ij}. Let t_{ij} denote the transition time from mode i to j, then the reset law assigns probabilities for the jump/transition of the continuous-state, i.e.

$$\Pr[X^{q_j}(t_{ij}) \in \mathcal{A}] = R_{ij}(X^{q_i}(t_{ij}^-), \mathcal{A}),\ \mathcal{A} \subset \mathcal{X}^{q_j}$$

  In [5] for example, the GSHS uses the equivalent state-holding rate $\Lambda_i : \mathcal{X}^{q_i} \to \mathbb{R}_+$ and a more general probability law $R^{\Lambda}_i : \mathcal{X}^{q_i} \times \mathcal{H} \to [0, 1]$ describing both the discrete transition choice and the continuous-state reset at the same time.

  An observation here is that, while transitions from mode i leading back to i were not legal for Markov chains, these are allowed for GSHS because of the continuous-state reset.

- forced transitions triggered when the continuous state is about to leave the (invariant) domain,
  - the domain of discrete state i is the open set $\mathcal{X}^{q_i}$, and the trigger for the forced transition is reaching in the limit the boundary of the set, i.e. $X^q(t^-) \in \partial\mathcal{X}^{q_i}$;
  - discrete mode transition probabilities $\rho_i : \partial\mathcal{X}^{q_i} \times \mathcal{Q} \to [0,1]$ such that $\sum_{j\in\mathcal{Q}} \rho_i(X,j) = 1$, and a probabilistic reset law for the continuous state, $R_{ij}^f : \partial\mathcal{X}^{q_i} \times \mathcal{B}(\mathcal{X}^{q_j}) \to [0,1]$ or equivalently, a more general probability law describing the discrete-state and continuous state transition at the same time, $R_i^F : \partial\mathcal{X}^{q_i} \times \mathcal{H} \to [0,1]$;
- initial values for the hybrid state, (q_0, X_0) as a random variable.

TCL example. The GSHS accommodates all of the features of the TCL dynamic: noisy thermal dynamics, the thermostat logic and the logic of the minimum on/off times, and the random nature of the switching actuation. The hybrid state is composed of the on/off discrete-state q, the continuous state $X = (T, c)$ where T is the temperature state and c is state holding timer state.

The relevant GSHS elements capturing the TCL dynamic behavior with the Switching-Rate actuation are:

- discrete-state domain $\mathcal{Q} = \{q_0 = \text{OFF}, q_1 = \text{ON}\}$;
- continuous-state domains, $\mathcal{X}^{OFF} = (T_{\text{minmin}}, T_{\text{max}}) \times [0,\infty) \in \mathbb{R}^2$, and $\mathcal{X}^{ON} = (T_{\text{min}}, T_{\text{maxmax}}) \times [0,\infty) \in \mathbb{R}^2$, corresponding to the temperature and timer states;
- spontaneous transitions elements are:

$$\lambda_{\text{OFF,ON}}\big(X = (T,c)\big) = \begin{cases} \lambda_1, \ T \in [T_{\text{min}} + \Delta T_1, T_{\text{max}}) \wedge c > M_{\text{OFF}} \\ 0, \ \text{otherwise} \end{cases} \tag{49a}$$

$$\lambda_{\text{ON,OFF}}\big(X = (T,c)\big) = \begin{cases} \lambda_0, \ T \in (T_{\text{min}}, T_{\text{max}} - \Delta T_2) \wedge c > M_{\text{ON}} \\ 0, \ \text{otherwise} \end{cases} \tag{49b}$$

$$R^{\lambda}_{q_i,q_{1-i}}\big(X = (T,c), \mathcal{A}\big) = \begin{cases} 1, \ \{T,0\} \in \mathcal{A}; \\ 0, \ \text{otherwise} \end{cases} \tag{49c}$$

The transition rates are piecewise constant on the continuous state-domain, and the state reset is deterministic, the temperature is maintained and the state holding timer state is reset to zero.

The Switching-Rate demand response concept is based on the fact that the transition rate parameters λ_0 and λ_1 are external inputs. Although the GSHS definition does not explicitly include external inputs, this is a reasonable concept addressed in the literature for other subclasses of SHSs such as piecewise deterministic Markov processes and switching-diffusions.

- forced transitions occur at the temperature boundaries of the domains, and have deterministic characteristics

$$\rho_{\text{OFF}}\big((T_{\max}, c),\ \text{ON}\big) = 1,$$

$$R^f_{\text{OFF,ON}}\big((T_{\max}, c), \mathcal{A}\big) = \begin{cases} 1, (T_{\max}, 0) \in \mathcal{A} \\ 0, \text{ otherwise} \end{cases} \tag{50a}$$

$$\rho_{\text{OFF}}\big((T_{\text{minmin}}, c),\ \text{OFF}\big) = 1,$$

$$R^f_{\text{OFF,ON}}\big((T_{\text{minmin}}, c), \mathcal{A}\big) = \begin{cases} 1, (T_{\text{minmin}}, c) \in \mathcal{A} \\ 0, \text{ otherwise} \end{cases} \tag{50b}$$

$$\rho_{\text{ON}}\big((T_{\min}, c),\ \text{OFF}\big) = 1,$$

$$R^f_{\text{ON,OFF}}\big((T_{\min}, c), \mathcal{A}\big) = \begin{cases} 1, (T_{\min}, 0) \in \mathcal{A} \\ 0, \text{ otherwise} \end{cases} \tag{50c}$$

$$\rho_{\text{ON}}\big((T_{\text{maxmax},c)},\ \text{ON}\big) = 1,$$

$$R^f_{\text{ON,ON}}\big((T_{\text{maxmax}}, c), \mathcal{A}\big) = \begin{cases} 1, (T_{\text{maxmax}}, c) \in \mathcal{A} \\ 0, \text{ otherwise} \end{cases} \tag{50d}$$

The above description includes the thermostat rules, the reset of the state holding times, and a barrier or reflection mechanism at the temperature points T_{minmin} and T_{maxmax}. Referring to the latter, an alternative is to define one-sided infinite domains for the temperature state, $(-\infty, T_{\max})$, and $(T_{\min}, +\infty)$.

A stochastic process $\{Z(t) = (q(t), X(t)\}$ that evolves according to the rules of GSHS dynamic is a concatenation of diffusion processes, and is a Markov process. Similar to the other two classes of Markov processes presented above, Markov chains and SDEs, GSHSs should allow for a form of Forward and Backward differential forms. This is addressed in [6], and the Forward form in particular in [3].

TCL example. This work give an explicit form for the Forward differential form of the TCL model with the Switching-Rate as a PDE system with boundary conditions, see Paper C. Based on this formulation, analysis and control results are obtained.

It is noted that the work of [1](Ch.1.3) argues for the elimination of the forced transitions. This is done by introducing an approximation procedure using on additional state-dependent transition rates in increasing value as the state approaches the triggering boundary. In this way, the deterministic rules are replaced by an approximately equivalent stochastic mechanism, and it is argued that this leads to a model

simplification. The approach was not analyzed in the current work.

6 Computational methods

6.1 Numerical Simulation of SHS

Simulations are an important tool in the process of understanding a particular system and for validating design changes and control strategies in a fast and economic way. In the case of the TCL population, the real system as such does not yet exist: A communication infrastructure is not set up and local controllers with necessary functionality are not present in large-scale for the TCLs currently connected to the grid. Even if this was the case, it would be unwise to, for example, test the principle of the Switching-Rate actuation on live conditions before it was validated in simulation. This work uses a simulation of a TCL population that is composed a large number of independent individual TCLs simulations, each build using a SHS model. This is considered as a virtual replacement for a physical TCL population.

Simulation of SHS is not always straightforward, as some delicate points can emerge from interplay of the continuous dynamics and discrete dynamics, such as the issue of detecting boundary crossings.

6.1.1 Numerical Methods for SDE

Numerical methods for approximating the solution of SDE are based on stochastic Taylor expansions [16, 21]. In general lines, this parallels the approach used for approximating the solution of an Ordinary Differential Equation (ODE). An informal overview follows next.

For a deterministic dynamic characterized by

$$\frac{dx(t)}{dt} = f(x,t),\ x(t_0) = x_0, \tag{51}$$

numerical methods used to calculate $x(t_1)$ are based on the direct relation,

$$x(t_1) = x(t_0) + \int_{t_0}^{t_1} f(x(t),t)dt \tag{52}$$

and a Taylor approximation for $g(t) = f(x(t),t)$,

$$\begin{aligned} g(t) &= g(t_0) + \frac{dg(t)}{dt}\Big|_{t=t_0}(t-t_0) + \ldots + \frac{1}{k!}\frac{d^k g(t)}{dt^k}\Big|_{t=t_0}(t-t_0)^k + \ldots \\ &= g(t_0) + \left(\frac{\partial f(x,t)}{\partial t} + \frac{\partial f(x,t)}{\partial x}\frac{dx(t)}{dt}\right)\Big|_{t=t_0}(t-t_0) + \\ &+ \frac{1}{2}\left(\frac{\partial^2 f(x,t)}{\partial t^2} + 2\frac{\partial^2 f(x,t)}{\partial t \partial x}\frac{dx}{dt} + \frac{\partial f^2(x,t)}{\partial x^2}\left(\frac{dx}{dt}\right)^2 + \frac{\partial f(x,t)}{\partial x}\frac{d^2x}{dt^2}\right)\Big|_{t=t_0}(t-t_0)^2 + \ldots. \end{aligned} \tag{53}$$

Approximation schemes with increasing order of accuracy can be obtained by keeping more terms of the Taylor series in the final expression. The most simple choice, $g(t) \approx$

$g(t_0)$ leads to the Euler method,

$$\hat{x}(t_1) = x(t_0) + f(x(t_0), t_0)\Delta t_1, \tag{54a}$$

$$\hat{x}(t_k) = \hat{x}(t_{k-1}) + f(\hat{x}(t_{k-1}), t_{k-1})\Delta t_k. \tag{54b}$$

Mentioning the order of accuracy requires clarification. In the Euler truncation case, the local order of accuracy is two, meaning that the local error $|x(t_1) - \hat{x}(t_1)|$ is proportional to $(\Delta t)^2$. The repeated recursion in constructing the solution $x(t_k)$ however leads to a global order of accuracy one, meaning that global error $|x(t_k) - \hat{x}(t_k)|$ is proportional to Δt. There are two (independent) ways to obtain better numerical approximations/solutions: decrease the time step Δt, and choose a method with an increased order of accuracy.

For a stochastic dynamic characterized by

$$dX(t) = a(X,t)dt + b(X,t)dW(t),\ X(t_0) = x_0, \tag{55}$$

numerical methods used to calculate $X(t_1)$ are based on the direct relation,

$$X(t_1) = X(t_0) + \int_{t_0}^{t_1} a(X(t),t)dt + \int_{t_0}^{t_1} b(X(t),t)dW(t) \tag{56}$$

and stochastic Taylor approximations for $U(t) = a(X(t),t)$ and $V(t) = b(X(t),t)$. The trajectory of $X(t)$ is continuous, but not differentiable, therefore a differential form of the Taylor series cannot be used to expand $U(t)$ and $V(t)$. However, the Itô chain rule of derivation (36) can be used on the terms $a(y,t)$ and $b(y,t)$,

$$\begin{aligned} dU(t) = da(X(t),t) &= \left(\frac{\partial a}{\partial t} + a\frac{\partial a}{\partial y} + \frac{1}{2}b^2\frac{\partial^2 a}{\partial y^2}\right)(X(t),t)dt + \left(b\frac{\partial a}{\partial y}\right)(X(t),t)dW(t) \equiv \\ \equiv \int_{t_0}^{t} da(X(t),t) &= a(X(t),t) - a(X(t_0),t_0) = \\ = \int_{t_0}^{t}\left(\frac{\partial a}{\partial u} + a\frac{\partial a}{\partial y} + \frac{1}{2}b^2\frac{\partial^2 a}{\partial y^2}\right)(X(u),u)du &+ \int_{t_0}^{t}\left(b\frac{\partial a}{\partial y}\right)(X(u),u)dW(u), \end{aligned} \tag{57}$$

$$\begin{aligned} b(X(t),t) - b(X(t_0),t_0) &= \\ = \int_{t_0}^{t}\left(\frac{\partial b}{\partial u} + a\frac{\partial b}{\partial y} + \frac{1}{2}b^2\frac{\partial^2 b}{\partial y^2}\right)(X(u),u)du &+ \int_{t_0}^{t}\left(b\frac{\partial b}{\partial y}\right)(X(u),u)dW(u). \end{aligned} \tag{58}$$

For the expansion of $X(t_1)$, this leads to

$$\begin{aligned} X(t_1) = X(t_0) &+ \int_{t_0}^{t_1}\left[a(X(t_0),t_0) + \int_{t_0}^{t}\left(\frac{\partial a}{\partial u} + a\frac{\partial a}{\partial y} + \frac{1}{2}b^2\frac{\partial^2 a}{\partial y^2}\right)(X(u),u)du + \int_{t_0}^{t}\left(b\frac{\partial a}{\partial y}\right)(X(u),u)dW(u)\right]dt + \\ &+ \int_{t_0}^{t_1}\left[b(X(t_0),t_0) + \int_{t_0}^{t}\left(\frac{\partial b}{\partial u} + a\frac{\partial b}{\partial y} + \frac{1}{2}b^2\frac{\partial^2 b}{\partial y^2}\right)(X(u),u)du + \int_{t_0}^{t}\left(b\frac{\partial b}{\partial y}\right)(X(u),u)dW(u)\right]dW(t) = \\ &= X(t_0) + a(X(t_0),t_0)\int_{t_0}^{t_1} dt + b(X(t_0),t_0)\int_{t_0}^{t_1} dW(t) + \\ &+ \int_{t_0}^{t_1}\int_{t_0}^{t}\left(\frac{\partial a}{\partial u} + a\frac{\partial a}{\partial y} + \frac{1}{2}b^2\frac{\partial^2 a}{\partial y^2}\right)(X(u),u)dudt + \int_{t_0}^{t_1}\int_{t_0}^{t}\left(b\frac{\partial a}{\partial y}\right)(X(u),u)dW(u)dt + \\ &+ \int_{t_0}^{t_1}\int_{t_0}^{t}\left(\frac{\partial b}{\partial u} + a\frac{\partial b}{\partial y} + \frac{1}{2}b^2\frac{\partial^2 b}{\partial y^2}\right)(X(u),u)dudW(t) + \int_{t_0}^{t_1}\int_{t_0}^{t}\left(b\frac{\partial b}{\partial y}\right)(X(u),u)dW(u)dW(t). \end{aligned} \tag{59}$$

A first computation approximation for $X(t_1)$ is thus

$$\hat{X}(t_1) = X(t_0) + a(X(t_0), t_0)\Delta t_1 + b(X(t_0), t_0)\Delta W(t_1) \tag{60a}$$
$$\hat{X}(t_k) = \hat{X}(t_{k-1}) + a(\hat{X}(t_{k-1}), t_{k-1})\Delta t_k + b(\hat{X}(t_{k-1}), t_{k-1})\Delta W(t_k), \tag{60b}$$

known as the Euler-Maruyama. Advanced computations use further expansions for all or just some of the terms in the double integrals above. For example, expanding only the $dW(u)dW(t)$ term leads to the following computational approximation

$$\begin{aligned}\hat{X}(t_1) = X(t_0) &+ a(X(t_0), t_0)\Delta t_1 + b(X(t_0), t_0)\Delta W(t_1) + \\ &+ \frac{1}{2} b(X(t_0), t_0)\frac{\partial b}{\partial y}(X(t_0), t_0)\left(\Delta W^2(t_1) - \Delta t_1\right)\end{aligned} \tag{61a}$$

$$\begin{aligned}\hat{X}(t_k) = \hat{X}(t_{k-1}) &+ a(X(t_{k-1}), t_{k-1})\Delta t_k + b(X(t_{k-1}), t_{k-1})\Delta W(t_k) + \\ &+ \frac{1}{2} b(X(t_{k-1}), t_{k-1})\frac{\partial b}{\partial y}(X(t_{k-1}), t_{k-1})\left(\Delta W^2(t_k) - \Delta t_k\right) ,\end{aligned} \tag{61b}$$

known as the Milstein method.

To compare and decide on appropriate truncations, it is important to define the (global) order of accuracy, similar to the deterministic case. The stochastic context leads to two definitions. The strong order of accuracy γ is defined with respect to the exact trajectory of the random process, such that the error quantity $\mathrm{E}\left[|X(t_k) - \hat{X}(t_k)|\right]$ is proportional with $(\Delta t)^\gamma$. The weak order of accuracy β is defined by a proxy, the expected value of a function of the random process, such that the error $\left|\mathrm{E}\left[g(X(t_k))\right] - \mathrm{E}\left[g(X(t_k))\right]\right|$ is proportional with $(\Delta t)^\beta$, for any function g of an appropiate class. Given a particular numerical approximation scheme, the strong order is always small or equal to the weak order, $\gamma \leq \beta$.

It is well known that the Euler-Maruyama scheme has a strong order $\gamma = \frac{1}{2}$ and a weak order $\beta = 1$, while for the Milstein method $\gamma = \beta = 1$. Depending on the objectives of the simulation (focus on individual trajectory simulation or focus on statistical properties), either the strong order or the weak order is a more relevant measure of accuracy. The choice of terms for expansion and the necessary truncation terms in the Stochastic Taylor relation can be customized to yield desired strong/weak accuracies. Similar to the derministic case, there are two (independent) ways to obtain better numerical approximations/solutions: decrease the time step Δt, and choose a method with an increased order of accuracy.

TCL example. For the Ornstein-Uhlenbeck process as discussed in Sec. 5.4.3, the Euler-Maruyama and the Milstein method are equivalent because the diffusion term is a constant, $b(X(t), t) = \sigma$ and the term $\frac{\partial b}{\partial y}$ is thus zero. The thermal dynamics of the TCL can be simulated using this method leading to an accuracy $\gamma = \beta = 1$. Alternatively, the explicit solution for this dynamic was given by (40), and this can also be used for simulation. An observation is that the objective of simulating a TCLs population is on generating individual trajectories (scenario simulations) for each TCL (each with each own set of parameters in general).

6.1.2 Simulation of Rate-based Events

For continuous-time Markov chains, the simulation consists of an event-based scheduling scheme [7](Ch.10). Given an initial state, random trigger times are generated for all possible events. The events are then sorted by the increasing ordered of their times, and the first event is executed. This causes the system to change state. In the new state, all events that are no longer feasible are canceled from the ordered list, and new events that become available are added. The event with the smallest time is again executed, leading to a new state.

Generating random trigger times is one of the main important tasks in this process. For constant transition rates, the waiting time until a new event is exponentially distributed with the given rate, leading to a simple procedure for generating a trigger time using the inverse transform sampling method (see e.g [9]),

$$t_{e_i} = t + \left(-\frac{1}{\lambda_i} \ln(1-U) \right) \equiv t + \left(-\frac{1}{\lambda_i} \ln(U) \right), \tag{62}$$

where U is a uniform random variable with domain $[0, 1]$.

TCL example. The Switching-Rate demand response mechanism introduces Markov-chain-like stochastic jumps between the ON and OFF modes. Transition rates are externally controlled, but have a piecewise constant profile in time. This is in part a limitation of the broadcast channel, but can also be seen as an inherent part of the design. The transition rates are in addition also piecewise constant with respect to the temperature of the TCLs, see (49). The software/logic implementation of switching mechanism is the main part of the TCL local controller, and can be based on the generation of exponentially distributed waiting times with constant rates, as discussed above.

6.1.3 Simulation of SHS

The combination of continuous and discrete dynamics leads to two new simulation issues: arrival of non-stochastic events when the continuous state reaches a domain boundary, and transition rates with varying characteristics depending on the continuous state.

Detection of boundary crossings and SDE simulation near the boundaries can increase the error level in the simulation. This is because, near the boundaries, using a relatively coarse time step Δt can mask a crossing: the start state and the end state are within the domain, but simulations with a finer step would have crossed the boundary with a high probability. This aspect can be accounted for in different ways, such as adapting to smaller time steps next to the boundary (reduce the chance of missed detections) or using an auxiliary variable to explicitly track the boundary hitting probability, see for example [20, 22] and reference within.

If transition rates are varying with the continuous-state, the mechanism for triggering stochastic jumps needs to be adapted. Only constant rates were addressed in the computational discussion for Markov chains in the above Sec. 6.1.2, but there exist a number of techniques available for generating events with time-inhomogeneous

rates, such as the thinning method [9, 17]. This further requires an adaptation in the SDE numerical integration scheme, to be able to evaluate the continuous-state at the candidate times given by the thinning scheme (meaning not just at the equally spaced time points t_k).

TCL example. Simulation of the individual TCL dynamic behavior requires only boundary crossing detection, both for the thermostat switching rule and for the transition rates mechanism. For mode ON, crossings to detect are $T_{\min}$, $T_{\max} - \Delta T_2$, $T_{\max\max}$, and for mode OFF $T_{\max}$, $T_{\min} + \Delta T_1$, $T_{\min\min}$. It can also be said that the crossings of the reflective boundaries $T_{\max\max}$ and $T_{\min\min}$ are highly unlikely if the diffusion coefficient is low or if these boundaries are reasonably far away placed from the thermostat limit values. The timer state $c(t)$ has deterministic dynamics, meaning that its crossings are trivial to address.

TCL example. Alternatively, a more relaxed simulation strategy can be adopted for the TCLs scenario. Provided that the time-step of the simulation is not too coarse, the boundary crossing detection can be handled with the naive approach of checking after each SDE integration step. This relaxed approach can be easily justified if we consider that the TCL discrete dynamics are not time-synchronized with the thermal dynamics, but are rather features build into a computer controller and relying on a (low grade) sensor input. Thus, the boundary detection cannot be expected to be sharp in the real system itself. Furthermore, the rate switching can also be handled with a simplified approach that does not require an event scheduling scheme. For a relatively small time step t_c, the infinitesimal description of the transition rates (20) can be used as a direct approximation in deciding a transition,

$$\Pr\big[\text{TurnOFF} \mid m = \text{ON and } T \in [T_{\min}, T_{\max} - \Delta T_2)\big] = \min(\lambda_0 t_c, 1)$$
$$\Pr\big[\text{TurnON} \mid m = \text{OFF and } T \in (T_{\min} + \Delta T_1, T_{\max}]\big] = \min(\lambda_1 t_c, 1),$$

where λ_0 and λ_1 are the most recent rates received by the unit. This is reasonable in both simulation and in the implementation of the TCL local controller. Performing random number generation operations at a relatively fast time step might be more simple than implementing an event scheduler scheme in the TCL control software. This is was the chosen method in the simulations carried out in this work.

6.2 PDE Numerical Integration

Finding exact, analytical solutions for partial differential equations is, in general, an even more difficult task than for ODE (and SDEs). And similar to the ODE and SDE cases, in practice and engineering, it is very useful to use numerical algorithms and discretization to obtain approximate solutions.

Numerical methods for ODEs perform a discretization of the coordinate/variable of the unknown function. For Partial Differential Equations (PDEs), there are multiple

coordinates/variables that need to be discretized. On top of the discretization mesh (or grid), approximate relations are used to transform differential equations into algebraic forms. Given an initial value, the algebraic equations (either in a recursive or in a closed system form) can be solved to obtain approximate solution values at the points of the discretization partition.

There are three main types of discretization and numerical approximation methods for PDEs:

- Finite-Difference methods
- Finite-Volume methods, and
- Finite-Element methods.

An useful introductory reference is, for example, [10].

> *TCL example.* The model of a TCL population used in this work consists of a PDE system with coupling boundary conditions and terms. Each PDE is based on the Forward differential equation associated with an Ornstein-Uhlenbeck process (47). For this type of model, the Finite-Difference approach is the numerical tool of choice reported in the TCL literature. In this work, the Finite-Volume approach is used, and it is argued that it presents a number of advantages. The main argument is that Forward differential equations are intrinsically conservation laws, and the Finite-Volume approach is specifically designed to preserve the conservation balance. This is discussed in Paper D.

References

[1] Alessandro Abate. *Probabilistic reachability for stochastic hybrid systems: Theory, computations, and applications*. ProQuest, 2007.

[2] Rajeev Alur and David L Dill. A theory of timed automata. *Theoretical computer science*, 126(2):183–235, 1994.

[3] Julien Bect. A unifying formulation of the fokker–planck–kolmogorov equation for general stochastic hybrid systems. *Nonlinear Analysis: Hybrid Systems*, 4(2):357–370, 2010.

[4] Michael S Branicky, Vivek S Borkar, and Sanjoy K Mitter. A unified framework for hybrid control: Model and optimal control theory. *Automatic Control, IEEE Transactions on*, 43(1):31–45, 1998.

[5] Manuela L Bujorianu and John Lygeros. General stochastic hybrid systems: Modelling and optimal control. In *Decision and Control, 2004. CDC. 43rd IEEE Conference on*, volume 2, pages 1872–1877. IEEE, 2004.

[6] Manuela L Bujorianu and John Lygeros. Toward a general theory of stochastic hybrid systems. In *Stochastic Hybrid Systems*, pages 3–30. Springer, 2006.

[7] Christos G Cassandras and Stephane Lafortune. *Introduction to discrete event systems*. Springer Science & Business Media, 2008.

[8] B De Schutter, WPMH Heemels, J Lunze, Christophe Prieur, et al. Survey of modeling, analysis, and control of hybrid systems. *Handbook of Hybrid Systems Control–Theory, Tools, Applications*, pages 31–55, 2009.

[9] Luc Devroye. *Non-Uniform Random Variate Generation*. Springer-Verlag, 1986.

[10] Joel H Ferziger and Milovan Perić. *Computational methods for fluid dynamics*, volume 3. Springer Berlin, 2002.

[11] Crispin W Gardiner. *Handbook of stochastic methods: for Physics, Chemistry and the Natural Sciences*. Springer Berlin, 1985.

[12] Rafal Goebel, Ricardo G Sanfelice, and Andrew R Teel. *Hybrid Dynamical Systems: modeling, stability, and robustness*. Princeton University Press, 2012.

[13] Floyd B Hanson. *Applied stochastic processes and control for Jump-diffusions: modeling, analysis, and computation*, volume 13. Siam, 2007.

[14] Thomas A Henzinger, Peter W Kopke, Anuj Puri, and Pravin Varaiya. What's decidable about hybrid automata? In *Proceedings of the twenty-seventh annual ACM symposium on Theory of computing*, pages 373–382. ACM, 1995.

[15] Soren Johansen. Product integrals and markov processes. *CWI Newsletter*, 12:3–13, 1986.

[16] Peter E Kloeden and Eckhard Platen. *Numerical solution of stochastic differential equations*, volume 23. Springer Science & Business Media, 1992.

[17] Peter A Lewis and Gerald S Shedler. Simulation of nonhomogeneous poisson processes by thinning. *Naval Research Logistics Quarterly*, 26(3):403–413, 1979.

[18] John Lygeros, Karl Henrik Johansson, Slobodan N Simic, Jun Zhang, and Shankar S Sastry. Dynamical properties of hybrid automata. *Automatic Control, IEEE Transactions on*, 48(1):2–17, 2003.

[19] John Lygeros and Maria Prandini. Stochastic hybrid systems: a powerful framework for complex, large scale applications. *European Journal of Control*, 16(6):583–594, 2010.

[20] EAJF Peters and Th MAOM Barenbrug. Efficient brownian dynamics simulation of particles near walls. i. reflecting and absorbing walls. *Physical Review E*, 66(5):056701, 2002.

[21] Eckhard Platen and Nicola Bruti-Liberati. *Numerical solution of stochastic differential equations with jumps in finance*, volume 64. Springer Science & Business Media, 2010.

[22] Derek Riley, Xenofon Koutsoukos, and Kasandra Riley. Modeling and simulation of biochemical processes using stochastic hybrid systems: The sugar cataract development process. In *Hybrid Systems: Computation and Control*, pages 429–442. Springer, 2008.

Summary of Contributions

This chapter summarizes the main contributions to the problem of enabling large-scale demand response of Themostatically Controlled Loads (TCLs).

7 Switching-Fraction Actuation

Paper A argues for a distributed approach to the problem of Demand Response (DR) from TCLs while maintaining the idea of a *direct* control, and in this way outlines the Automated Direct Demand Response via Broadcast (ADDRB) principles. The approach is realized by introducing the Switching-Fraction randomized actuation strategy, supported by a preliminary simulation. The Switching-Fraction actuation can be seen to be closely related to, and a variation of, the "toggle control" as introduced in [2], but with some clear advantages related to the practical implementation. In particular, the footprint of the broadcast signal is much lower, and the resolution of the temperature sensor does not need to be high.

The Switching-Fraction actuation, although not so named, is at the same time introduced, modeled and elaborated by another group of authors in the works [1, 4]. Paper B performs a parallel modeling task, introduces the feature of temperature-safe zones, and brings a control result based on numerical optimization. An standout feature is that both switch-on and switch-off actions are used at the same time. This increases (although only slightly) the controllability of the system and has the advantage of making the non-convex optimization more numerically tractable. A key conclusion is that the actuation offers partial control robustness to modeling inaccuracies such as population heterogeneity.

A schematic overview of Switching-Fraction actuation is given in Fig. 13. Each TCL responds as soon as the command signal $u = [p, \bar{p}] \in [0, 1]^2$ is received by performing a Bernoulli trial. The success rate of the trial is chosen between the values $\{0, p, \bar{p}\}$ based on the current power mode m, temperature T, and mode counter/timer c. The schematic implies a temperature-safe zone $(T_{\min}, T_{\max} - \Delta T_1]$ for mode on, and a temperature-safe zone $[T_{\min} + \Delta T_0, T_{\max})$ for mode off. Temperature-safe zones are discussed also in Papers B and D. If the trail is successful, a mode switch action takes place. Otherwise, the unit does not perform any action. The thermostat mechanism itself is not part of the actuation, it is a part of the free/autonomous dynamics.

The modeling of the Switching-Fraction actuation at the population level is based on the probabilistic method developed in [3] for TCLs without actuation as a Partial Differential Equation (PDE) system. The PDE system is first discretized in its spatial

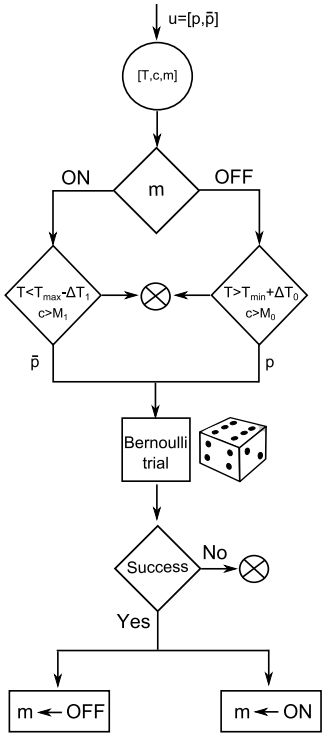

Fig. 13: Overview of the Switching-Rate randomized actuation.

coordinates, and then in the time coordinate. The result is a medium/high (but finite) dimensional linear system in discrete time. Because of its discrete-time nature, the Switching-Fraction can be naturally introduced at this point. The Switching-Fraction contributes with a bilinear input term to the discrete-time dynamic of the TCL population.

8 Switching-Rate Actuation

Paper C introduces and models the Switching-Rate actuation. This extension is strongly motivated by the existence of a short but very high power-peak occurring at the beginning of the on-cycle in the TCL operation, see App. Z and Fig. D.1. The peak is related to the operation of the single phase induction motor that powers the compressor, namely the secondary or start-up winding mechanism. The power peak makes the discrete-time and synchronized population response to the Switching-Fraction signal undesirable. The Switching-Rate mechanism distributes the response of the TCL population in time, in a way that remains highly controllable. Furthermore, the overall response is more smooth than in the case of the Switching-Fraction actuation.

Under the Swiching-Rate actuation, the unit receives a command $u = [\lambda, \bar{\lambda}] \in \mathbb{R}^2_+$, consisting of rates instead of probabilities. The main idea is that the TCL does not respond with a switching action as soon as the command is received, but instead

performs a random sampling to select an appropriate waiting time, see Fig. 14. The waiting time can be very long, such that the switch action may become invalid (e.g. the unit already changed modes due to the thermostat), leading to a situation similar to a failed Bernoulli trial in the case of the Switching-Fraction. As discussed in Sec. 6.1.3, a complete algorithm for implementing the Switching-Rate actuation must include further elements, such as detection of temperature and timer crossings from the safe-zones to the "unsafe" zones, or, equivalently, a fast sample time.

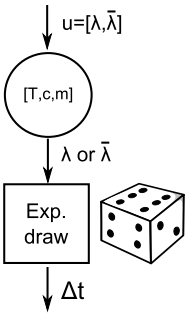

Fig. 14: Random sampling of the waiting time for the Switching-Rate actuation.

The Switching-Rate actuation has a continuous-time characteristic. Modeling it requires an extension of the original PDE system from [3]. This PDE system is the Forward differential equation of the stochastic hybrid TCL model without actuation, and is composed of individual Fokker-Planck equations with coupling boundary conditions. Because of the design the Switching-Rate, the extension proves to be relatively straightforward, consisting in the addition of bilinear input terms in the individual Fokker-Planck equations. The supplementary features of temperature-safe zones and minimum on/off time are also clarified. The new PDE model can be spatially discretized to give a medium/high (but finite) dimensional system with linear autonomous dynamics and bilinear input terms. This serves as the control model.

Paper D puts the Switching-Actuation to use in a control loop design. Two control algorithms are presented, and a state observation scheme. Using numerical simulations, it is argued that the switching actuation is an efficient way of enabling the power flexibility, as coherent aggregated power responses are obtained from the TCL population. Furthermore, a case is made to favor Finite-Volume methods as numerical algorithms for the spatial discretization of the PDE system, due to its conservation from. Special care must still be taken under the spatial discretization to preserve other structural properties when needed, such as the transition-rate matrix form for the continuous-time linear autonomous dynamics.

References

[1] Chin-Yao Chang, Wei Zhang, Jianming Lian, and Karanjit Kalsi. Modeling and control of aggregated air conditioning loads under realistic conditions. In *Innovative Smart Grid Technologies (ISGT), 2013 IEEE PES*, pages 1–6. IEEE, 2013.

[2] Stephan Koch, Johanna L Mathieu, and Duncan S Callaway. Modeling and control of aggregated heterogeneous thermostatically controlled loads for ancillary services. In *Proc. PSCC*, pages 1–7, 2011.

[3] Roland Malhame and Chee-Yee Chong. Electric load model synthesis by diffusion approximation of a high-order hybrid-state stochastic system. *Automatic Control, IEEE Transactions on*, 30(9):854–860, 1985.

[4] Wei Zhang, Jianming Lian, Chin-Yao Chang, and K. Kalsi. Aggregated modeling and control of air conditioning loads for demand response. *Power Systems, IEEE Transactions on*, 28(4):4655–4664, Nov 2013.

Closing Remarks and Perspectives

This chapter concludes on the work, and lists some of the remaining open questions.

In recent years, appliance producers have been embedding possibilities for communication and computation into their products for user functionality. It is believed that embedding possibilities for communication and computation for grid functionality, either as a free initiative incentivized by a new electricity markets or nudged by upcoming grid regulations, is a logical next step.

The aim of this research has been to look at control methods for enabling large-scale demand response from small appliances and devices, and in particular thermostatic loads. Because of the truly large-scale and distributed aspect, the small capacity of - and the small expected monetary gains rewarding power flexibility for - the individual devices, and because of security and privacy concerns, it is believed that realistic solutions must be content in the near future with only a fraction of the communication and computation capabilities promised by the big Smart Grid picture. As a result, the parsimonious Automated Direct Demand Response via Broadcast (ADDRB) principles have been put forward in Sec. 2.2: broadcast command, local decision making, and anonymous, infrequent centralization of local information.

The work then focused on developing a specific actuation, namely the Switching Actuation, and associated modeling and algorithmic control tools. The Switching Actuation is a randomized form of direct control from a central entity that leaves part of the decision making under the control of the individual units to allow for adaptation to local conditions. At the same time, the control logic of the individual units is predesigned, and known at the central level. Through modeling and simulation, it was shown that the approach is viable, and that the power flexibility of a Themostatically Controlled Load (TCL) population can indeed be controlled. Furthermore, the switching actuation is in principle suitable for the design of large-scale demand response of other types of on/off powered appliances, such as (electrical vehicle) batteries, dishwashers, washing machines, dryers.

A natural direction for future work is to instrument and setup a small fleet of refrigerators, to analyze the main sources of disturbance that could occur at the aggregate level, and, more generally, gather field experience on the population system.

Furthermore, a number of questions about the TCL modeling and control problem have been collected through the project work, but have not so far been addressed.

- The switching actuations have been successfully used to control the power *output* of a TCL population. In doing so, the overall system *state* is moved from

equilibrium. Although the switching actuation can be used to keep the aggregated power *output* close to the baseline value for an indefinite amount of time, stopping the actuation when the system *state* is away from equilibrium will lead to an oscillatory free response behavior. The TCL population naturally returns to equilibrium, but it is of clear interest to investigate methods for minimizing the transient period and the amplitudes. It is an open question how this can be best achieved using the switching actuation. It is also possible to consider a separate desynchronization/stabilization protocol, e.g. [1].

- The population model is based on a homogeneity assumption. As discussed in Paper B, this is not a theoretical limitation, as the state-space can be extended to account for parameters as states with dynamic zero. However, it leads to a computational limitation. The spatial discretization in a multi-dimensional space leads to exponentially larger systems. The homogeneity assumption is reasonable for cases where there is a very small level of parameter heterogeneity between the units in the population. With the increase in the heterogeneity level, relatively fast aggregate measurements and the robustness properties of the actuation and of a closed control loop start to play an important role. Instead of relying on a relatively fast control loop, it would be desirable to rely on a partial or approximate model for the heterogeneity effects. High levels of heterogeneity require an explicit strategy, such as the clustering approach in [7], which is essentially equivalent to a coarse spatial discretization of the parameter space.

  As such, the topic of partial or approximate models for heterogeneous TCL populations is one of interest for capturing more accurately the dynamics of subpopulation clusters with moderate levels of heterogeneity. Two techniques are present in literature. In [6], heterogeneity is approximated by an increase in the diffusion coefficient of the thermal dynamics. This accounts for a higher dampening factor in the power output oscillations of the free response evolution. However, this only improves the *output* modeling, and does not specifically improve the *state* modeling. The control algorithms proposed in this work require state information to evaluate the amount of non-responsive units (units in the "nonsafe" temperature and timer ranges) and to send out accurate switching commands. In the original work [5], the authors propose a perturbation-based analysis for the population of dynamical systems. Applied to linear systems, this approach was found to work well only for low dimensional systems. After the spatial discretization of the Partial Differential Equation (PDE) system however, a large dimensional system is obtained (>100 states). The perturbation approach has not so far been successful in these cases, as the numerical results showed incorrect behaviors. A likely explanation is that perturbation techniques [3] for large dimensional systems require a (too) large number of Taylor terms to be considered before the results become appropriate.

- The population model as discussed in this work contains high dimensional matrix elements. This is not a problem for the simple calculations required by the control strategies proposed in this work. However, such a model is not suitable for optimization tasks at a planning level. More specifically, it is not

well suited for characterizing the overall flexibility of the TCL population and planning reference trajectories in a scenario with many other assets. Such a planning scenario is discussed in [2], where an heuristic "leaky-bucket" flexibility model (without guarantees or theoretical properties) is proposed for the TCL population asset. A flexibility model is a model that describes all (or a subclass) of tractable power references. The question of whether a given reference is tractable or not depends on the initial state of the population, the population parameters, and the control method.

- The average parameters of the TCL population were considered given/know and fixed in this work. The issue of population parameter identification from available data (aggregate measurements, and partial unit level measurements), as well as adaptively adjusting these parameters in operation is of interest. A recent work in this direction is [4].

References

[1] Jan Bendtsen and Srinivas Sridharan. Efficient desynchronization of thermostatically controlled loads. *arXiv preprint arXiv:1302.2384*, 2013.

[2] Morten Juelsgaard, Luminita C Totu, S Ehsan Shafiei, Rafael Wisniewski, and Jakob Stoustrup. Control structures for smart grid balancing. 2013.

[3] Tosio Kato. *Perturbation theory for linear operators*, volume 132. Springer Science & Business Media, 1976.

[4] Nariman Mahdavi, Cristian Perfumo, and Julio H Braslavsky. Bayesian parameter estimation for direct load control of populations of air conditioners. In *World Congress*, volume 19, pages 9924–9929, 2014.

[5] Roland Malhame and Chee-Yee Chong. Electric load model synthesis by diffusion approximation of a high-order hybrid-state stochastic system. *Automatic Control, IEEE Transactions on*, 30(9):854–860, 1985.

[6] Scott Moura, J Bendtsen, and V Ruiz. Modeling heterogeneous populations of thermostatically controlled loads using diffusion-advection pdes. In *Proceedings of the 2013 ASME Dynamic Systems and Control Conference, Stanford, California*, 2013.

[7] Wei Zhang, Jianming Lian, Chin-Yao Chang, and K. Kalsi. Aggregated modeling and control of air conditioning loads for demand response. *Power Systems, IEEE Transactions on*, 28(4):4655–4664, Nov 2013.

Part II

Publications

Paper A

Control for Large-Scale Demand Response of Thermostatic Loads

Luminița C. Totu, John Leth and Rafael Wisniewski

The paper has been published in the
proceedings of the American Control Conference, 2013

© 2013 IEEE
The layout has been revised, and small editorial changes have been made. Content relavant changes, if any, are marked with explicit footnotes.

Abstract

Demand response is an important Smart Grid concept that aims at facilitating the integration of volatile energy resources into the electricity grid. This paper considers a residential demand response scenario and specifically looks into the problem of managing a large number thermostat-based appliances with on/off operation. The objective is to reduce the consumption peak of a group of loads composed of both flexible and inflexible units. The power flexible units are the thermostat-based appliances. We discuss a centralized, model predictive approach and a distributed structure with a randomized dispatch strategy.

1 Introduction

In many countries including Denmark [1, 2], energy generation from volatile resources such as wind or solar radiation is planned to increase. While these resources are sustainable and have overall capacity to cover the growing energy demand and even replace capacity currently served by fossil-fuels, large-scale use is challenging. This is because the power system needs to be in balance between consumption and production at all times. When a large percentage of the generation is volatile, the balancing effort increases beyond the possibilities of the traditional grid.

Smart Grid is a developing technology that proposes real-time information exchange, distributed generation, distributed storages, and intelligent solutions for the electrical network. It can facilitate the large-scale integration of volatile generation, reduce infrastructure investments and decrease the need for large, stand-by energy reserves. An important Smart Grid concept is demand response, which can be described as the active, continuous participation of the consumption in the energy balance: use less electricity when it is scarce and difficult to produce, and more otherwise.

We present a demand response scenario where a large group of thermostat-based appliances with on/off operation represent power flexible units. We can think of the flexible units as many, small and "leaky" thermal storages.

Next, we briefly refer to works on a similar topic to outline our focus. Dynamic demand, a concept closely related to demand response, is addressed in [4] for a population of domestic refrigerators acting as grid frequency stabilizers. In this case, and in contrast to the demand response scenario, the units cannot be used for planning, e.g., storing energy minutes or hours before a consumption peak.

The demand-side management structures in [12] and [5] are more appropriate for operating appliances as distributed storages. Important techniques used here are randomization and broadcasting. Furthermore, [10] discusses three different structures for demand response (price signal, individual power reference, and individual temperature reference) and concludes that a successful scheme must combine optimization and feedback. It is on these four ideas that we build the distributed approach proposed in this work.

We start by investigating centralized optimization techniques that are commonly used for production planning [7, 9]. While these can offer an insight into the consumption problem, such a direct approach alone is impractical. Due to non-convex elements (the on/off device level control) and the large number of variables that need to be communicated and computed, algorithms become impracticable. Consequently, we propose a distributed structure with two levels: a supervisor center and local con-

trollers. The supervisor center broadcasts a global coordination signal and uses power measurements of the cumulated consumption as feedback. A modified thermostat algorithm acts as the local controller of each appliance. The algorithm handles device specific operation and responds to the coordination signal in a randomized manner.

The article is organized as follows. First, models based on physical principles are introduced in Section 2. The centralized optimization is presented in Section 3, and the distributed structure in Section 4. Simulations for both approaches are discussed in Section 5, while Section 6 concludes and points to future work.

2 Models

We assume given $N + M$ power consuming devices, where N units have thermal storage capabilities and thermostat driven on-off behavior, and M units have a purely stochastic, time-varying on-off behavior and no energy storage properties. We think of the first type as refrigerators, heat-pumps, air-conditioning or water boilers, and of the second type as lights, TVs, or ovens. With respect to the energy needed for nominal operation, the devices of the first category have power flexibility and are considered controllable, while those of the second category are power inflexible and are considered uncontrollable. It is also assumed that power consumption is constant during the on-cycle for all devices.

The aim is to control the N flexible devices, within the boundaries of their nominal operation and in the presence of the M inflexible devices, such that the peak of the cumulated consumption is reduced.

For both device categories, simplified physical models combined with stochastic elements are used to capture the main behaviors related to power consumption. Essential aspects of the problem are scale and variability: the objective is to manage a very large number of units and to tolerate parameter variations.

2.1 Basic models for the flexible units

The flexible devices have an on/off consumption pattern based on thermostat control. In the on-cycle, power is consumed and thermal energy (heat or "coldness") is stored. In the off-cycle, the thermal energy is lost in the surrounding environment. Modeling based on physical principles is described next.

The power active component (e.g. vapor-compression cycle, resistive heater, etc.) is modeled with a constant coefficient of performance. A number of compartments of uniform temperatures are modeled by heat balance affine differential equations. Since the control and communication will be based on digital systems, it is natural to work directly in discrete time. We will use models of the form (A.1) where the notation is summarized in Table A.1. A random term is introduced in the dynamics. It can be designed to account for the variety of disturbances coming from usage profiles and the environment.

$$\mathbf{F_i}: \begin{cases} T_i(k+1) &= A_i T_i(k) + b_i u_i(k) + c_i + q_i(k) & \text{(A.1a)} \\ y_i(k) &= p_i u_i(k), & \text{(A.1b)} \end{cases}$$

Nominal operation is the evolution of $\mathbf{F}_i$ within a set of constraints, e.g., temperature ranges and minimum on and off times. The unit has operational flexibility

Table A.1: Notation and symbols for models of flexible units

	Signals	
$T_i(\cdot)$	temperature vector for the compartments	$\mathbb{R}^{n_i}$
$u_i(\cdot)$	on/off value of the power consuming comp.	$\{0,1\}$
$u(\cdot)$	collective on/off values	$\{0,1\}^N$
$y_i(\cdot)$	power consumption (Watts)	$\mathbb{R}_+$
$y(\cdot)$	collective power consumption (Watts)	$\mathbb{R}_+^N$
$q_i(\cdot)$	random contributions	$\mathbb{R}^{n_i}$
	Parameters	
N	number of flexible units	$\mathbb{N}_+$
n_i	number of thermal compartments for a unit	$\mathbb{N}_+$
A_i	linear map, 2D-matrix	$\mathbb{R}^{n_i} \to \mathbb{R}^{n_i}$
b_i, c_i	linear map, 1D-vector	$\mathbb{R} \to \mathbb{R}^{n_i}$
p_i	power rating of the device (Watts)	$\mathbb{R}_+$
p	collective power ratings	$\mathbb{R}_+^N$
DT_i	minimum down(off) time periods	$\mathbb{N}_+$
UT_i	minimum up(on) time periods	$\mathbb{N}_+$
	Indexes	
$()_i$	unit index	$1, \ldots, N$
k	discrete time index	$1, 2, \ldots, K$

because there are different possibilities of controlling the on/off power cycle, i.e. the u_i signal, to maintain nominal operation, see Fig. A.3.

Next, we collect the u_i and p_i terms in the following notations, $u(k) = (u_1(k), \ldots, u_N(k))$, $p = (p_1, \ldots, p_N)$ and write the total consumption of the N flexible units at time k as

$$y(k) = \langle p, u(k) \rangle \stackrel{\Delta}{=} \sum_{i=1}^{N} p_i u_i(k). \tag{A.2}$$

2.2 Basic models for the inflexible units

Inflexible units have a stochastic on-off behavior with time varying properties. As example, an indoor light appliance is more likely to be turned on in the early morning and in the evening, and less at midday and after midnight. A natural choice for modeling the random on/off behavior at the unit level is using the discrete-time Markov chain formalism. We will use notations similar to [8].

Each inflexible unit j will be modeled as a discrete time Markov chain, with $X_j(k) \in \{1(\text{on}), 0(\text{off})\}$ the random variable representing the state of the unit at time k, $P_j(k) = (p_0^j(k), p_1^j(k)) = (P[X_j(k) = 0], P[X_j(k) = 1])$ the state probability row vector at time k, and $p_{01}^j(k)$ and $p_{10}^j(k)$ time varying transition probabilities, "turn on"

and ‘"turn off" respectively. The evolution in time of the state probability and the power consumption output can be described as

$$\mathbf{I}_j : \begin{cases} P_j(k+1) & = P_j(k) M_j(k) \\ w_j(k) & = p_j' X_j(k), \end{cases} \tag{A.3}$$

where $M_j(k) = \begin{bmatrix} 1 - p_{01}^j(k) & p_{01}^j(k) \\ p_{10}^j(k) & 1 - p_{10}^j(k) \end{bmatrix}$ is the transition probability matrix.

This Markov chain is also depicted in Fig. A.1 and notation and symbols are summarized in Table A.2. The transition probabilities can be parameterized to approximate usage patterns for different device types.

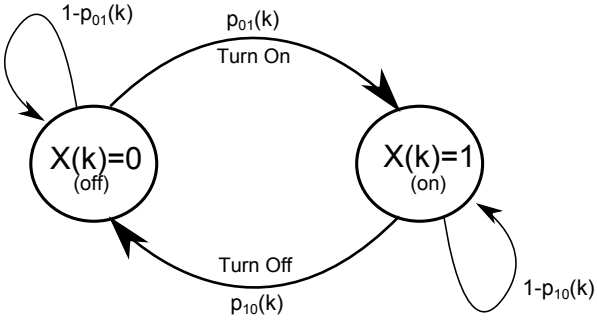

Fig. A.1: Markov chain for the inflexible units

We further collect the X_j and p_j' terms in the notations, $X(k) = (X_1(k), \ldots, X_M(k))$ and $p' = (p_1'(k), \ldots, p_M'(k))$ to compactly express the total power consumption of the M inflexible units, a random process, as

$$w(k) = \langle p', X(k) \rangle . \tag{A.4}$$

In this work, we use the probabilistic construction only for numerical simulations. In the optimization formulation, a deterministic sequence $\bar{w}(k)$ is used as a forecast for the expected power consumption of the inflexible units over a required time horizon. This deterministic sequence is constructed by replacing each $w(k)$ random variable with its expected value, $E[w(k)]$. Given an initial state probability vector $P_j(0)$ and knowing the transition matrices $M_j(k)$,

$$E[w(k)] = \sum_{j=1}^{M} p_j' P_j(0) M_j^k \begin{bmatrix} 0 & 1 \end{bmatrix}^T , \tag{A.5}$$

where $M_j^k = M_j(0) M_j(2) \ldots M_j(k-1)$.

Using the above models for the flexible and inflexible units, the total power consumption of the $N + M$ devices can be expressed, depending on the context, as one of the following two random processes:

$$z(k) = y(k) + w(k) = \langle p, u(k) \rangle + \langle p', X(k) \rangle , \tag{A.6a}$$

$$\bar{z}(k) = y(k) + \bar{w}(k) = \langle p, u(k) \rangle + \bar{w}(k). \tag{A.6b}$$

Table A.2: Notation and symbols for models of inflexible units

	Signals	
$P_j(\cdot)$	probabilities for Markov states on and off	$\mathbb{R}^{1\times 2}$
$X_j(\cdot)$	random variable, state of the unit: on(1) or off(0)	$\{0,1\}$
$w_j(\cdot)$	power consumption (Watts)	$\mathbb{R}_+$
$w(\cdot)$	cumulated power consumption	$\mathbb{R}_+$
$\bar{w}(\cdot)$	forecast/mean consumption profile (Watts)	$\mathbb{R}_+$
	Parameters	
M	number of inflexible units	$\mathbb{N}$
$M_j(\cdot)$	right stochastic matrix, time varying	$\mathbb{R}^{2\times 2}$
$p^j_{xy}(\cdot)$	pr. of transition from state x to y, time varying	$[0,1]$
$p^j_x(\cdot)$	pr. of being in state x	$[0,1]$
p'_i	power rating of the device (Watts)	$\mathbb{R}_+$
p'	collective power ratings	$\mathbb{R}^M_+$
	Indexes	
j	unit index	$1,\ldots,M$
k	discrete time index	$1,\ldots,K$

It is noted that while $\bar{w}(k)$ has been introduced as a deterministic sequence, $\bar{z}(k)$ remains a random process for all practical cases. This is because the dynamics of the flexible units are affected by noise, and this fact will reflect into the power consumption, the term $u(k)$.

3 A Centralized Approach

A straightforward approach to reduce the peak consumption is to employ optimization techniques based on an objective, models and constraints to compute the on/off controls for the flexible units. In this section, we formulate and analyze a mixed integer linear optimization that is the core component of the model predictive control (MPC) [11] approach.

We want to calculate the $u_i(k)$ values for all the flexible units $\mathbf{F}_i$ and over the entire time horizon $\{1,\ldots,K\}$, such that the maximum value of the sequence $\bar{z}(k)$ is minimized. This opaque minimax objective,

$$\min_{u(\cdot)} \|\bar{z}(k)\|_\infty = \min_{u(\cdot)} \|\langle p, u(k)\rangle + \bar{w}(k)\|_\infty, \tag{A.7}$$

can be written in a convenient linear form by adding a new variable, $m \in \mathbb{R}$ and a set

of inequality constraints, see [6],

$$\min_{u(\cdot)} \|\bar{z}(k)\|_\infty \Leftrightarrow \begin{cases} \min\limits_{u(\cdot),m} \; m \\ -m \leq \bar{z}(k) \leq m; \; \forall k. \end{cases} \tag{A.8}$$

Furthermore, because $z(k)$, the cumulated instantaneous power consumption, is always non-negative, the left inequality, $-m \leq \bar{z}(k)$, can be dismissed. Next, we detail three main constraints.

First, the model dynamics must be included to indicate the relation between the states $T_i(\cdot)$ and the decision variables $u_i(\cdot)$. For each flexible unit i, and $k \in \{1, \ldots, K\}$, equation (A.1a) without the random term is accounted as an equality constraint. It is noted that the $T_i(1)$ temperatures are already decided by the $u_i(0)$, and act as initial conditions. These constraints apply on $T_i(2)$ to $T_i(K+1)$.

Second, the states $T_i(k)$ must be within the allowable ranges, $T_i^{\min} \leq T_i(k) \leq T_i^{\max}$, where $T_i^{\min}, T_i^{\max} \in \mathbb{R}^{n_i}$ are individual parameters of the flexible unit i and $k \in \{2, \ldots, K+1\}$.

Third, we include minimum on and off times associated with the power consumption of each $\mathbf{F}_i$. These constraints can be written in a linear form, see [7]. Expressions (A.9) are for the minimum on-time and (A.10) are for the minimum off-time.

$$\sum_{k=1}^{(\mathrm{UT}_i - C_i)u_i(0)} u_i(k) = (\mathrm{UT}_i - C_i)u_i(0) \tag{A.9a}$$

$$\sum_{k=t}^{t+\mathrm{UT}_i-1} u_i(k) \geq \mathrm{UT}_i \left(u_i(t) - u_i(t-1)\right), \quad \forall t \in \{(\mathrm{UT}_i - C_i)u_i(0) + 1, \ldots, K - \mathrm{UT}_i + 1\} \tag{A.9b}$$

$$\sum_{k=t}^{K} u_i(k) - \left(u_i(t) - u_i(t-1)\right) \geq 0, \; \forall t \in \{K - \mathrm{UT}_i + 2, \ldots, K\};. \tag{A.9c}$$

$$\sum_{k=1}^{(\mathrm{DT}_i - C_i)(1-u_i(0))} u_i(k)) = 0, \tag{A.10a}$$

$$\sum_{k=t}^{t+DT_i-1} (1 - u_i(k)) \geq \mathrm{DT}_i \left(u_i(t-1) - u_i(t)\right), \quad \forall t \in \{(\mathrm{DT}_i - C_i)(1 - u_i(0)) + 1, \ldots, K - \mathrm{DT}_i + 1\} \tag{A.10b}$$

$$\sum_{k=t}^{K} 1 - u_i(k) - \left(u_i(t-1) - u_i(t)\right) \geq 0, \forall t \in \{K - \mathrm{DT}_i + 2, \ldots, K\}. \tag{A.10c}$$

It can be seen that a number of approximately $2K$ linear inequalities are used for each unit to assure the minimum on and off time conditions. The inequalities have different expressions at the beginning (A.9a), (A.10a) and at the end (A.9c), (A.10c) of the time horizon. C_i is a counter value that holds number of samples that the unit has been in the initial state, and is part of the optimization initialization. Thus the value $(\mathrm{UT}_i - C_i)$ represents the number of periods that the unit must remain in its initial

state and not change. The term $u_i(t) - u_i(t-1)$ equals to 1 for a turn-on event at time t, and thus the next UT_i commands $u_i(t+1), \ldots, u_i(t+\mathrm{UT}_i-1)$ must remain on (=1). The term $u_i(t-1) - u_i(t)$ equals to 1 for a turn-off event at time t.

The optimization can now be passed to a mixed integer linear solver. Simulation results are presented in Section 5.

We present next implementation considerations. In total, the problem has $2 \times N \times K + 1$ decision variables (temperatures are also decision variables) and about $5 \times N \times K$ constraints. A sample period $T_s = 60$ seconds is considered a good choice with respect to the dynamic characteristics of the controllable units, the level of detail in the modeling, and the on/off control behavior. Ideally, the time horizon K should cover 24 hours, the main period of the inflexible consumption pattern. In the model predictive control solution, such an optimization needs to be solved every sample period. Although good algorithms exist for solving mixed integer linear optimizations [3], memory and execution time requirements will grow exponentially with the number of units and the time horizon, and make computation infeasible for large-scale problems. Another disadvantage here is related to the centralized nature of the approach: the computation center must send and receive data from geographically distributed locations in a short period of time, requiring a robust, fast, double way communication infrastructure.

4 A Distributed Approach

In the centralized approach, the non-convex elements and the large number of local variables and constraints make the numerical computations impracticable. It seems reasonable to carry out part of the control task at the local level where knowledge of the state variables and operational constraints is inherent. If the power consumption decisions are made locally, some type of information sharing becomes necessary to achieve a consistent global behavior.

We construct a demand response structure that has distributed characteristics, two control levels, and requires minimal communication. A diagram is shown in Fig. A.2(a), where blocks $\mathbf{F}_1, \ldots, \mathbf{F}_n$ represent flexible units equipped with the local controllers K_L and the $(\mathbf{I}_1 + \ldots + \mathbf{I}_L)$ block corresponds to the cumulated inflexible consumption process.

4.1 Supervisory control and estimation

Using consumption forecasts and an aggregation model with approximate knowledge of type and number of cooling units in the system, the supervisor control generates the power reference signal r. The power reference has the purpose of scheduling periods of thermal energy storage and discharge. Furthermore, estimated values are needed to characterize the refrigeration population. These are $\tilde{N}^{\mathrm{on}}$ and $\tilde{N}^{\mathrm{off}}$, estimates for the number of units in the state ON and OFF respectively that are in the flexibility range, and $\bar{p}_i$ the average specific power rating of a cooling unit in the group. The flexibility range refers to the temperature of a unit i being some distance away from the hard limits, that is in the range $[T_i^{\min} + \Delta T_i,\ T_i^{\max} - \Delta T_i']$. This is done to avoid successive on/off cycling due to conflicting local and global objectives.

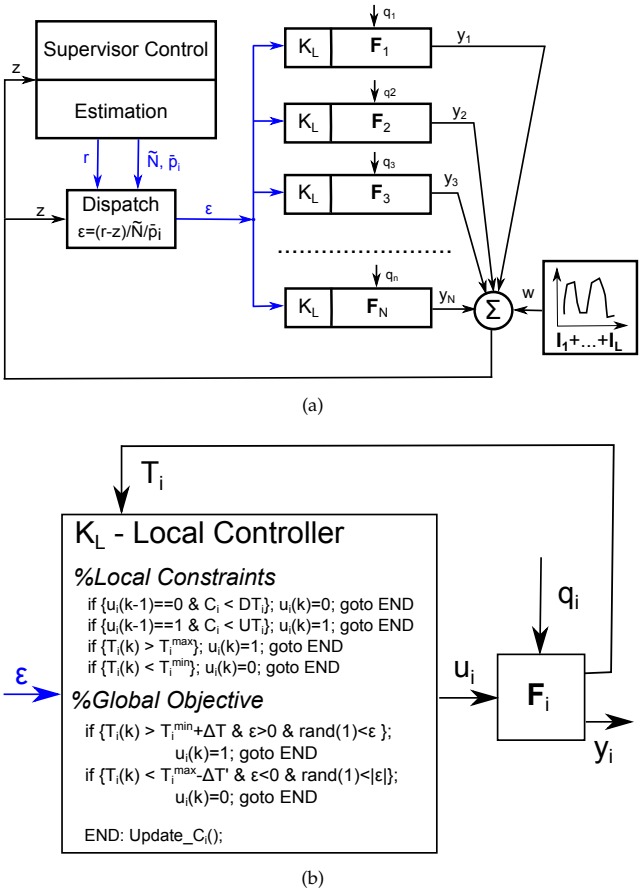

Fig. A.2: Distributed control structure (a), and the local controller block K_L (b)

4.2 Local controller

The local controller, shown in Fig. A.2(b), is a computationally inexpensive extension of the thermostat cooling logic. The on/off decision is made with first priority on constraints, in this case temperature and timer limits. If they are all satisfied, the operational flexibility is used to respond to the broadcast signal ϵ in a randomized manner. Fig. A.3 shows a normal thermostat operation versus an extended thermostat reacting in a randomized manner to an external signal ϵ.

4.3 Dispatch strategy

The ϵ signal is similar to the error signal in a classic control structure. It is build as a scaled difference between the reference signal r and the actual power consumption z. It can either encourage consumption ($\epsilon > 0$), or discourage it ($\epsilon < 0$). The scaling is performed such that the absolute value has the meaning of a fraction of the total

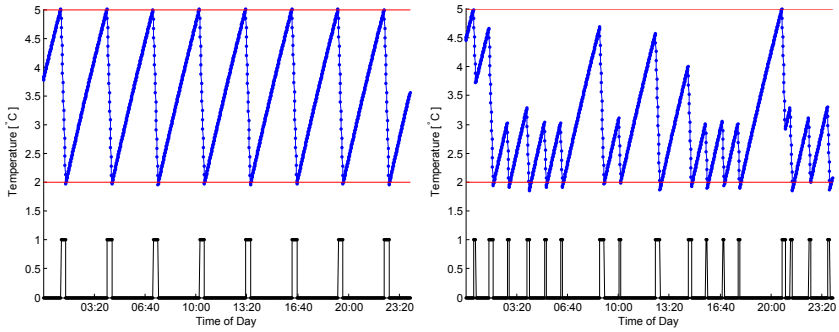

(a) Normal duty-cycle (b) Randomized duty-cycle

Fig. A.3: Operation of flexible unit. Temperature is shown in blue, and the on/off state in black.

number of refrigerators. For example, if $\epsilon = -0.1$, the broadcast information is that 10% of the refrigerators should turn off. The formula for computing ϵ is thus

$$\epsilon = \begin{cases} (r-z)/(\tilde{N}^{\text{off}}\bar{p}_i), \text{if } \ r > z \\ (r-z)/(\tilde{N}^{\text{on}}\bar{p}_i), \text{if } \ r < z. \end{cases} \tag{A.11}$$

Refrigerator units in the flexibility range respond to the ϵ signal by making random trial with success rate $|\epsilon|$. If the trial is successful, the unit reacts by turning on ($\epsilon > 0$) or respectively off ($\epsilon < 0$). For a sufficiently large number of refrigerators and good $\tilde{N}$ estimates, by the law of large numbers, the cumulated responses of the individual units will be close to the requested fraction. It is thus possible to follow a power reference signal r that is well-designed.

We have organized a dispatch strategy that can support an arbitrarily large number of individual units, is computationally and communication-wise cheap, and is robust to faults in the coordination level. The dispatch is intrinsically noisy, but the relative noise ratio will decrease with the number of units. This can be seen in the next section. Some of the complexity of the problem remains to be handled at the coordination level, where good aggregation models and algorithms are needed for tracking the thermal storage level and for estimating the $\tilde{N}^{\text{on}}$ and $\tilde{N}^{\text{off}}$ values.

5 Numerical Experiments

This section puts forward specific models for the flexible and inflexible units, and presents simulation results for the centralized optimization control and the distributed control.

We take the case of a 1-compartment cooling unit in constant ambient temperature, similar to [4], [12] or [5],

$$\mathbf{F}_i : \begin{cases} T_i(k+1) & = a_i T_i(k) + (1-a_i)\left(T_i^a - u_i(k)T_i^g\right) + q(k) \\ y_i(k) & = p_i u_i(k), \end{cases} \tag{A.12}$$

where $a = \exp(-\text{UA} \cdot T_s/C)$, $T^g = \text{COP} \cdot p/\text{UA}$ and $T_s = 60$ seconds. A random, white component $q(k)$ with normal distribution has been added to the temperature dynamics to simulate disturbances. Overall, this is a simple model with the purpose of evaluating the control approaches, and is a particular case of the general affine linear state-space representation (A.1).

We work with two parameter sets, described in Table A.3. Parameters marked with "*" will be generated with a $\pm 10\%$ normal variation around the given value. In uncontrolled operation mode, the thermostat drives the power consumption cycle in regular intervals[1] of approximately 20 minutes on and 162 minutes off for the first parameter set (refrigerators) and 43 minutes on and 490 minutes off for the second parameter set (freezers).

Table A.3: Numerical parameters for the flexible unit model

	Description	Units	Refrigerator	Freezer
C^*	heat capacity	$J/^\circ C$	$9.4 \cdot 10^4$	$13.5 \cdot 10^4$
UA^*	overall heat transfer	$W/^\circ C$	1.432	0.8
T^{a*}	ambient temp.	$^\circ C$	24	22
COP^*	coeficient of perf.	-	2.8	2.8
p^*	power rating	W	100	140
$T^{\min}$	min operational temp.	$^\circ C$	2	-22
$T^{\max}$	max operational temp.	$^\circ C$	5	-15
UT	min up time	min	5	5
DT	min down time	min	5	5
$q(\cdot)$	random, normal distrib.	$^\circ/s$	$\sigma = 0.05$	$\sigma = 0.05$

The inflexible unit j is described by the transition probabilities $p^j_{01}(k)$ and $p^j_{10}(k)$ specified over the time horizon of a day. The transition probabilities have been designed piece-wise constant, and create a state probability profile $p^j_1(k)$ with two exaggerated peaks, shown in Fig. A.4. The probability behavior is identical for all units, such that the cumulated consumption has the same shape.

For the MPC approach, the optimization problem defined in Section 3 has been implemented for the Gurobi solver MATALB interface. It was parameterized for a group of identical 1-compartment cooling units with identical ambient temperatures and inflexible consumption profile $\bar{w}(k)$. The largest number of controllable units for which it was possible to obtain solutions in a reasonable amount of time was $N = 20$. The optimized commands associated corresponding to the first time step, $u(1)$, are dispatched to each unit. The new temperatures are then collected and used as initial conditions for the next optimization, which is carried out with a receded horizon.

For the distributed approach, a simulation was set-up in MATLAB as described in Sec. 4. The elements of the Supervisor Control and Estimation block have not been completely developed for this simulation. The reference signal r was designed manually such that periods of energy storage were scheduled prior to the peaks, and periods of energy discharge were scheduled during the peaks. In addition, the $\tilde{N}^{\text{off}}$

[1] *Added Note:* For clarification, it is remarked that the ON and OFF duration are calculated for a deterministic operation, without considering the white noise contributions.

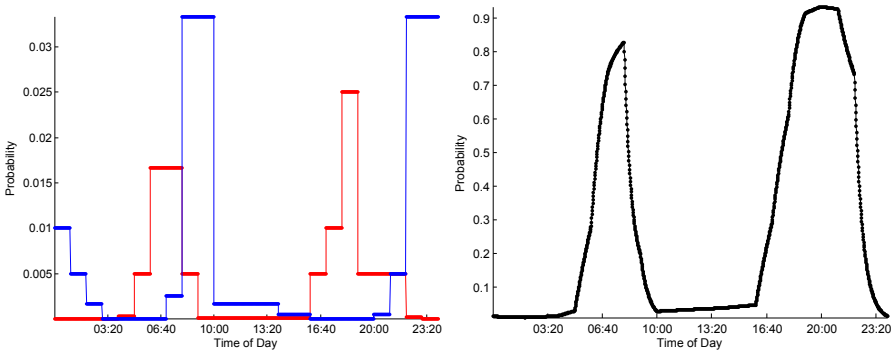

(a) Transition probabilities

(b) Probability profile for state ON

Fig. A.4: Properties for the inflexible units across the time horizon of a day. In the left figure, TURNON transition probabilities are shown in red, and TURNOFF transition probabilities are shown in blue. In the right figure, resulting steady-state probabilities for ON are shown.

and $\tilde{N}^{\text{on}}$ estimates were constructed using simulation data that would not normally be available to the supervisor center.

Fig. A.5 shows realizations for the small scale case. The differences between the planned schedule (Fig. A.5(a)) and the MPC realization (Fig. A.5(b)) are due to model parameter variations and noisy dynamics in the simulation of the flexible units, and also because of errors in the inflexible consumption forecast. For the distributed control A.5(d), it can be seen that the reference signal for the total consumption is followed in an imprecise manner. This is mainly due to large relative granularity of the system as the response from the refrigerator group is in steps of approximately $\pm$100W. Furthermore, at this scale, the dispatch strategy is imprecise due to the randomization. For both the MPC and the distributed control, the peak has been reduced.

Fig. A.6 shows realizations for the large-scale case. The dispatch strategy is now able to keep the response smooth and precise. The shortcomings in this experiment are only related design of the power reference signal. This remains to be addressed in future work. It can also be noticed that the second peak starting around 16:40 has a longer duration. The refrigerator units simply do not have enough storage capacity to completely ride through this peak and after the 20:00 mark, power consumption increases over the reference value. Fig. A.6(c) shows a distributed control run for a group of freezers, units with a larger individual flexibility. In this case, it is possible to keep the peak close to the level of the inflexible consumption.

6 Conclusion

We have proposed in this work a demand response scenario with a power peak reduction objective and emphasis on large-scale. First, a centralized MPC framework was evaluated as infeasible. Subsequently, we presented a distributed control structure with good performance for large numbers of control units. A main contribution is the randomized dispatch strategy, which keeps decision making at the local level where

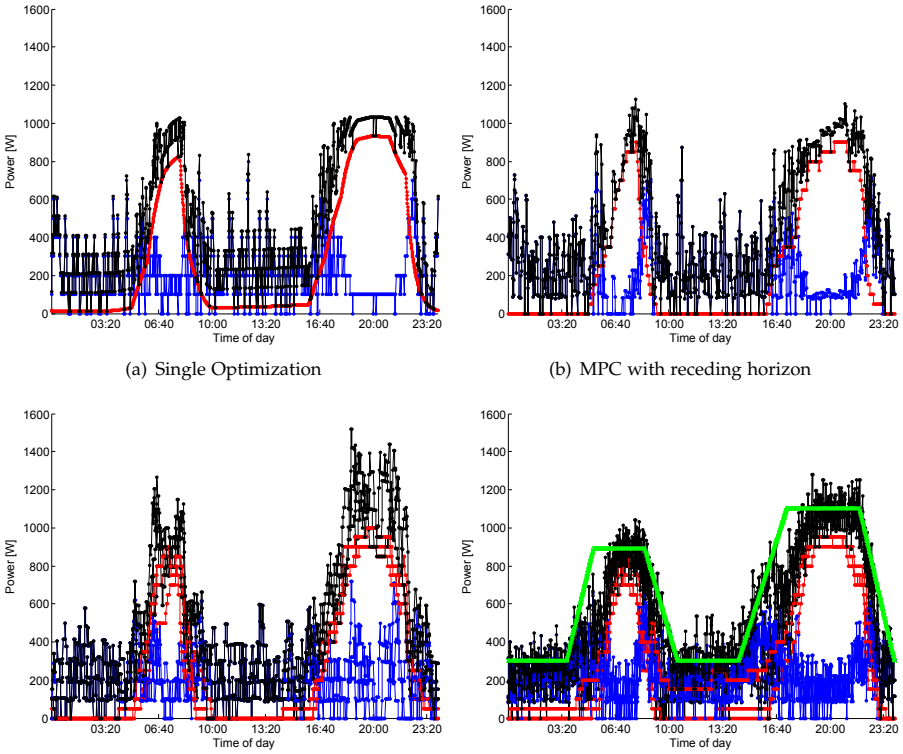

(a) Single Optimization

(b) MPC with receding horizon

(c) Uncontrolled operation

(d) Distributed control

Fig. A.5: Small scale experiments for refrigerator units, $N = 20$. Blue shows the consumption of the flexible units $y(\cdot)$, red shows the consumption of the inflexible units $w(\cdot)$, and black represents the total power $z(\cdot)$. For the distributed control, the power reference $r(\cdot)$ is shown in green. In figures A.5(c) and A.5(d), data from theree simulated days is plotted in an overlapped manner.

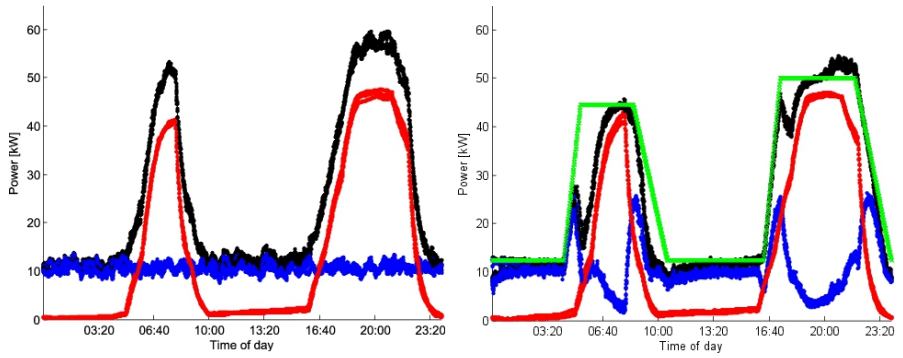

(a) Uncontrolled operation

(b) Distributed control

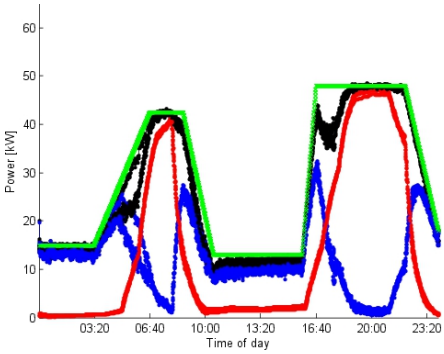

(c) Distributed control, freezer units

Fig. A.6: Large-scale experiments, number of controllable units is $N = 1000$. Same conventions as in Fig. A.5

.

specific operation is easy to manage. The approach has only minimal communication requirements. Future work will address in detail the design of the supervisor level control based on an aggregated model of the group of thermostat-based devices.

References

[1] Our future energy, 2011.

[2] Strategic research agenda 2035, 2012.

[3] Karen Aardal and Stan Van Hoesel. Polyhedral techniques in combinatorial optimization. *Statistica Neerlandica*, 50:3–26, 1995.

[4] D. Angeli and P.-A. Kountouriotis. A stochastic approach to dynamic-demand refrigerator control. *Control Systems Technology, IEEE Transactions on*, 20(3):581 –592, may 2012.

[5] T. Bigler, G. Gaderer, P. Loschmidt, and T. Sauter. Smartfridge: Demand side management for the device level. In *Emerging Technologies Factory Automation (ETFA), 2011 IEEE 16th Conference on*, pages 1 –8, sept. 2011.

[6] Stephen Boyd and Lieven Vandenberghe. *Convex optimization*. Cambridge University Press, Cambridge, 2004.

[7] M. Carrion and J.M. Arroyo. A computationally efficient mixed-integer linear formulation for the thermal unit commitment problem. *Power Systems, IEEE Transactions on*, 21(3):1371 –1378, aug. 2006.

[8] Christos G Cassandras and Stephane Lafortune. *Introduction to discrete event systems*, volume 11. Kluwer academic publishers, 1999.

[9] Kristian Edlund. *Dynamic Load Balancing of a Power System Portfolio*. PhD thesis, Aalborg University, 2010.

[10] Kirsten Molgaard Nielsen, Tom Sondergaard Pedersen, and Palle Andersen. Heat pumps in private residences used for grid balancing by demand desponse methods. In *Transmission and Distribution Conference and Exposition (T D), 2012 IEEE PES*, pages 1 –6, may 2012.

[11] J.B. Rawlings. Tutorial overview of model predictive control. *Control Systems, IEEE*, 20(3):38 –52, jun 2000.

[12] Michael Stadler, Wolfram Krause, Michael Sonnenschein, and Ute Vogel. Modelling and evaluation of control schemes for enhancing load shift of electricity demand for cooling devices. *Environmental Modelling & Software*, 24(2):285 – 295, 2009.

Paper B

Demand Response of Thermostatic Loads by Optimized Switching-Fraction Broadcast

Luminița C. Totu and Rafael Wisniewski

The paper has been published in the
proceedings of the 19th IFAC World Congress, 2014.

© 2014 IFAC
The layout has been revised, and small editorial changes have been made. Content relavant changes, if any, are marked with explicit footnotes.

Abstract

Demand response is an important Smart Grid concept that aims at facilitating the integration of volatile energy resources into the electricity grid. This paper considers the problem of managing large populations of thermostat-based devices with on/off operation. The objective is to enable demand response capabilities within the intrinsic flexibility of the population. A temperature distribution model based on Fokker-Planck partial differential equations is used to capture the behavior of the population. To ensure probability conservation and high accuracy of the numerical solution, a Finite Volume Method is used to spatially discretize these equations. Next, a broadcast strategy with two switching-fraction signals is proposed for actuating the population. This is applied in an open-loop scenario for tracking a power reference by running an optimization with a multilinear objective.

1 Introduction

We consider a large group of devices of the same type, where each unit has on/off power consumption controlled by an internal thermostat. These devices are of special interest for Smart Grid scenarios since they have the potential to deliver demand response services in an automated way. The focus of this work is on aggregating a very large numbers of units. The challenge is twofold. Firstly, communication flows must be carefully designed to be feasible under cost, security and privacy criteria because of the large-scale and large geographic spread of the system. Secondly, computational complexity must be kept in check.

The study of large groups of thermostatic loads started in the power system and in the control literature in the '80s with the works of [3] and [5]. The interest was on modeling the oscillatory effects in the power consumption after a planned (direct load control) or unplanned interruption (black-out). After three decades, the problem got a resurgence motivated by the advancement of demand response concepts, which in turn are motivated by new challenges in power system operations, mainly the integration of intermittent generation.

The modeling approach that we are focused on is based on physical principles and stochastics. The thermostatic unit is described by a stochastic hybrid lumped-state dynamical model, while a thermostatic population can be described by a distribution function over the hybrid state-space.

If the distribution function is taken in its continuous form (a density), an infinite dimensional state-space description is obtained where dynamics are given in the form of a Partial Differential Equation (PDE) system and boundary conditions. This form was first derived in [5], and has been subsequently used in e.g. [2], [1], [6]. Another approach is to divide the hybrid state-space into a finite number of partitions, and work with a discrete distribution i.e. probability mass. Careful considerations based on the unit model can be made to derive transition probabilities from one partition to another, and thus the dynamics can be expressed in form of a Markov chain, e.g. in [4], [9], [7]. These two forms are essentially equivalent, leading to a standard, linear state-space description.

However, in terms of numerical performance not all methods all equivalent. For example, in [1] a finite-difference numerical scheme is used to obtain the Markov chain representation from the PDE description. This method does not inherently

conserve probability and the solution might require periodic rescaling. In [4] the transition probabilities of the Markov chain are derived based on an uniformity approximation over each partition. In this work, we propose Finite Volume Methods (FVM) for obtaining the Markov chain transition matrix from the PDE system. The main advantage is that the overall probability is guaranteed to be conserved as the resulting dynamic matrix has columns that sum to zero[1]. Furthermore, numerical results have a high degree of accuracy also over long horizons, since the PDE form is exact and the only errors are related to the size of the state-space partitions. Finally, there is an advantage in using a well-developed framework with recognized robustness and performance as opposed to custom solutions.

Other important aspects for population modeling are heterogeneity and minimum on/off times. Heterogeneity is a difficult problem because exact descriptions suffer from the "curse of dimensionality". We add a few remarks, but do not address directly the modeling of heterogeneity. Nonetheless, results show that the used control appears to have good robustness to heterogeneity. The effects of enforcing minimum on/off times at the unit level are modeled using a technique essentially equivalent to [9].

For control, our focus is on broadcasting strategies since we believe that these have an implementation advantage. In particular, we are interested in a particular form of toggling control [4] that involves the broadcast of only two switching fractions. This is a randomized method of actuation, and has been introduced in [9] and [8] in a closed-loop form where just one switching fraction is used at a time. In this work, we set-up and analyze an open-loop configuration based on a non-convex, predictive horizon optimization.

Section 2 presents the modeling used for the individual Thermostatically Controlled Load (TCL) and for the population, Section 3 introduces the randomized broadcast actuation with the switching fractions, Section 4 sets up the optimization formulation and presents numerical results, and Section 5 concludes.

2 TCL Modeling

For this work, we consider cooling units, in particular domestic refrigerators. As under realistic conditions, the TCLs are independent of each other, do not communicate nor share states. A main object of interest is the aggregated power consumption, which is simply the sum of the individual power consumptions.

2.1 TCL unit model

Stochastic Hybrid Unit Model:

The basic model for a TCL is a hybrid dynamical system with two modes, corresponding to the "on" or "off" state of the vapor-compression cooling cycle. When the TCL is "on", it is consuming power and the temperature in the food storage compartment is lowering. When the TCL is "off", it is not consuming power and the temperature in

[1] *Added Note*: The original print contains "the resulting dynamic matrix has a proper rate transition form, i.e., columns that sum to zero." For a proper transition-rate form, the resulting dynamic matrix must also have all non-diagonal elements non-negative. This property is not by default fulfilled by using FVM. This is further discussed in Paper D, and the claim of a proper transition rate-matrix is removed from this paper.

the food storage compartment is rising due to ambient conditions. The heating and cooling processes are modeled with a first-order dynamic. This is similar to [3], [2], [1] and others. Although more complex, second-order dynamics should be studied for air-conditioning or heat-pumps TCLs [9], this is not considered necessary in the case of domestic refrigerators, because there is no dominant secondary temperature mass. Additionally, random fluctuation are introduced in the dynamics as a white noise term.

Other possible random disturbances not pursued at this time are jump processes that would correspond to "door-opening" events. Furthermore, power consumption is considered to be constant when the mode is "on". This assumption might need to be revisited in future work.

Summing up, the model of a TCL unit is a stochastic hybrid system of the following form:

$$dT(t) = -\frac{\mathrm{UA}}{C}\left(T(t) - T_a + m(t)\frac{\eta W}{\mathrm{UA}}\right)dt + \sigma dw \tag{B.1a}$$

$$= \Big(aT(t) + b + m(t)c\Big)dt + \sigma dw \tag{B.1b}$$

$$y(t) = dm(t) \tag{B.1c}$$

where $T(t) \in \mathbb{R}$ is the continuously-valued temperature state, $m(t) \in \{0,1\}$ is the discrete-valued state corresponding to the "off" and "on" modes respectively, $y \in \mathbb{R}_+$ is the power consumption viewed here as model output, and a, b, c, d and σ are time invariant coefficients.

The dynamics of the discrete-valued state, m_i, are given by

$$m(t^+) = \begin{cases} 1, & T(t) \geq T_{\max} \\ m(t^-), & T(t) \in (T_{\min}, T_{\max}) \\ 0, & T(t) \leq T_{\min} \end{cases}, \tag{B.2}$$

a standard thermostat mechanism with boundaries at $T_{\min}$ and $T_{\max}$. This is a deterministic, state-dependent switching.

Probabilistic unit model

Because of the random influences introduced in the continuous dynamics, the hybrid state $\big(T(t), m(t)\big) \in \mathbb{R} \times \{0,1\}$ is a stochastic variable. It can be characterized by a probability density function (pdf) defined in the following way,

$$f_y(x,t) = \lim_{\delta x \searrow 0} \frac{1}{\delta x} \Pr[T(t) \in [x, x+\delta x) \wedge m(t) = y] \,. \tag{B.3}$$

The Fokker-Planck equation

The temperature dynamics corresponding to each of the two modes (on and off) are continuous-time continuous-state Markov processes, and in particular diffusions. If we look at any of the modes in isolation and do not take the switches into consideration, given the probability distribution of the temperature state at time t_0, we can determine the probability distribution at any future time $t \geq t_0$ using the Fokker-Planck

(Forward Kolmogorov) equation, which can be seen as a transport and conservation law for probability.

PDE system for the hybrid dynamic

The result in [5] gives the pdf dynamics in the particular case of the TCL hybrid dynamic (B.1), (B.2). It consists of Fokker-Planck equations written for each mode (B.4), and a set of boundary conditions (B.5).

Before stating the result, some preliminaries need to be addressed. The temperature domain needs to be divided into three subsets: the thermostat range $[T_{\min}, T_{\max}]$, the left hand side $(-\infty, T_{\min})$ and the right hand-side $(T_{\max}, \infty)$. This is a natural partition with respect to the operation of the TCL unit, and is necessary because boundary conditions apply in the points $T_{\min}$ and $T_{\max}$, and also because the pdf is not x-differentiable here. It is convenient to denote the three subsets with the letters b, a and c respectively. It is also important to note that in normal operation the pdf corresponding to the off mode, $f_0(x,t)$, is zero-valued on the c domain, because if the temperature becomes greater than $T_{\max}$ the thermostat mechanism ensures that the mode can not remain "off". The c domain accounts only for units in state "off", whose temperature becomes greater than $T_{\max}$ due to diffusion effects. Similarly, the pdf corresponding to the on-mode, $f_1(x,t)$ is zero-valued on the a-domain. In numerical work, the infinity domains limits can be cut short since it is realistic to assume that the temperature inside a working refrigerator cannot drop below some T_{minmin} value and cannot rise above some T_{maxmax} value.

$$\frac{\partial f_{0j}}{\partial t} + \frac{\partial}{\partial x}\left((ax+b)f_{0j}\right) = \frac{\sigma^2}{2}\frac{\partial^2 f_{0j}}{\partial^2 x}, j \in \{a,b\} \tag{B.4a}$$

$$\frac{\partial f_{1j}}{\partial t} + \frac{\partial}{\partial x}\left((ax+b+c)f_{1j}\right) = \frac{\sigma^2}{2}\frac{\partial^2 f_{1j}}{\partial^2 x}, j \in \{b,c\} \tag{B.4b}$$

$$f_{1b}(T_{\min}, t) = 0, f_{0b}(T_{\max}, t) = 0 \tag{B.5a}$$

$$f_{0a}(T_{\text{minmin}}, t) = 0, f_{1c}(T_{\text{maxmax}}, t) = 0 \tag{B.5b}$$

$$f_{0b}(T_{\min}, t) = f_{0a}(T_{\min}, t), f_{1b}(T_{\max}, t) = f_{1c}(T_{\max}, t) \tag{B.5c}$$

$$\frac{\partial}{\partial x} f_{1b}(T_{\min}, t) = \frac{\partial}{\partial x} f_{0b}(T_{\min}, t) + \frac{\partial}{\partial x} f_{0a}(T_{\min}, t) \tag{B.5d}$$

$$\frac{\partial}{\partial x} f_{1b}(T_{\max}, t) = \frac{\partial}{\partial x} f_{0b}(T_{\max}, t) - \frac{\partial}{\partial x} f_{1c}(T_{\max}, t) \tag{B.5e}$$

Fig. B.1(a) shows the temperature domains, and the stationary shape of the pdfs obtained after a long operation time of the TCL unit. In this case, the pdf is almost uniform across the thermostat temperature range. An important quantity of interest, the probability that the TCL is on, is given by the area under the pdf associated with the on-mode,

$$\Pr[m(t) = 1] = \int_{T_{\min}}^{T_{\text{maxmax}}} f_1(T, t) dT. \tag{B.6}$$

Furthermore, the area under both pdfs equals to 1, as it represents total probability.

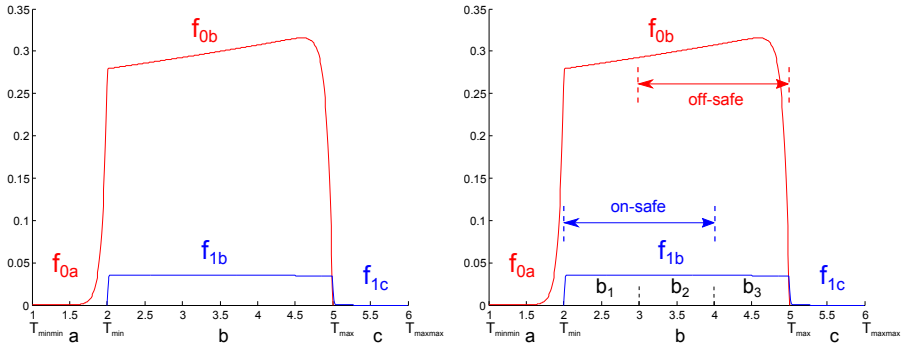

(a) Prob. density functions (b) Actuation ranges

Fig. B.1: Temperature domains and sketch of the temperature distributions at equilibrium

A PDE system can be recovered using the Fokker-Planck framework also for extensions of the continuous dynamics, such as multidimensionality (e.g. second order temperature dynamics) and jump-noises (modeling user interaction /door opening events).

Finite Volume Method

To solve the PDE, or equivalently propagate the pdf in time starting from an initial condition, numerical methods are employed and special care must be taken not to introduce unnecessary errors. Because of the conservation form of the Fokker-Planck equations, we choose FVM. This assures that the invariant of the system, probability, is conserved.

The idea is to partition the temperature domain, consisting of the sub-domains a, b, c, into a finite number of cells N_a, N_b, N_c. For convenience, we choose cells of equal sizes ΔT_a, ΔT_b and respectively ΔT_c for each domain. The continuous pdf function is replaced by a finite number of approximations points $F = [F_0^a, F_0^b, F_1^b, F_1^c]^T \in \mathbb{R}^{(N_a+2N_b+N_c)\times 1}$, each representing the average density value over a cell. This means that $F_{0a}(i)$ is designed to approximate the value $\int_{\text{Cell}_i} f_{0a}(T)dT$. Because of the linear form of the equations (the PDEs (B.4) are linear in the unknown function f) and of the boundary conditions, a linear finite-dimensional approximation dynamic can be obtained,

$$\dot{F}(t) = AF(t). \tag{B.7}$$

The resulting matrix A has the property that the columns sum to 0. This is consistent with the fact that the space discretized description is a Markov chain representation of the stochastic hybrid TCL model[2]. Furthermore, as a consequence of the fact that the columns sum to one, the matrix Ahas stable eigen values except one, which is exactly zero.

[2] *Added Note*: As mentioned, the non-diagonal elements are not guratanteed to be non-negative by a generic FVM technique alone, meaning that the matrix A will not have a true transition-rate form.

Lastly, the expected power consumption output of the TCL unit can be written as

$$y(t) = CF(t), \tag{B.8}$$

with $C = d \cdot \begin{bmatrix} 0_{1\times N_a} & 0_{1\times N_b} & \Delta T_b 1_{1\times N_b} & \Delta T_c 1_{1\times N_c} \end{bmatrix}$.

2.2 Population model

Homogeneous population

The state distribution model has so far been developed for a single TCL. If we consider a population of N *identical* units, the dynamic model (B.7) holds, where the vector F simply changes meaning from probabilities to fractions[3] of the population. The expected power consumption of the population is given by

$$y(t) = NCF(t). \tag{B.9}$$

Heterogeneous population

"Small" heterogeneities of the TCL population should not cause severe modeling errors, but "large" heterogeneities will cause a significant departure from the homogeneous case. If we consider heterogeneity given in the form of parameter distribution, an exact modeling approach is to augment the TCL model and add parameters as states with dynamic zero. This is sketched below for a single branch of the hybrid dynamic,

$$dT = \Big(aT(t) + b + m(t)c\Big)dt + \sigma dw \tag{B.10a}$$

$$\dot{a} = 0 \tag{B.10b}$$

$$\dot{b} = 0 \tag{B.10c}$$

$$\dot{c} = 0 \tag{B.10d}$$

$$\dot{\sigma} = 0 \tag{B.10e}$$

The corresponding multidimensional Fokker-Planck equation in the pdf $f(\mathbf{x}, t) = f([T, a, c, b, \sigma], t)$ resolves to

$$\frac{\partial f(\mathbf{x},t)}{\partial t} + \frac{\partial}{\partial x_1}\Big((x_2 x_1 + x_3) f(\mathbf{x},t)\Big) = \frac{x_5^2}{2}\frac{\partial^2 f(\mathbf{x},t)}{\partial^2 x_1}. \tag{B.11}$$

Unfortunately the approach suffers from the curse of dimensionality, since the space-variable $\mathbf{x} \in \mathbb{R}^5$ and a fine meshing of the five dimensional space is required to accurately recover the dynamics. Another observation is that, since the dynamics of the parameter-state are not connected to the dynamics of the temperature state, this formulation essentially leads to a clustering strategy, as used in [9]. The clustering strategy corresponds to a rough partitioning of the parameter space.

Another approach to modeling heterogeneous dynamics is by adding an extra term in the PDE (B.4) that can be fitted to account for the empirically observed damping/dissipation effect. This approach is taken in [6] using an increase of the already

[3] The state vector $F \in \mathbb{R}^{N_a+2N_b+N_c}$ is defined to represent average density values. It can be scaled by the cell sizes to yield probability quantities, which are equivalent to fractions in the population case.

present diffusion term $\frac{\partial^2}{\partial x^2}$. Other operators could be consider for obtaining a better fit, perhaps taking inspiration from mechanical modeling.

2.3 Numerical verification

For a population composed of identical TCLs with known parameters, the only sources of inaccuracies are the fact that the number of units in the population is finite (this error is small for large populations) and the spatial discretization of the PDE (this error is also small in the FVM case). A more concerning source of errors is that a real population would not be composed of identical units.

The graphs in Fig. B.2 compare the power output of the model (B.7), (B.9) with Monte Carlo simulations of populations composed of $N = 10000$ units and different levels of heterogeneity. The scenario is that of a free response to synchronized initial condition where all units start from the same state $(T_{\max}, 0)$. This type of synchronization that generates a well known oscillatory behavior.

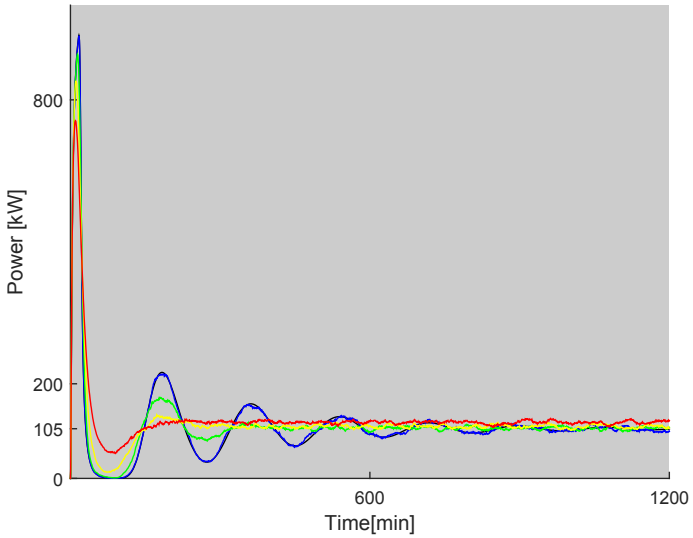

Fig. B.2: Free response of the power consumption. The model is shown in black, and Monte Carlo simulations in blue (identical units), green (10% heterogeneity), yellow (20% heterogeneity) and red (30% heterogeneity).

The heterogeneous populations are composed of units where the key Equivalent Thermal Parameters (ETP) of the TCL model (C, UA, W) and σ are each distributed according to a Gaussian profile with standard deviations 10%, 20% and 30% respectively, and truncated at $\pm 3\sigma$. It can be seen that the model matches well the power consumption of the population with identical units, but starts to degrade in performance with the increase of heterogeneity.

The parameters used for the TCL unit model are given in Table B.1, resulting in a duty-cycle[4] with an on-time of about 18 minutes and off-time of 160 minutes.

[4] *Added Note:* For clarity, it is remarked that the ON and OFF duration are calculated for a deterministic operation, without considering the white noise contributions.

Table B.1: TCL unit parameters

C (J/K)	UA (W/K)	T_a (°C)	W (W)
93920	1.432	24	100
η	σ (°C/s)	$T_{\min}$(°C)	$T_{\max}$(°C)
2.8	0.0065	2	5

3 Switching-Fraction Modeling

In order to externally influence the power consumption of the TCL population, a switching-fraction signal is introduced. This is composed of two rational numbers that have the meaning of percentages, $\epsilon = \{\epsilon_0, \epsilon_1\} \in \mathbb{Q}^2$, and is broadcast every T_c seconds. The signal triggers a percentage ϵ_0 of the units "on", which are also in the "on-safe" temperature range (to be defined next), to "switch-off", and a percentage ϵ_1 of the units "off", which are also in the "off-safe" temperature range, to "switch-on". The "on-safe" range is $[T_{\min}, T_{\max} - \Delta T_0]$, and the "off-safe" range is $[T_{\min} + \Delta T_1, T_{\max}]$.

3.1 Actuation at the unit-level

While the switching-fractions are given at the population level, the actual switch is decided at the unit level. The TCLs have to meet the requested fractions without communicating with each other. To do so, an individual TCL that is in the target group switches based on the result of a binomial trial with success rate equal to the broadcast fraction value. If the target group is large enough, by the law of large numbers, the response of the population will be close to the requested one.

Referring to the stochastic hybrid model from Section 2.1, this represents a change in the discrete dynamic (B.2). The thermostat mechanism that generates deterministic state-dependent switches remains in place, and in addition, a stochastic component is introduced. This can generate spontaneous switches in response to the external signal. The temperature safe-zones are specially defined to ensure that switches do not occur close to a relevant boundary, since they would quickly be reversed by the thermostat. Furthermore, minimum on/off guards can be introduced to block the generation of an external switch, again to avoid the undesirable fast switching behavior.

3.2 Actuation in the population model

The switching-fractions broadcast actuation has been introduced as a discrete-time strategy. We will therefore introduce it into a discrete-time state space form of (D.16), specifically

$$F(k+1) = A_d F(k), \quad A_d = e^{A \cdot T_c}. \tag{B.12}$$

Figure B.1(b) shows the temperature ranges of the switching-fraction signal. A switch-off fraction ϵ_0 will instantaneously transport probability from the temperature zone $[T_{\min}, T_{\max} - \Delta T_0]$ of f_{1b} to f_{0b}. Similarly, a switch-on fraction ϵ_1 will transport probability from the temperature zone $[T_{\min} - \Delta T_1, T_{\max}]$ of f_{0b} to f_{1b}. Notations b_1, b_2 and b_3 have been introduced in Fig.B.1(b) to define the safe-range partitions of the thermostat domain.

At the time step k^+, right after the broadcast, the pdfs over the temperature domain $[T_{\min}, T_{\max}]$ change in the following way,

$$F_{0b_1}(k^+) = F_{0b_1}(k) + \Delta F_{1b_1}(k) \tag{B.13a}$$
$$F_{1b_1}(k^+) = F_{1b_1}(k) - \Delta F_{1b_1}(k) \tag{B.13b}$$
$$F_{0b_2}(k^+) = F_{0b_2}(k) - \Delta F_{0b_2}(k) + \Delta F_{1b_2}(k) \tag{B.13c}$$
$$F_{1b_2}(k^+) = F_{1b_2}(k) + \Delta F_{0b_2}(k) - \Delta F_{1b_2}(k) \tag{B.13d}$$
$$F_{0b_3}(k^+) = F_{0b_3}(k) - \Delta F_{0b_3}(k) \tag{B.13e}$$
$$F_{1b_3}(k^+) = F_{1b_3}(k) + \Delta F_{0b_3}(k)\ . \tag{B.13f}$$

If the minimum on-off time effects are not considered, then

$$\Delta F_{1b_1} = \epsilon_0 F_{1b_1} \tag{B.14a}$$
$$\Delta F_{1b_2} = \epsilon_0 F_{1b_2} \tag{B.14b}$$
$$\Delta F_{0b_2} = \epsilon_1 F_{0b_2} \tag{B.14c}$$
$$\Delta F_{0b_3} = \epsilon_1 F_{0b_3}\ , \tag{B.14d}$$

leading to the following bilinear form

$$F(k+1) = E(k+1)A_d F(k)\ , \tag{B.15}$$

where $E(k)$ is a matrix depending on $\epsilon_0(k)$ and $\epsilon_1(k)$. The block form[5] of the $E(k)$ matrix is

$$\begin{bmatrix} I & 0 & 0 & 0 & 0 & 0 & 0 & 0 \\ 0 & I & 0 & 0 & \epsilon_{10}(k)I & 0 & 0 & 0 \\ 0 & 0 & (1-\epsilon_{01}(k))I & 0 & 0 & \epsilon_{10}(k)I & 0 & 0 \\ 0 & 0 & 0 & (1-\epsilon_{01}(k))I & 0 & 0 & 0 & 0 \\ 0 & 0 & 0 & 0 & (1-\epsilon_{10}(k))I & 0 & 0 & 0 \\ 0 & 0 & \epsilon_{01}(k)I & 0 & 0 & (1-\epsilon_{10}(k))I & 0 & 0 \\ 0 & 0 & 0 & \epsilon_{01}(k)I & 0 & 0 & I & 0 \\ 0 & 0 & 0 & 0 & 0 & 0 & 0 & I \end{bmatrix}. \tag{B.16}$$

To include the minimum on-off effects, it is required to account for the units that are "locked", meaning that they have recently switched and cannot do so again. This reduces the amount of TCL units that are responsive to the broadcast signal. The population modeling needs to be extended to include tracking of the locked units. The following is similar to [9].

Let us assume that the on-lock duration (minimum on time) is 300[s], the same for all units, and equivalent to $l_1 = 5$ control steps for $T_c = 60$[s]. Similarly, off-lock duration (minimum off time) is associated with l_0. Initially, after a period with no control, all units are available for external switching. The first broadcast actuation causes a change in the distribution state F as described in (B.15). After the broadcast, the units that have switched become locked. We have direct information about the distribution of the locked states, this is $[\Delta F_{0b_2}(k), \Delta F_{0b_3}(k)]$ (just switched on), and $[\Delta F_{1b_1}(k), \Delta F_{1b_2}(k)]$ (just switched off). These proportions of the distribution are

[5] *Added Note:* The block form has been added for clarity.

locked for a number l_1 and l_0 respectively of time steps, and we have to also take into account that these distribution will evolve in the temperature space during this time.

The following additional states are added to the model, representing the distribution of on-locked units and off-locked units respectively, at different locking stages.

$$F_{1L}^l = [F_{1Lb_1}^l, F_{1Lb_2}^l, F_{1Lb_3}^l, F_{1Lc}^l]^T, l \in \{0, \cdots, l_1 - 1\} \tag{B.17}$$

$$F_{0L}^l = [F_{0La}^l, F_{0Lb_1}^l, F_{0Lb_2}^l, F_{0Lb_3}^l]^T, l \in \{0, \cdots, l_0 - 1\}. \tag{B.18}$$

These states propagate in the following way,

$$F_{1L}^{l+1}(k+1) = A_{d1} F_{1L}^l(k) \tag{B.19}$$

$$F_{0L}^{l+1}(k+1) = A_{d0} F_{0L}^l(k), \tag{B.20}$$

where matrices A_{d1} and A_{d0} represent temperature dynamics without thermostat switches.

In the end, the population model with switching-fraction actuation and minimum on/off times can be written as an augmented form of (B.15), namely

$$\bar{F}(k+1) = \bar{E}(k+1)\bar{A}_d F(k). \tag{B.21}$$

The bilinear form of the actuation in (B.15) and (B.21) can be seen as intrinsic to the TCL problem. It also appears in the case of a thermostat set-point actuation [1]. This is because when using a physically based modeling approach, the actuation does not represent an external input to the system, but rather an internal transformation/change. Although the work in [4] proposes a linear formulation of the control, by letting the decision variables be the $\Delta F(k)$ quantities from (B.13), this has some disadvantages. In this case, there are as many independent control channels as bins in the relevant b_1, b_2 and b_3 temperature zones. The control is therefore dependent on a particular spatial discretization, and multiple switching fractions need to be broadcast at every time step.

4 Open-Loop Control

The objective of this section is to use models (B.15) and (B.21) for controling the aggregate power consumption of the TCL population. We define an optimization to generate an actuation sequence consisting of switching fractions $\epsilon_0(k)$ and $\epsilon_1(k)$. This actuation sequence is applied in open loop to drive the population to consume power in a manner that closely matches a given external reference.

4.1 Optimization problem

Given a power reference over a time horizon with Tsteps, and the initial state of the TCL population as the distribution F_0, an optimization for minimizing the power consumption tracking error can be written as

$$\begin{aligned} \underset{\epsilon_1(k),\epsilon_0(k)}{\text{minimize}} \quad & f(\epsilon) = \textstyle\sum_{k=1}^{T} \Big(CF(k) - r(k) \Big)^2 \\ \text{subject to} \quad & \\ & 0 \leq \epsilon_0(k) \leq 1 \\ & 0 \leq \epsilon_1(k) \leq 1 \end{aligned} \tag{B.22}$$

where, using model (B.15),

$$F(k) = E(k)A_d E(k-1)A_d \cdots E(1)A_d F_0. \tag{B.23}$$

Gradient of the objective function

The first order optimality conditions on (B.22) lead to,

$$\begin{aligned}\frac{\partial f(\epsilon)}{\partial \epsilon_x(l)} &= 2\Big(\sum_{k=l}^{T}[CF(k) - r(k)]C^*_{l,k}\Big)E_x(l)AdF(l-1)\\ &= 0\end{aligned} \tag{B.24}$$

$$\text{with } C^*_{l,k} = C \cdot \prod_{l+1}^{i=k\downarrow} E(i)A_d, \forall k \geq l, \tag{B.25}$$

matrix $E_x(l) = \partial E(l)/\partial \epsilon_x(l)$, and the subscript $()_x$ standing in for either 0 or 1. Since the optimization problem is not convex (the objective expression is multilinear in the decision variables), it is important to specify this gradient information to the numerical solver to improve computational time and performance. Furthermore, the line-vector $C^*_{l,k}$ can be computed recursively

$$C^*_{l,k} = C^*_{l+1,k}E(l)A_d, \tag{B.26}$$

and the sparse structure of the matrices involved, especially E and A_d, can be used to reduce computation time.

The optimization has the same form when considering the minimum on/off effects, requiring only to replace F, C, A_d, E with the augmented versions, $\bar{F}, \bar{C}, \bar{A}_d, \bar{E}$.

4.2 Numerical examples

This section[6] presents numerical results for tracking two references composed of step segments over a time horizon of two hours. The control time-step is $T_c = 60$[s] and the initial state of the population is close to the equilibrium distribution shown in Fig. B.1. The optimization is implemented numerically in MATLAB with a generic interior point algorithm. Figure B.3 shows the results, and it can be seen that model without the locking mechanism can be driven to consume closely to the desired reference. The power flexibility of the model with the locking mechanism is somewhat reduced. Although this is a good solution, because of the non-convex formulation we cannot conclude that these results represent the optimum.

Figure B.4 shows the results of actuating Monte Carlo populations ($N = 10000$) using the optimized switching fraction signals. The performance is good for both the homogeneous and the heterogeneous populations suggesting that the switching fractions broadcast is robust to heterogeneity[7]. On the other hand, as can be seen from Fig. B.4(a) and B.4(c), the locking effect is significant and cannot be avoided in the modeling.

[6] *Added Note:* The numerical results and figures presented in this section are updated versions of published paper. The changes are not significant to alter the conclusion.

[7] Results are shown here for Gaussian distributed parameters. Similar results are obtained also for uniformly distributed parameters.

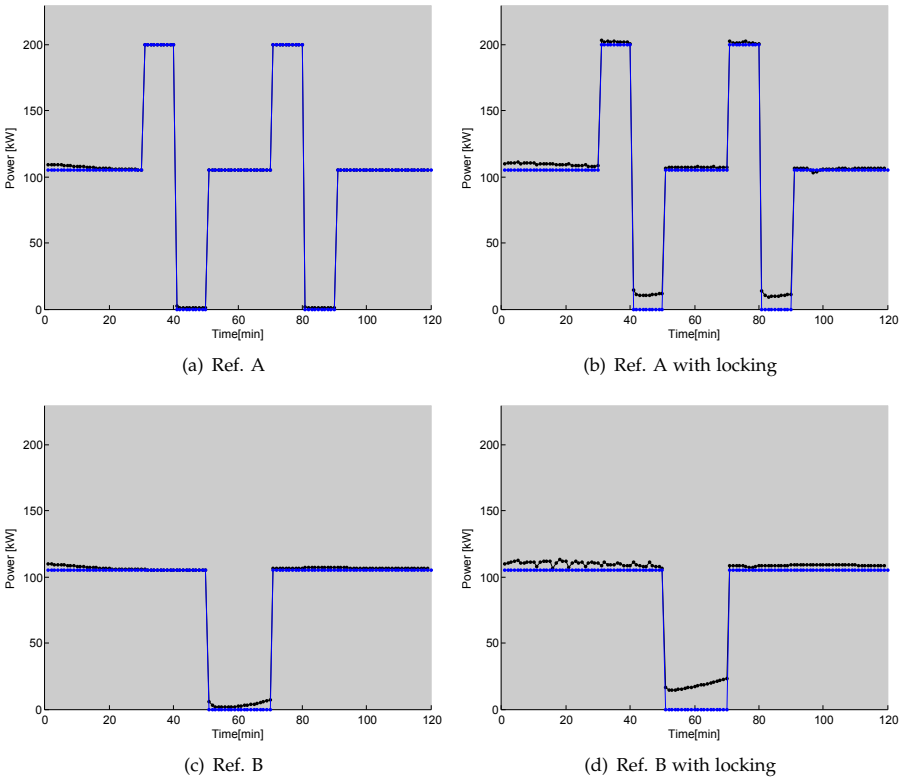

(a) Ref. A

(b) Ref. A with locking

(c) Ref. B

(d) Ref. B with locking

Fig. B.3: Power reference (blue) and the optimized consumption (black) of the model with (B.21) and without locking (B.15).

5 Conclusion

Demand response of TCL populations can provide a great support to the electrical grid by reducing the capacity need for fast reserves. The switching fraction broadcast is a reliable way of engaging and controlling the power output of such populations within their natural flexibility. This intrinsic flexibility is most accurately represented by a physically based modeling technique. We have introduced a switching-fraction actuation entering the system in a bilinear form. While this is not an ideal form for control, we have shown that an open-loop model predictive strategy can still be computationally tractable and robust to heterogeneity. Future work will make use of these results to complete a control architecture with feedback and state-estimation.

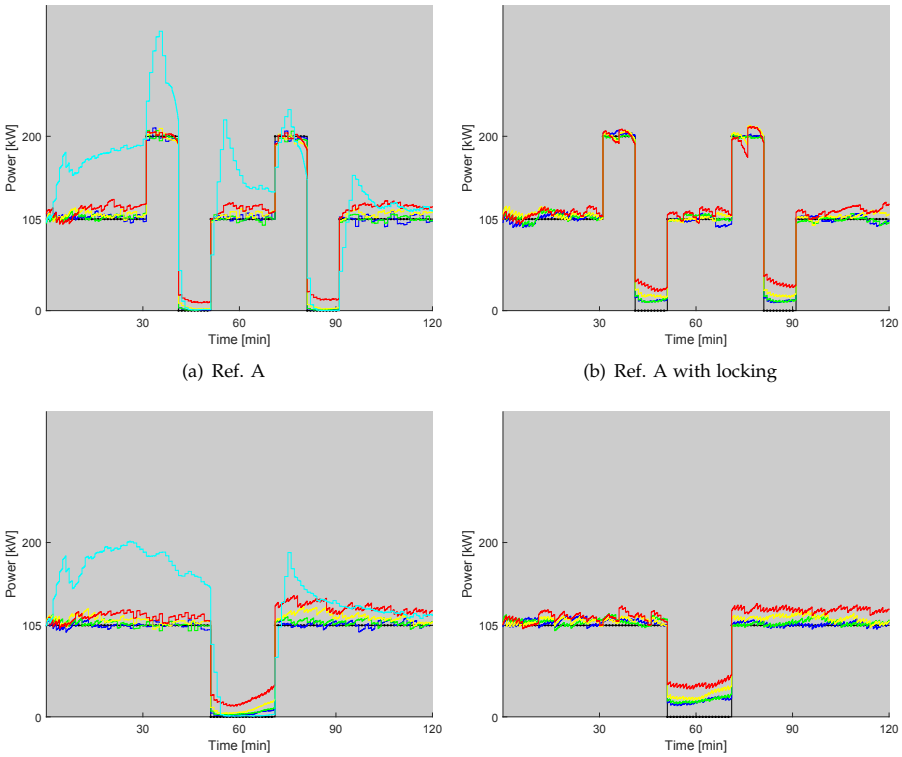

(a) Ref. A

(b) Ref. A with locking

(c) Ref. B

(d) Ref. B with locking

Fig. B.4: TCL populations under optimized actuation. The color legend is the same as in Fig. B.2. The Monte Carlo populations on the left do not have the locking mechanism implemented (except cyan), while the populations on the right all have it.

References

[1] Saeid Bashash and Hosam K Fathy. Modeling and control of aggregate air conditioning loads for robust renewable power management. *Control Systems Technology, IEEE Transactions on*, 21(4):1318–1327, 2013.

[2] Duncan S Callaway. Tapping the energy storage potential in electric loads to deliver load following and regulation, with application to wind energy. *Energy Conversion and Management*, 50(5):1389–1400, 2009.

[3] Satoru Ihara and Fred C Schweppe. Physically based modeling of cold load pickup. *Power Apparatus and Systems, IEEE Transactions on*, (9):4142–4150, 1981.

[4] Stephan Koch, Johanna L Mathieu, and Duncan S Callaway. Modeling and control of aggregated heterogeneous thermostatically controlled loads for ancillary services. In *Proc. PSCC*, pages 1–7, 2011.

[5] Roland Malhame and Chee-Yee Chong. Electric load model synthesis by diffusion approximation of a high-order hybrid-state stochastic system. *Automatic Control, IEEE Transactions on*, 30(9):854–860, 1985.

[6] Scott Moura, J Bendtsen, and V Ruiz. Modeling heterogeneous populations of thermostatically controlled loads using diffusion-advection pdes. In *Proceedings of the 2013 ASME Dynamic Systems and Control Conference, Stanford, California*, 2013.

[7] S. Soudjani and A. Abate. Aggregation of thermostatically controlled loads by formal abstractions. In *ECC 2013: Eropean Control Conference*, pages 4232–4237, Zurich, Switzerland, July 2013.

[8] Luminita C Totu, John Leth, and Rafael Wisniewski. Control for large scale demand response of thermostatic loads. In *American Control Conference (ACC), 2013*, pages 5023–5028. IEEE, 2013.

[9] Wei Zhang, Jianming Lian, Chin-Yao Chang, and Karanjit Kalsi. Aggregated modeling and control of air conditioning loads for demand response. *IEEE Transactions on Power Systems*, 28(4):4655 – 4664, 2013.

Paper C

Modeling Populations of Thermostatic Loads with Switching-Rate Actuation

Luminița C. Totu, Rafael Wisniewski and John Leth

The paper has been published in the
proceedings of the 4th Workshop on Hybrid Autonomous Systems, 2014.

The layout has been revised, and small editorial changes have been made. Content relavant changes, if any, are marked with explicit footnotes.

Abstract

We model thermostatic devices using a stochastic hybrid description, and introduce an external actuation mechanism that creates random switches in the discrete dynamics. We then conjecture the form of the Fokker-Planck equation and successfully verify it numerically using Monte Carlo simulations. The actuation mechanism and subsequent modeling result are relevant for power system operation.

1 Introduction

In the context of power system operation and Smart Grids technologies, thermostatically controlled loads (TCLs), such as refrigerators, air-conditioners or heat-pumps, are seen as a promising resource of demand response services [3, 9]. Essentially, TCLs have the potential of acting as distributed energy storages that can be scheduled and controlled to balance out grid fluctuations. Arguably, this can be used to decrease the overall capacity requirements for spinning reserves, and contribute towards the integration of more intermittent generation, such as wind, into the grid.

Since the individual TCL has a very small energy storage capacity relative to the scale of power system operation, any relevant demand response strategy requires the participation of a very large number of TCLs. For this reason, developing demand response algorithms requires not only models for individual TCLs, but also models for TCL populations. An overview of recent population modeling results can be found in [7].

This work presents an aggregate model for a TCL population under a specific demand response strategy, the Switching Rate broadcast actuation. This actuation is closely related to the Switching Fraction broadcast proposed and analyzed in [10–12], but has the added advantage that the switching actions are not synchronized across the population. An individual TCL unit is modeled as a Stochastic Hybrid System (SHS) with the Markov property, and the resulting population model is in the form of a Partial Differential Equation (PDE) or Partial Integro-Differential Equation (PIDE) system and boundary conditions. This PDE form corresponds to a generalized Fokker-Planck (Forward Kolmogorov) operator [1] associated with the TCL stochastic hybrid system.

The Fokker-Planck approach for TCL population modeling is not in itself new. It was first used in [8] for modeling a TCL population without (continuous) external actuation. However, to the best knowledge of the authors, the Switching Rate actuation variant and the resulting population model are new and should be a useful contribution to the topic.

The article is organized as follows. The stochastic hybrid model of the TCL unit and the Switching Rate actuation are presented in Section 2. PDE population models are then given in Section 3. Numerical simulations and results addressed in Section 4, while Section 5 points to future work.

2 Stochastic Hybrid Model for the TCL Unit

Similar to other works, we consider that the TCL unit can be abstracted as a hybrid dynamical system with temperature as a continuous state and the power mode, "on"

or "off", as a discrete state. An informal presentation follows next where mathematical constructions are not rigorously addressed, but remarks about the formal setting are made towards the end of the section.

2.1 Unactuated TCL

We consider the dynamics of the continuous state represented by Stochastic Differential Equations (SDE) of the following form,

$$dT_t = u_0(T_t, t)dt + \sigma_0(T_t, t)dw_t, \quad \text{for } m_t = 0 \tag{C.1a}$$

$$dT_t = u_1(T_t, t)dt + \sigma_1(T_t, t)dw_t, \quad \text{for } m_t = 1, \tag{C.1b}$$

where $T \in \mathbb{R}$ is the temperature state, $u_0(\cdot), u_1(\cdot) : \mathbb{R} \times [0, \infty) \to \mathbb{R}$ are deterministic, (potentially) time-varying vector fields, $w_t \in \mathbb{R}$ is a Wiener process, $\sigma_0(\cdot), \sigma_1(\cdot) : \mathbb{R} \times [0, \infty) \to \mathbb{R}^{n \times m}$ are diffusion coefficients, and $m_t \in \{0, 1\}$ is the mode state. We choose one-dimensional spaces for the continuous state T_t and the Brownian motion w_t since it simplifies presentation, but other low-dimensional spaces (e.g. [12] uses a two-dimensional temperature state) could also be considered and the subsequent population model carries over in a straightforward manner. However, it is noted that numerical analysis becomes more difficult as the state space increases, since the Fokker-Planck approach suffers from the curse of dimensionality and can become intractable.

The dynamics of the discrete state involve a thermostat mechanism that is considered equivalent to a state dependent, deterministic rule. For example, in the case of a cooling unit, this can be described as

$$m_{t^+} = \begin{cases} 0, & \text{if } T_t \leq T_{\min} \text{ and } \ m_{t^-} = 1 \\ 1, & \text{if } T_t \geq T_{\max} \text{ and } \ m_{t^-} = 0 \\ m_{t^-}, & \text{otherwise} \end{cases}, \tag{C.2}$$

where function argument notations t^+ and t^- denote limit from the right and from the left respectively, and $T_{\min}$ and $T_{\max}$ are the thermostat boundaries. In the multi-dimensional case, the thermostat-triggering temperature has to be one of the states.

The output of the TCL unit is represented by the instantaneous power consumption $y_t \in \mathbb{R}_+$, which must be a function of at least m_t. More specific, we consider that the power consumption is constant $r > 0$ if the mode is "on" and is zero otherwise,

$$y_t = r m_t, \ r > 0 \, . \tag{C.3}$$

2.2 Switching-Rate actuation

To make demand response possible, a control element needs to be introduced. The objective is to create the possibility of modifying the power consumption pattern of the TCL unit (and thus also that of the population) in a non-disruptive manner, from an external channel. Non-disruptive means that the TCL temperature is maintained within the thermostat dead-band at all times and no other operational constraints are broken. The Switching Rate mechanism achieves this objective by adding a control element to the discrete-state dynamics.

The idea is to introduce, in addition to the thermostat, a new type of switching: rate-switching. While the thermostat switching is governed by a deterministic law, rate-switching will take place according to a probabilistic law parameterized by an external signal. The external signal will control the rate of occurrence of the probabilistic switches (the average number of switching events in a given period of time).

Furthermore, a practical consideration needs to be addressed. A frequent switching behavior is undesirable because it can damage the equipment (e.g. compressor components) and because it is inefficient. If the cooling/heating cycle is active for only a short period of time, it will not produce any significant temperature effect. In addition, temperature dynamics of type (C.1) will be highly inexact in such cases.

To avoid frequent switching, two heuristics are added. First, we will prevent the pattern of a thermostat- and a rate-switch occurring closely in time. This is done by allowing rate-switching only if the temperature is a safe distance away from the relevant thermostat boundary. For example, in the case of a cooling unit, switch-off actions are allowed only when the temperature is some distance away from the upper bound (hot zone) of the thermostat interval, and similarly, switch-on actions are allowed only if the temperature is some distance away from the lower bound (cold zone). In this way, thermostat- and rate-switches will not compete. Second, we will prevent multiple rate-switches to occur closely in time. This is done by imposing a minimum dwell time for modes "on" and "off".

The Switching Rate mechanism is described next using more mathematical terms, but the presentation remains informal.

We introduce ΔT_0 and ΔT_1 as the safe distances from the thermostat boundaries, and add a new continuous state $d_t \in \mathbb{R}_+$, the dwell time. The dwell time acts as a clock variable, $\dot{d}_t = 1$, and resets to zero after each switch. We denote by M_0 the minimum dwell time in the "off" state, and by M_1 the minimum dwell time in the "on" state. The external control signals for the switch-off and switch-on rates are ϵ_t^0 and ϵ_t^1 respectively. The probability of a rate-switching event in a small time interval $\tau << 1$ can be described as,

$$\Pr\big[\, m_{t+\tau} = 1 \;\big|\; m_t = 0 \wedge T_t \in [T_{\min} + \Delta T_1, T_{\max}) \wedge d_t \geq M_0 \wedge \epsilon_t^1 \,\big] = \\ = \lambda_1(\epsilon_t^1, T_t)\tau + o(\tau)\,, \qquad \text{(C.4a)}$$

$$\Pr\big[\, m_{t+\tau} = 0 \;\big|\; m_t = 1 \wedge T_t \in (T_{\min}, T_{\max} - \Delta T_0] \wedge d_t \geq M_1 \wedge \epsilon_t^0 \,\big] = \\ = \lambda_0(\epsilon_t^0, T_t)\tau + o(\tau)\,, \qquad \text{(C.4b)}$$

where the temperature ranges in the conditional part of the probability are exemplified for a cooling unit, and λ_1 and λ_0 are real and positive valued rate-functions, which can be seen as part of the (control) design. A straightforward and simple choice for these functions is a temperature-independent form,

$$\lambda_i(\epsilon, T) = \epsilon,\ i \in \{0, 1\}\,. \qquad \text{(C.5)}$$

Compared to the Switching Fraction approach [10–12], the Switching Rate actuation has the advantage that individual switch events will not be synchronized across the population. This is useful for at least one reason. It is well known that the power consumption of an individual TCL exhibits a peak (compressor peak) right after switch-on and before converging to the nominal value. This is not captured in

the modeling (C.3), and could in practice cause short but high demand peaks that negatively impact grid stability if the switch-on actions are synchronized.

2.3 Remarks on a GSHS description

The TCL unit could formally be described in the framework of Generalized Stochastic Hybrid Systems (GSHS) [2]. A GSHS is a hybrid system where the continuous states evolve according to a SDEs (as is the case of (C.1)), and where the discrete dynamics can produce jumps in the continuous state (as it the case with the reset of the dwell time state d_t). Furthermore, the discrete dynamics are described by probabilities (in the TCL case, the switch-rate laws (C.4)), or occur when the continuous state hits a certain domain boundary (in the TCL case, the thermostat mechanism). A GSHS has the strong Markov property and trajectories that are right continuous with left limits.

The only issue that needs to be addressed is the fact that the GSHS definition does not explicitly include dependences of an external control element, as is the case of the transition rate functions, or time, as is the case with the continuous dynamics. We postpone this technical discussion for future work.

3 Probability Density Model

In the absence of the Switching Rate mechanism, the TCL unit can be described, equivalent in effect with the SHS characterization, in terms of the probability density function (pdf) over the hybrid state space $(T, m) \in \mathbb{R} \times \{0, 1\}$, namely

$$f_i(x,t) = \frac{1}{dx}\Pr\big[T(t) \in (x, x+dx] \ \wedge \ m(t) = i \ \big] \ . \tag{C.6}$$

Building on elements and results from Markov process theory (e.g. [4, 6]), [8] showed that the dynamic of $f_i(x,t)$ can be described analytically. In particular, the dynamic of $f_i(x,t)$ represents the generator of the forward-operator linear semigroup associated with the TCL SHS. For dynamical systems characterized by regular SDEs, without hybrid elements, this generator is known as the Fokker-Planck equation. Therefore, the result in [8] can be seen as a Fokker-Planck operator specific to the TCL SHS.

Unlike the SHS form, a TCL description in terms of the pdf translates almost directly into a (homogeneous) population model. Probability quantities simply change meaning to population fractions, see e.g. [8] and [11]. The latter contains also a discussion and results on heterogeneous populations.

3.1 Unactuated TCL

For an unactuated TCL unit, [8] showed that the dynamics of $f_i(x,t)$ can be described by a system of Fokker-Planck equations, each acting on a sub-domain of the hybrid state-space. These sub-domains are $0a = (-\infty, T_{\min}) \times \{0\}$, $0b = (T_{\min}, T_{\max}) \times \{0\}$, $1b = (T_{\min}, T_{\max}) \times \{1\}$, $1c = (T_{\max}, \infty) \times \{1\}$, and the pdf $f_i(x,t)$ is reconstructed from four segments, f_{0a}, f_{0b}, f_{1b}, and f_{1c}. The separation of the pdf into components f_0 and f_1 corresponds to the "off" and "on" discrete modes, and it appears naturally as seen already in (C.6). The partition of the temperature domain into the regions a, b and c, is a result of the pdf $f_i(x,t)$ not being x-differentiable at $T_{\min}$ and $T_{\max}$.

Furthermore, the pdf is zero over the omitted domains $1a$ and $0c$. These features are a result of the thermostat. The dynamic for each pdf segment is given by the Fokker-Planck equations

$$\frac{\partial f_{ip}}{\partial t}(x,t) = -\frac{\partial}{\partial x}\left(u_i(x,t)f_{ip}(x,t)\right) + \frac{\partial^2}{\partial x^2}\left(\frac{1}{2}\sigma_i^2(x,t)f_{ip}(x,t)\right), \tag{C.7}$$

and the following boundary conditions apply,

$$f_{1b}(T_{\min},t) = 0,\ f_{0b}(T_{\max},t) = 0 \tag{C.8a}$$
$$f_{0a}(-\infty,t) = 0,\ f_{1c}(+\infty,t) = 0 \tag{C.8b}$$
$$f_{0b}(T_{\min},t) = f_{0a}(T_{\min},t),\ f_{1b}(T_{\max},t) = f_{1c}(T_{\max},t) \tag{C.8c}$$
$$h_{0a}(T_{\min},t) = h_{0b}(T_{\min},t) + h_{1b}(T_{\min},t) \tag{C.8d}$$
$$h_{1c}(T_{\max},t) = h_{0b}(T_{\max},t) + h_{1b}(T_{\max},t) \tag{C.8e}$$

where $i \in \{0,1\}$ and $p \in \{a,b,c\}$, in the allowed combinations mentioned above, $h_{ip}(x,t)$ are probability flows defined as $\int \frac{\partial f_{ip}}{\partial t}dx$, and (C.8d) and (C.8e) are particular to the case of a cooling unit. For the differential forms in the right hand side of (C.7) to exist, it is implied that the functions u_i and σ_i need to be sufficiently smooth.

3.2 Switching-Rate actuation

We first consider Switching Rate actuated TCLs without the feature of the minimum dwell time. The pdf dynamic corresponding to a TCL unit with rate-switching can be described in this case by the PDE system

$$\frac{\partial f_{0a}}{\partial t} = -\frac{\partial}{\partial x}\left(u_0 f_{0a}\right) + \frac{\partial^2}{\partial x^2}\left(\frac{1}{2}\sigma_0^2 f_{0a}\right) \tag{C.9a}$$
$$\frac{\partial f_{0b}}{\partial t} = -\frac{\partial}{\partial x}\left(u_0 f_{0b}\right) + \frac{\partial^2}{\partial x^2}\left(\frac{1}{2}\sigma_0^2 f_{0b}\right) - \bar{\lambda}_1 f_{0b} + \bar{\lambda}_0 f_{1b} \tag{C.9b}$$
$$\frac{\partial f_{1b}}{\partial t} = -\frac{\partial}{\partial x}\left(u_1 f_{1b}\right) + \frac{\partial^2}{\partial x^2}\left(\frac{1}{2}\sigma_1^2 f_{1b}\right) + \bar{\lambda}_1 f_{0b} - \bar{\lambda}_0 f_{1b} \tag{C.9c}$$
$$\frac{\partial f_{1c}}{\partial t} = -\frac{\partial}{\partial x}\left(u_1 f_{1c}\right) + \frac{\partial^2}{\partial x^2}\left(\frac{1}{2}\sigma_1^2 f_{1c}\right) \tag{C.9d}$$

together with the boundary conditions (C.8). The notation $\bar{\lambda}$ is used to extend the function λ with zero values over the unsafe temperature distances ΔT_0 and ΔT_1. In the case of a cooling unit, this translates into

$$\bar{\lambda}_1(\epsilon,T) = \begin{cases} 0,\ T \in (T_{\min}, T_{\min}+\Delta T_1) \\ \lambda_1(\epsilon,T),\ T \in [T_{\min}+\Delta T_1, T_{\max}) \end{cases} \tag{C.10}$$

$$\bar{\lambda}_0(\epsilon,T) = \begin{cases} \lambda_0(\epsilon,T),\ T \in (T_{\min}, T_{\max}-\Delta T_0] \\ 0,\ T \in (T_{\max}-\Delta T_0, T_{\max})\ . \end{cases} \tag{C.11}$$

The reason why adding terms $\bar{\lambda}_1 f_{0b}$ and $\bar{\lambda}_0 f_{1b}$ gives a fitting dynamic in (C.9a) is related to the exponential behavior of the survival and jump switch-rate times as

$\Delta t \to 0$. We refer to [1] for a more elaborate mathematical discussion in the context of GSHS.

We now include minimum dwell time conditions and consider the complete Switching Rate actuation. The idea is to continuously track the part of the pdf that becomes locked for the external actuation. The same approach is used in [12] and [11] in the context of the Switching Fraction actuation. We introduce two new density functions corresponding to the locked condition for mode "off" and for mode "on", $L_0 : (-\infty, T_{\max}) \times [0, M_0) \times [0, \infty) \to \mathbb{R}_+$ and $L_1 : (T_{\min}, \infty) \times [0, M_1) \times [0, \infty) \to \mathbb{R}_+$, defined as

$$L_i(x, y, t) = \frac{1}{dxdy} \Pr\left[\ T_t \in (x, x + dx] \ \wedge d_t \in (y, y + dy] \ \wedge m_t = i \ \right]. \tag{C.12}$$

Using these pdfs, we can evaluate the part of $f_i(x, t)$ which remains responsive to the actuation. The terms $\bar{\lambda}_1 f_{0b}$ and $\bar{\lambda}_0 f_{1b}$ will thus be replaced in (C.9a) by $\bar{\lambda}_1 \left(f_{0b} - \int_0^{M_0} L_0(x, y, t) dy \right)$ and $\bar{\lambda}_0 \left(f_{1b} - \int_0^{M_1} L_1(x, y, t) dy \right)$.

The new pdfs must also be propagated in time. Their dynamic is given by normal Fokker-Planck equations, since no switching mechanism is active in the interior of the domains. These are

$$\frac{\partial L_i}{\partial t}(x, y, t) = -\frac{\partial}{\partial x}\left(u_i(x, t) L_i(x, y, t) \right) - \frac{\partial}{\partial y} L_i(x, y, t) + \frac{\partial^2}{\partial x^2}\left(\frac{1}{2}\sigma_i^2(x, t) L_i(x, y, t) \right), \tag{C.13}$$

with boundary conditions that follow naturally,

$$L_i(x, 0, t) = \bar{\lambda}_i \left(f_{\bar{i}b} - \int_0^{M_{\bar{i}}} L_{\bar{i}}(x, y, t) dy \right) \tag{C.14a}$$

$$L_i(x, M_i, t) = 0 \tag{C.14b}$$

$$L_0(-\infty, y, t) = 0, \ L_0(T_{\max}, y, t) = 0 \tag{C.14c}$$

$$L_1(T_{\min}, y, t) = 0, \ L_1(\infty, y, t) = 0 \tag{C.14d}$$

where $i \in \{0, 1\}$, and $\bar{i} = 1 - i$. Eq. (C.14b), (C.14c) and (C.14d) represent absorbing boundaries, while (C.14a) represents the incoming density current (or flow) of "newly locked" for which the dwell time state d_t has just been reseted to zero.

4 Numerical Simulation

This section verifies numerically the probability density model of the Switching Rate actuation, without the minimum dwell time feature. The verification procedure consists of two numerical simulations: a Monte Carlo analysis running multiple SHS model instances, and a finite dimensional linear approximation of the pdf PDE dynamics via a Finite Volume technique. The results show an equivalence between the two simulations.

The SHS simulation consists of time-discretized dynamics with a sample period $\tau_s = 1$s. The SDEs are simulated with the Euler-Maruyama method. The set-up is such that the control signal ϵ is constant during the sample period τ_s, and rate-switches are

generated as Bernoulli trials with success rate $1 - e^{-\epsilon_i \tau_s}$, when the temperature is in the safe-zone.

The PDE model is the basis for the second simulation. Eq. (C.9a) together with boundary condition (C.8) represent an infinite-dimensional dynamic. We approximate this dynamic with a finite-dimensional form via the Finite Volume Method (FVM), see e.g. [5]. This results in a numerical approximation of the weak solution of the PDE system. The FVM has the property of being locally and globally conservative, which will ensure that the probability in the system will always sum to one. We implement the FVM using an uniform grid, and a linear, cell-centered, piecewise-quadratic reconstruction scheme with an upstream flux rule[1]. Because of Godunov's order barrier theorem, this third order accurate reconstruction scheme can create spurious oscillations, but no significant effects have been noticed in practice. Applying non-linear elements to the reconstruction scheme to correct this possibility is not an option, as it is important to obtain a dynamic that is linear in the state. We obtain a finite-dimensional dynamic of the following form,

$$\dot{F}_t = (A + B_0\epsilon_0 + B_1\epsilon_1)F_t,\ F_t \in \mathbb{R}^n,\ A, B_0, B_1 \in \mathbb{R}^{n\times n}. \tag{C.15}$$

We use the following TCL model elements $u_i(T,t) = aT + b_i$, $\sigma_i(T,t) = \sigma$, with parameter values $a = -1.5247^{-05}$, $b_0 = 3.6593^{-04}$, $b_1 = -0.0026$, $\sigma = 0.0065$, $T_{\min} = 2$, $T_{\max} = 5$, meant to approximate a refrigerator unit similar to [10, 11]. Rate-functions λ of the form (C.5) have been used. A practical deployment scenario requires a coordination center broadcasting the actuation signal $\epsilon_t = (\epsilon_t^0, \epsilon_t^1)$. Between broadcasts, the TCL units operate with the previously received values, resulting in a scenario with piecewise constant actuation. The broadcast sample period is $\tau_c = 60$s. Simulations take place over a time horizon of two hours, and two actuation signals are tested. These signals have a specially chosen form derived from the results in [11], which is meant to show the power consumption flexibility. Figures C.1 and C.2 show comparisons between the Monte Carlo SHS simulation with 10000 identical units and the linear system model, for both pdf and power output.

5 Future Work

These successful numerical results motivate future work, in two directions. First, the modeling result could be consolidated by more rigorous mathematical considerations, such as completing the GSHS description. Moreover, a two dimensional FVM scheme needs to be set up to introduce the minimum dwell time feature. Secondly, the bilinear model (C.15) can be analyzed for control.

[1] *Added Note:* This is a control-volume-based finite element scheme, a hybrid finite-volume/finite-element method.

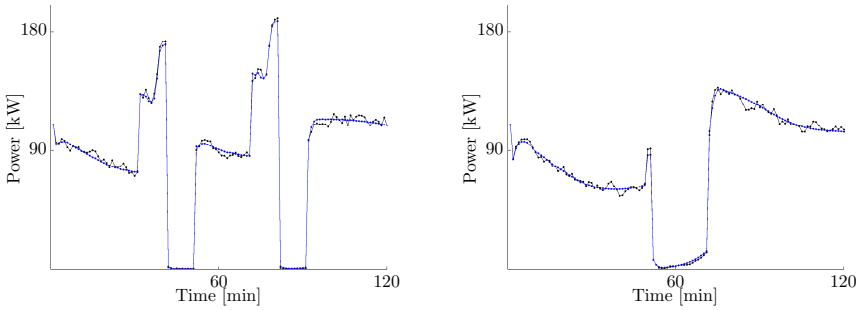

(a) Input signal A (b) Input signal B

Fig. C.1: Power consumption of the TCL population. The output of the Monte Carlo simulation is shown in black, and the PDE model is shown in blue.

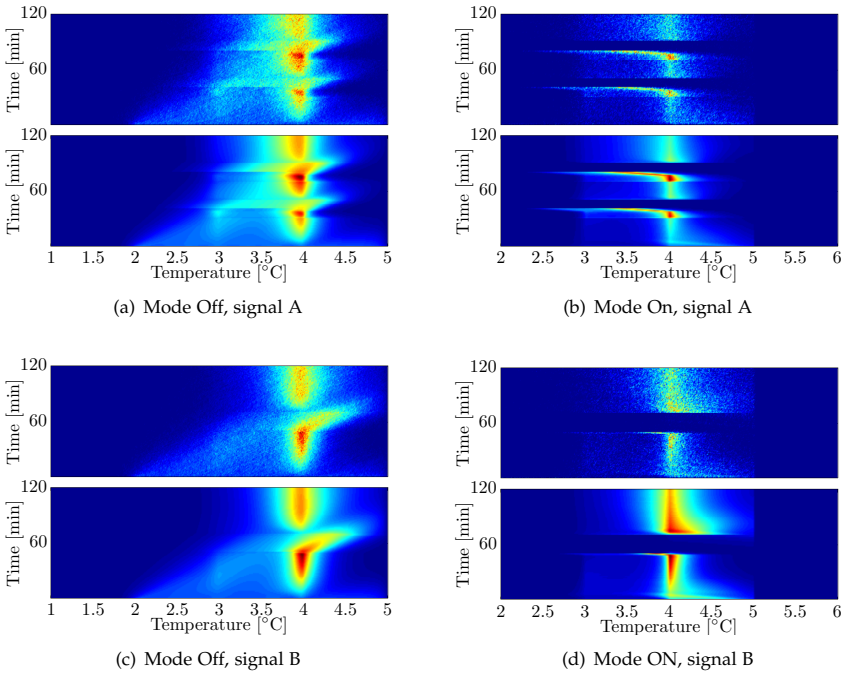

(a) Mode Off, signal A (b) Mode On, signal A

(c) Mode Off, signal B (d) Mode ON, signal B

Fig. C.2: Temperature densities across the TCL population. The empirical Monte Carlo pdf is shown in the top subplots, and the pdf from the PDE model is shown the bottom subplots. Blue represents low pdf values, and red high pdf values.

References

[1] Julien Bect. A unifying formulation of the fokker–planck–kolmogorov equation for general stochastic hybrid systems. *Nonlinear Analysis: Hybrid Systems*, 2010.

[2] Manuela L Bujorianu and John Lygeros. Toward a general theory of stochastic hybrid systems. In *Stochastic Hybrid Systems*. Springer, 2006.

[3] Duncan S Callaway and Ian A Hiskens. Achieving controllability of electric loads. *Proceedings of the IEEE*, 2011.

[4] E B Dynkin. *Markov processes*. Springer, 1965.

[5] Joel H Ferziger and Milovan Perić. *Computational methods for fluid dynamics*, volume 3. Springer Berlin, 2002.

[6] Crispin W Gardiner. *Handbook of stochastic methods: for Physics, Chemistry and the Natural Sciences*. Springer Berlin, 1985.

[7] Maryam Kamgarpour, Christian Ellen, Sadegh Esmaeil Zadeh Soudjani, Sebastian Gerwinn, Johanna L Mathieu, Nils Mullner, Alessandro Abate, Duncan S Callaway, Martin Franzle, and John Lygeros. Modeling options for demand side participation of thermostatically controlled loads. In *Bulk Power System Dynamics and Control-IX Optimization, Security and Control of the Emerging Power Grid (IREP), 2013 IREP Symposium*, pages 1–15. IEEE, 2013.

[8] Roland Malhame and Chee-Yee Chong. Electric load model synthesis by diffusion approximation of a high-order hybrid-state stochastic system. *Automatic Control, IEEE Transactions on*, 1985.

[9] Frauke Oldewurtel, Theodor Borsche, Matthias Bucher, Philipp Fortenbacher, Marina Gonzalez Vaya Tobias Haring, Johanna L Mathieu, Olivier Megel, Evangelos Vrettos, and Goran Andersson. A framework for and assessment of demand response and energy storage in power systems. In *Bulk Power System Dynamics and Control-IX Optimization, Security and Control of the Emerging Power Grid (IREP), 2013 IREP Symposium*, pages 1–24. IEEE, 2013.

[10] Luminita C Totu, John Leth, and Rafael Wisniewski. Control for large scale demand response of thermostatic loads. In *American Control Conference (ACC), 2013*, pages 5023–5028, June 2013.

[11] Luminita C Totu and Rafael Wisniewski. Demand response of thermostatic loads by optimized switching-fraction broadcast. In *IFAC World Congress*. To be published, 2014.

[12] Wei Zhang, Jianming Lian, Chin-Yao Chang, and Karanjit Kalsi. Aggregated modeling and control of air conditioning loads for demand response. *IEEE Transactions on Power Systems*, 2013.

Paper D

Demand Response of a TCL population using Switching-Rate Actuation

Luminița C. Totu, Rafael Wisniewski and John Leth

This work has been submitted for review and publication to the
IEEE Transactions on Control Systems Technology.

© IEEE
The layout has been revised, and small editorial changes have been made. Content relavant changes, if any, are marked with explicit footnotes.

Abstract

This work considers the problem of actively managing the power consumption of a large number of thermostatically controlled loads with on/off operation (TCLs), and a case-study on household refrigerators. Control is performed using a new randomized actuation that consists of switching units on and off at given rates, while at the same time respecting the nominal constraints on each individual unit. Both the free and the controlled behavior of the TCL units can be aggregated, making it possible to handle the TCL population as if it were a single system. The aggregation method uses the distribution of the unit states and across the population. The distribution approach has two main advantages. It scales excellently since the computational requirements do not increase with the number of units, and it allows data from individual units to be used anonymously, which solves privacy concerns relevant for consumer adoption. Using elements of Markov Theory for Stochastic Hybrid Systems, the dynamics of the distribution state can be written as a PDE system with boundary conditions. The PDE system is reduced to a finite dimensional form using finite-volume methods, resulting in a state-space description with linear autonomous dynamics and bilinear input terms. Based on this description, the power output of the population is controlled using model based techniques.

1 Introduction

Wind and solar power generation have seen a significant increase in the last decade. This global trend is predicted to continue, and it brings the promise of a more clean and economically stable energy future worldwide. Yet these renewables still represent only a small fraction of the overall power generation [13]. One of the problems is that large-scale integration in the power system is challenging. Wind and solar power production have a variable characteristic. While averages over long time scales are predictable, on the shorter time scales the generation output can be volatile and unpredictable. Because the power system needs to be in balance between consumption and production at all times, when a large percentage of the generation has a variable characteristic the balancing effort increases beyond the possibilities of the traditional grid. Integration levels over 30% require a transformation of the power system [1, 2]. One of the transformations needed is including demand-side as an active participant in the power system operations, both in the planning stage and in the real time balancing services. The idea is to access and organize existing demand flexibility, and utilize it to counteract variability in the grid and, additionally, optimize the economic dispatch of resources [17, 25, 28, 31].

This work is concerned with a demand response scenario consisting of a large number of thermostat-based appliances with on/off operation. We think of these as many, small and "leaky" thermal storages. These devices are of special interest since they have the potential to deliver a fast, automated response. The focus is on aggregating a very large numbers of units, in order to obtain a total power capacity relevant for power system operations. Using terminology introduced in [8], we want to achieve a control scheme that is *fully responsive* in terms of the aggregated power output and *nondisruptive* to the local unit operation.

The main technical challenges of the control problem are related to the large number of individual units and the distributed structure. Realistic solutions must keep computational complexity in check and use communication flows that are feasible

under cost and privacy criteria. We will therefore focus on solutions that are aligned with the following three principles. First, actuation should take place via broadcast communication. The network requirements for the actuation channel are thus reduced and communication is fast, since the same signal is sent to all units. Second, the actual physical decisions should take place at the individual unit and account for the local conditions. This guarantees a robust, nondisruptive local operation. Thirdly, measurements on the unit level should be used sparsely and anonymously. This is to ensure that network requirements for the measurement channel are not excessive, and that the overall solution is privacy friendly. Similar implementation principles are discussed also in [20].

The study of large groups of thermostatic loads started in the 1980s with the works of [18], [22] and [24]. The interest was on modeling oscillations in the power consumption after a planned (direct load control) or unplanned (black-out) interruption. Such oscillations are caused by the synchronization of the thermostatic duty-cycles, and can be seen as the free response of a TCL population subject to initial conditions. These early works set in place the "first principles" or "physically based" modeling paradigm for TCL populations. Previous approaches used data-driven models fitted using historical data. The new idea was to model the main behaviors at the unit level and then both simulate and mathematically lift the population behavior as the natural result of an aggregation operation. The important result in [22] realizes the mathematical aggregation of a homogeneous population of stochastic hybrid system as a partial differential system of equations with boundary conditions. The partial differential equations (PDEs) represent the dynamics of temperature distributions across the "on" and "off" modes in the population, and are obtained in a manner similar to the modeling of physical transport phenomena.

After three decades, the TCL problem got a resurgence motivated by the advance of demand response concepts and enabled by the low cost of computing and communication hardware. The focus is not only on modeling and prediction, but also control. The duty-cycles of individual TCL units can be modified and adjusted in order to shape the power output at the group level. A broadcast actuation method that shifts the thermostat set-point temperature is proposed in [7], and is also used in other works [3, 26]. The broadcast signal consists of a quantity ΔT, which is either positive or negative. All units in the receiving population immediately react by shifting their thermostat band with the ΔT amount. Another broadcast actuation is toggle control [23]. This actuation targets subgroups of units from the population based on the location (bin) in the temperature and mode distribution. Individual units switch-on or -off based on a random trial with success probability corresponding to their subgroup. The broadcast signal thus consists of a set of switching probabilities, one for each subgroup. A specialized form of toggling control involves the broadcast of only one or two switching probabilities [32, 33, 35]. In this case, there are only two target subgroups, the units in mode "on" and the units in mode "off". The broadcast signal consist of a switch-off and a switch-on probability. Units are protected against frequent switching by minimum on/off time constraints, and in [32, 33] a switching dead-zone is included for temperatures that are too close to the relevant thermostat limit. Other actuations and control methods are present in the literature, but fall outside the scope of this work. For example, there are a number of actuations that are meant to be used infrequently and ensure a particular power response, see [27], [4]

or [29]. While arguably useful and relevant for different scenarios, we consider these schemes as not fulfilling the *fully responsive* property, as they do not allow a continuous and smooth manipulation of the output power.

The switching actuation presents some important advantages compared to the thermostat set-point and toggle control. It is *nondisruptive*, as the temperature remains bound in the original thermostat band, it does not require a temperature sensor with high resolution to distinguish between narrow temperature bins, and the broadcast signal has a small footprint. Furthermore, the switching actuation has a direct and intuitive effect on the power consumption, which is a desirable implementation characteristic.

This work presents in detail the Switching-Rate actuation, which we briefly introduced in [34], and which extends the Switching-Fraction from [32, 33, 35]. The actuation is used to obtain relevant power responses under two control schemes, and the observation problem is also addressed. Another contribution of the paper is the use of Finite Volume techniques in the distribution model. Finally, this work takes into account a number of practical considerations for making the approach feasible for real-life, large-scale deployment.

The rest of the paper is structured as follows. Section 2 describes the modeling process. Section 3 presents model-based control algorithms. Section 4 presents a numerical case study and simulation results, showing the demand response capabilities of a TCL population and the effectiveness of the Switching-Rate actuation. Section 5 concludes.

2 Modeling

This work considers cooling units, and in particular domestic refrigerators. As under realistic conditions, the units are independent of each other, do not communicate nor share states. The main object of interest is the aggregated power consumption, which is the sum of the individual power consumptions. The model for an individual TCL unit is presented first, followed by the aggregation based on distributions[1]. The Switching-Rate actuation is addressed both for the unit and for the distribution models.

2.1 TCL stochastic hybrid model

The model aims to capture only those dynamic characteristics that are highly relevant at the population level, and is not meant to be high fidelity at the unit level. This approach is prevalent in literature and is supported by verifications using simulation in [35]. The main characteristics to be captured are the thermal dynamics, the hybrid nature of the thermostat operation, and stochasticity. We next present the established unit model, along with considerations about the underlying simplifications.

The basic model is a stochastic hybrid dynamical system (SHS) with two modes, corresponding to the "on" or "off" state of the cooling cycle. When the TCL is "on", it is consuming power and the temperature in the cold compartment is lowering. When

[1]The meaning is that of distribution functions in the physical sense, i.e. describing the scattering across a domain.

the TCL is "off", it is not consuming power and the temperature in the cold compartment is rising due to ambient conditions. The heating and cooling processes are modeled using a lumped approach and first-order dynamics. Although second-order dynamics should be studied for air-conditioning or heat-pump TCLs as argued in [35], this is not considered necessary in the case of domestic refrigerators, since there are no outstanding dynamical thermal masses coupled to cold compartment. Random temperature fluctuations are modeled by a white noise term. Other possible random disturbances, not pursued at this time, are jump processes that would correspond to "door-opening" events. Power consumption is considered to be a positive constant when the mode is "on", and zero when the mode is "off". The assumption is again an idealization, since it is well known that power consumption has a sharp peak at the start of the power cycle (the start of the single phase induction motor) and that it also exhibits an overall first order response pattern (the load dynamics from the vapour-compression cycle), see Fig. D.1.

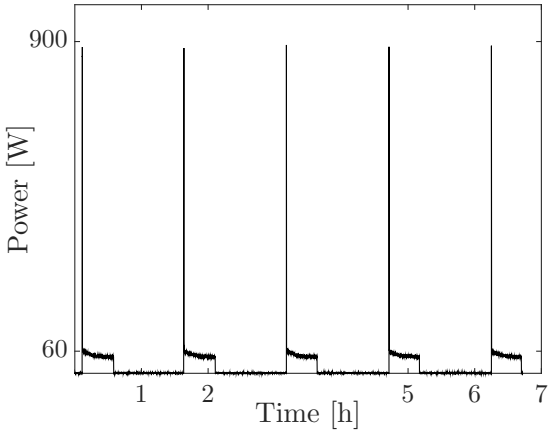

Fig. D.1: Power consumption pattern of a real domestic refrigerator (laboratory set-up)

Summing up, the model of a TCL unit is a SHS of the following form,

$$dT(t) = -\frac{\mathrm{UA}}{C}\left(T(t) - T_a + m(t)\frac{\eta W}{\mathrm{UA}}\right)dt + \sigma dw(t) \tag{D.1a}$$

$$= \big(aT(t) + b + m(t)c\big)dt + \sigma dw(t)\,, \tag{D.1b}$$

$$z(t) = Wm(t)\,, \tag{D.2}$$

where $T(t) : \mathbb{R}_+ \to \mathbb{R}$ is the continuously-valued temperature state, $m(t) : \mathbb{R}_+ \to \{0, 1\}$ is the discrete-valued state corresponding to the "off" and "on" modes respectively, $w(t)$ is a white noise process, and $z(t) : \mathbb{R}_+ \to \{0, W\}$ is the power consumption viewed here as model output. The temperature dynamics are expressed using equivalent thermal parameters in (D.1a) and using equivalent first order system parameters in (D.1b). All coefficients are considered to be time invariant. In the absence of external control, the dynamics of the discrete-valued state $m(t)$ are given by a standard

thermostat mechanism with boundaries at $T_{\min}$ and $T_{\max}$,

$$m(t) = \begin{cases} 1, & T(t) \geq T_{\max} \\ m(t^-), & T(t) \in (T_{\min}, T_{\max}) \\ 0, & T(t) \leq T_{\min} \, . \end{cases} \tag{D.3}$$

Since the discrete-valued state $m(t)$ has discontinuities at the switching times, notation t^- is used to represent limit from left. The convention is thus that $m(t)$ is càdlàg.

The switching actuation adds a random component on top of the deterministic thermostat mechanism, see Fig. D.2, and can be represented using the Markov chain formalism. It has a continuous-time characteristic, described by transition rates that are given over the broadcast input channel. In this way, a TCL unit that is "off" can be encouraged to consume power using input u_1, while a unit that is "on" can be discouraged from consuming power using input u_0. At the population level, the magnitude of the input will be reflected by the number/percentage of units that actually switch. This externally generated switching is always temperature safe since it can anticipate but not override the thermostat mechanism, which remains in place.

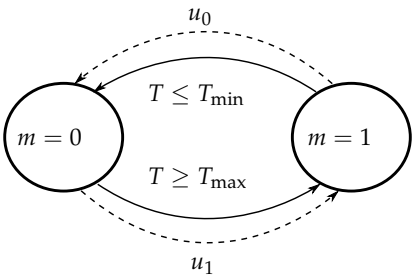

Fig. D.2: Dynamics of the discrete state $m(t)$ as a Markov chain, including deterministic, temperature-state dependent transitions (solid line) and random transitions (dashed line).

Furthermore, additional features are added to prevent the occurrence of multiple switches in a short time interval. Frequent switching can damage the physical components of the TCL unit such as the compressor, and can invalidate model (D.1) since the first-order thermal dynamic cannot be expected to be a good approximation on the short time scale. To this end, a timer state $\tau(t) : \mathbb{R}_+ \to \mathbb{R}_+$ with the straightforward dynamic

$$\dot{\tau}(t) = 1 \, , \tag{D.4}$$

is added to the model, and its value is reset to zero after a switch. Non-thermostatic switches are only allowed if a condition of the type $\tau(t) \geq M$ is satisfied, where M is chosen based on the specific TCL unit requirements for safe nominal operation. In addition, "safe-zones" are added to ensure that switches do not occur if the temperature is too close to a maximum or a minimum limit, as they would quickly be reversed by the thermostat action.

Switch-on actions are allowed only if the temperature is in the interval $\mathcal{S}_1$ and

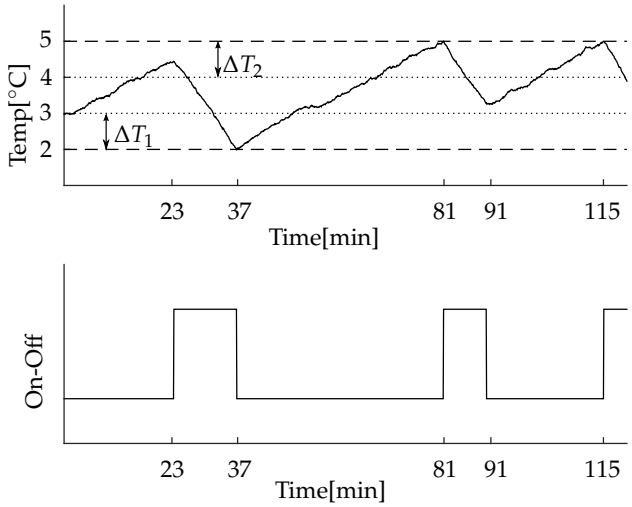

Fig. D.3: Temperature and mode trajectory with external actuation. Thermostat actions occur at minutes 37, 81 and 115, and external switches at minutes 23 and 91.

switch-off actions are allowed only if the temperature is in the interval $\mathcal{S}_0$,

$$\mathcal{S}_1 = [T_{\min} + \Delta T_1, T_{\max}) \tag{D.5a}$$

$$\mathcal{S}_0 = (T_{\min}, T_{\max} - \Delta T_2] \tag{D.5b}$$

where $\Delta T_1, \Delta T_2 < T_{\max} - T_{\min}$. Fig. D.4 gives a sketch of the complete Markov mechanism.

Both the Switching-Fraction [32, 33, 35] and the new Switching-Rate are randomized actuations, and the main difference is the time characteristic. After receiving a broadcast (which is considered to take place instantaneously), the TCL unit needs to take a decision about "if" and "when" to execute a mode switch. In the Switching-Fraction actuation case, the "when" moment is predefined to be "now", leaving only the "if" question to be answered. A consequence of the Switching-Fraction mechanism is that non-thermostatic switches are tightly synchronized across the population. Since the power consumption of an individual TCL exhibits a peak after switch-on, see Fig. D.1, synchronized switch-on actions lead to synchronized power peaks. The main objective of the Switching-Rate variant is to desynchronize the switch actions across the population. Not only is the switch decision random, but also the time of its occurrence. The mechanism is similar to the jumps in a Poisson process and is described by transition rates.

Given a small enough time interval h, and making the informal assumption that the temperature state T does not significantly change its value during this time (does not leave the safe interval $\mathcal{S}_{\bar{i}}$), the probability of a switch event can be written as

$$\begin{aligned} \Pr\big[m(t+h) = \bar{i} \;\big|\; m(t) = i, T(t) \in \mathcal{S}_{\bar{i}}, \tau(t) \geq M \,\big] \\ = u_{\bar{i}}(t_b)h + o(h) \,, \end{aligned} \tag{D.6}$$

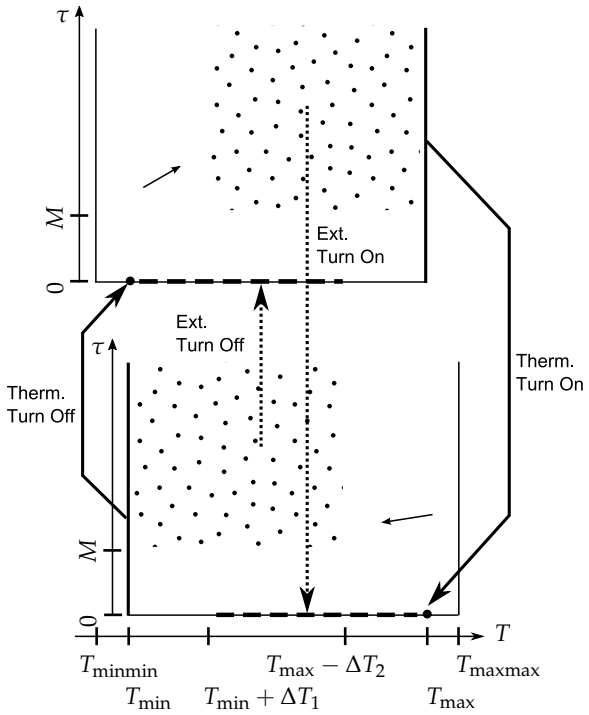

Fig. D.4: Dynamics of the discrete state $m(t)$ including temperature-state and timer-state partitions, extending the description from Fig. D.2.

where $\bar{i} \triangleq 1 - i$. The model of a TCL unit with Switching-Rate actuation can be formally constructed using the notion of General Stochastic Hybrid Systems (GSHS) [5, 6]. These objects include the three main characteristics of the TCL unit, dynamics given by stochastic differential equations (SDEs), jumps when the continuous state hits a boundary or according to transition rates, and state resets after jumps.

With a Switching-Rate actuation, switch-on and switch-off events can happen at any point along the continuous time line after the broadcast time, provided that temperature and timer conditions hold safe. In this way, switches are not synchronized across the population, although they might be densely clustered if the rate parameter is high. The switching mechanism is straight forward to implement in software. It consists of logic operations for checking the state safety conditions defined as inequalities, and a random number generator, see Alg 1.

2.2 Population model

The TCL unit can be described, equivalent in effect with the SHS characterization from Section 2.1, in terms of the probability density function (pdf) over the hybrid state space $(T, m) \in \mathbb{R} \times \{0, 1\}$,

$$f^i(x,t) = \lim_{dx \searrow 0} \frac{1}{dx} \Pr\left[\, T(t) \in (x, x+dx] \wedge m(t) = i \,\right] .$$

The continuous timer state $\tau(t)$ has been omitted for the moment, but will be reintroduced latter. Building on elements and results from Markov process theory (e.g. [9, 14]), [22] showed that the dynamic of $f^i(x,t)$ can be described analytically. In particular, the dynamic of $f^i(x,t)$ represents the generator of the forward linear semigroup associated with the TCL SHS. For dynamical systems characterized by regular SDEs, without hybrid elements, this generator is known as the Fokker-Planck equation and can be seen as a transport and conservation law for probability. Therefore, the result in [22] is a type of Fokker-Planck operator specific to the TCL SHS without actuation. The advantage of this modeling is that, unlike the SHS form, a TCL description in terms of the pdf translates almost directly into a (homogeneous) population model. Probability quantities simply change meaning to population fractions, see e.g. [7, 10, 22].

Distribution model without actuation

This section introduces the main result from [22] that gives the dynamics of $f^i(x,t)$ in the form of a PDE system with boundary conditions. Before stating the result, some preliminaries need to be addressed.

The temperature domain is divided into three subsets: the thermostat range $\mathcal{S}_b = [T_{\min}, T_{\max}]$, and $\mathcal{S}_a = (-\infty, T_{\min})$ and $\mathcal{S}_c = (T_{\max}, \infty)$. This is a natural division with respect to the operation of the TCL unit, and is necessary because boundary conditions apply in the points $T_{\min}$ and $T_{\max}$, and because the pdf $f^i(x,t)$ is not x-differentiable here. Superscript indices will then be used to denote subcomponents of

Algorithm 1 Switching-Rate

```
global T, m, τ, u_0, u_1
const ΔT_1, ΔT_2, M
function BroadcastReceived(new_u_0,new_u_1)
    if u_0 < 0 then return
    end if
    if u_1 < 0 then return
    end if
    u_0 ← new_u_0
    u_1 ← new_u_1
end function

function loop100ms
    if (m == 1) and (T > T_min) and (T ≤ T_max − ΔT_2) and (τ ≥ M) and (rand() ≤ u_0 · 0.1) then
        m ← 0
    end if
    if (m == 0) and (T < T_max) and (T ≥ T_min + ΔT_1) and (τ ≥ M) and (rand() ≤ u_1 · 0.1) then
        m ← 1
    end if
end function
```

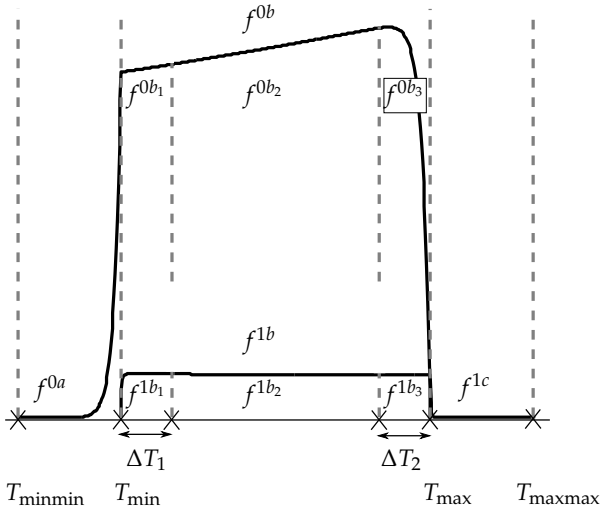

Fig. D.5: Partitions of the temperature domain and subcomponents

the pdf functions $f^i(x,t)$ over the specific partitions e.g., f^{0a} or f^{1b}. Temperatures outside the thermostat range must be accounted for because of the diffusive component in the thermal dynamics (D.1). For example, even though the TCL unit is automatically "on" and starting to cool when $T(t) = T_{\text{max}}$, the temperature might reach values $T(t) > T_{\text{max}}$ due to the contribution of the white noise term. It is also important to note that the pdf corresponding to the off mode, $f^0(x,t)$, is zero-valued on the $\mathcal{S}_c$ domain, because if the temperature becomes greater than T_{max} the thermostat mechanism ensures that the mode can not remain "off". Similarly, the pdf corresponding to the on-mode, $f^1(x,t)$ is zero-valued on the $\mathcal{S}_a$ domain. In numerical work, the infinity domains limits can be cut short since it is realistic to assume that the temperature inside a working refrigerator will not drop below some T_{minmin} value and cannot rise above some T_{maxmax} value, or equivalently, that probability of this happening is sufficiently low that it can be ignored. These elements are summarized on Fig. D.5, using a pdf function corresponding to the refrigerator unit from Section 4. Additionally, Fig. D.5 contains notations b_1, b_2 and b_3 for the intervals $(T_{\text{min}}, T_{\text{min}} + \Delta T_1)$, $[T_{\text{min}} + \Delta T_1, T_{\text{max}} - \Delta T_2]$ and $(T_{\text{max}} - \Delta T_2, T_{\text{max}})$, relevant for the actuation part. With this notation, the safe-temperature zones (D.5) can be expressed as,

$$\mathcal{S}_0 = \mathcal{S}_{b_1} \cup \mathcal{S}_{b_2};\ \mathcal{S}_1 = \mathcal{S}_{b_2} \cup \mathcal{S}_{b_3}\ . \tag{D.7}$$

The evolution of the temperature state $T(t)$ in the interior of the $\mathcal{S}_j$ domains, $j \in \{a, b, c\}$, is driven only by the SDE component (since the discrete dynamics only come into play at the boundaries of the $\mathcal{S}_j$ domains). As a result, the dynamic of the pdf $f^{ij}(x,t)$ on the interior $\mathcal{S}_j$ is given by a standard Fokker-Planck equations

matching the thermal dynamics (D.1b) for the corresponding mode,

$$\frac{\partial f^{0j}(x,t)}{\partial t} + \frac{\partial}{\partial x}\Big((ax+b)f^{0j}(x,t)\Big) = \frac{\sigma^2}{2}\frac{\partial^2 f^{0j}(x,t)}{\partial x^2},\ j \in \{a,b\} \tag{D.8a}$$

$$\frac{\partial f^{1j}(x,t)}{\partial t} + \frac{\partial}{\partial x}\Big((ax+b+c)f^{1j}(x,t)\Big) = \frac{\sigma^2}{2}\frac{\partial^2 f^{1j}(x,t)}{\partial x^2},\ j \in \{b,c\}. \tag{D.8b}$$

The switching dynamics (D.3) are included in the boundary conditions. We first introduce the probability flows $h^{ij}(x,t)$ as the integral over the temperature (x-) coordinate of the probability fluxes $\frac{\partial f^{ij}}{\partial t}(x,t)$,

$$h^{0j}(x,t) = -(ax+b)f^{0j}(x,t) + \frac{\sigma^2}{2}\frac{\partial f^{0j}(x,t)}{\partial x} \tag{D.9a}$$

$$h^{1j}(x,t) = -(ax+b+c)f^{1j}(x,t) + \frac{\sigma^2}{2}\frac{\partial f^{1j}(x,t)}{\partial x}. \tag{D.9b}$$

The boundary conditions can then be written as

$$h^{0a}(T_{\text{minmin}},t) = 0,\ h^{1c}(T_{\text{maxmax}},t) = 0 \tag{D.10a}$$

$$f^{1b}(T_{\min},t) = 0,\ f^{0b}(T_{\max},t) = 0 \tag{D.10b}$$

$$f^{0b}(T_{\min},t) = f^{0a}(T_{\min},t),\ f^{1b}(T_{\max},t) = f^{1c}(T_{\max},t) \tag{D.10c}$$

$$h^{0a}(T_{\min},t) = h^{0b}(T_{\min},t) + h^{1b}(T_{\min},t) \tag{D.10d}$$

$$h^{1c}(T_{\max},t) = h^{0b}(T_{\max},t) + h^{1b}(T_{\max},t)\ . \tag{D.10e}$$

Equations (D.10a) represent impenetrable wall conditions, i.e. there is no probability flow out-of or in-to the domain $\mathcal{S}_a$ from the left side, and similarly there is no flow out-of or in-to the domain $\mathcal{S}_c$ from the right side. The rest of the boundary conditions are associated with the thermostat switching mechanism. First, (D.10b) account for the "absorption" action of the thermostat process causing $\Pr[\ T(t) = T_{\min} \wedge m(i) = 1\ ] = 0$ and $\Pr[\ T(t) = T_{\max} \wedge m(i) = 0\ ] = 0$. Second, the fact that the temperature state does not jump (is not reset) by the switching mechanism is reflected in the continuity condition (D.10c). Finally, (D.10d) and (D.10e) describe of the flow of probability from mode "on" to mode "off" at $T_{\min}$, and the flow of probability from mode "off" to mode "on" at $T_{\max}$.

Finite Volume Methods

The system (D.8), together with boundary conditions (D.10), represents a linear, infinite-dimensional dynamic. We approximate it with a finite-dimensional form using FVM [12, 30]. While other works use a Finite Difference approach [3, 16], FVMs are arguably more suitable. A main argument is that FVMs are locally and globally conservative. The obtained approximate solution will conserve the probability invariant of the system (probability will always scale to 1 in the numerical solution).

The FVM consists of three main steps. First, the continuous spatial domain is partitioned using a relatively fine grid of non-overlapping cells[2]. The second step consists

[2]This is the semi-discrete FVM approach, as only the spatial domain is discretized. The result is a finite-dimensional, continuous-time dynamic in the form of an ODE system. The discrete-time dynamics can be obtained later, and separate from the spatial discretization process. Fully-discrete FVM techniques grid the spatial and temporal coordinate simultaneously.

of building the master FVM equation. This is done by integrating the dynamical PDE equation over a cell of the grid. For a generic conservation dynamic in one spatial dimension x with drift field $\phi(x,t)$, diffusion coefficient $D = \frac{\sigma^2}{2}$, and source term $s(x,t)$,

$$\frac{\partial \rho}{\partial t}(x,t) + \frac{\partial\big(\phi(x,t)\rho(x,t)\big)}{\partial x} = D\frac{\partial^2 \rho(x,t)}{\partial x^2} + s(x,t) \tag{D.11}$$

integrating over the spatial cell K_q gives

$$\int_{K_q} \frac{\partial \rho}{\partial t}(x,t)dx = \Big(-\phi(x,t)\rho(x,t) + D\frac{\partial \rho(x,t)}{\partial x}\Big)\Big|_{K_q^-}^{K_q^+} + \int_{K_q} s(x,t)dx\ , \tag{D.12}$$

where $q \in \{1,\dots,N\}$ is the cell index, and K_q^-, K_q^+ are the left and right edge points of the cell. Notice that flow quantities evaluated at K_q^- appear with a negative sign (outgoing) in the dynamic of the cell K_q, and with a positive sign (incoming) in the dynamic of the cell K_{q-1}. The outgoing flow from one cell is incoming flow to the neighbor cell, resulting in the conservative property of the method. Next, the left side of (D.12) can be further expressed as

$$\int_{K_q} \frac{\partial \rho}{\partial t}(x,t)dx = \frac{d}{dt}\int_{K_q} \rho(x,t)dx = \Delta x_q \frac{d\Theta_q}{dt}, \tag{D.13}$$

with Θ_q the average value of $\rho(x,t)$ over the cell K_q and Δx_q the cell size. Equations (D.12) and (D.13) can be combined to give an exact expression for the evolution in time of the average quantity Θ_q,

$$\Delta x_q \frac{d\Theta_q}{dt} = \Big(-\phi(x,t)\rho(y,t) + D\frac{\partial \rho(x,t)}{\partial x}\Big)\Big|_{K_q^-}^{K_q^+} + \int_{K_q} s(x,t)dx\ . \tag{D.14}$$

However, the master equation (D.14) is not closed since the right side expression uses the $\rho(x,t)$ terms, which are unknowns. The third step thus consists of applying a numerical scheme for approximating the right side of (D.14) using only $\Theta_q, \Theta_{q+1}, \Theta_{q-1}, \dots$ terms. This step is a combination of reconstruction techniques (interpolation and extrapolation) on neighborhood stencils, numerical approximation for differentiation and integration operations, and also heuristics such as the "up-wind" rule. Once this step is complete, a finite dimensional ODE system with N equations can be used as an approximation of the original infinite dimensional dynamic.

Regarding domain boundaries, the zero flow conditions (D.10a) are straightforward to implement, while conditions associated with the thermostat mechanism (D.10b), (D.10c), (D.10d) and (D.10e) need to be handled in combination by solving an algebraic system within the reconstruction scheme.

In the particular case of the TCL PDE system, the temperature sub-domains $j \in \{a,b,c\}$ are each divided into a number N_j of cells, $\mathcal{S}_j = \cup_{k=1}^{N_j} K_{jq}$. It is convenient to use uniform griding, meaning equal cell sizes $\Delta x_{jq} = \Delta x,\ \forall j,q$. As a result of the FVM spatial discretization procedure, the pdf function states $f^{ij}(x,t)$ are replaced by vector states $F^{ij} \in \mathbb{R}^{N_j}$, see Fig. D.6. These components are ordered as $F = (F^{0a}, F^{0b}, F^{1b}, F^{1c})$, resulting in a complete vector-state of dimension $N^a + 2N^b + N^c = N$. Subcomponents F^{ib_1}, F^{ib_2} and F^{ib_3} are relevant when considering actuation. Their dimensions

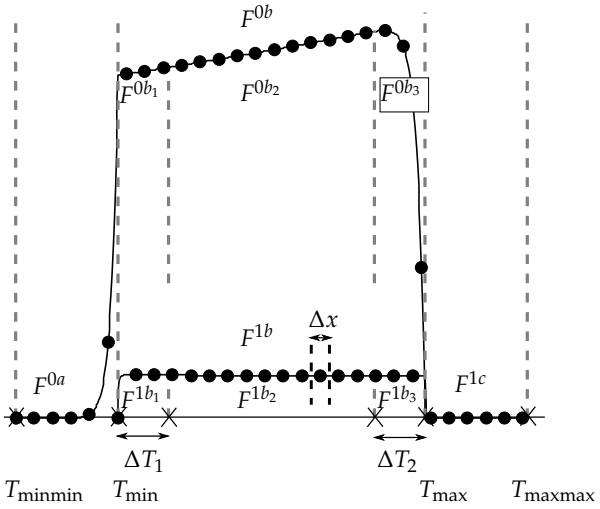

Fig. D.6: From the infinite dimensional state f to the final dimensional state $F \in \mathbb{R}^N$, $N = N_a + 2N_b + N_c$, $N_b = N_{b_1} + N_{b_2} + N_{b_3}$.

are N^{b_1}, N^{b_2}, and N^{b_3}, with $N^{b_1} + N^{b_2} + N^{b_3} = N^b$. Each entry in the vector state F represents the average probability density value in its corresponding cell,

$$F^{ijq}(t) = \frac{1}{\Delta x} \Pr\left[m(t) = i \wedge T(t) \in \mathrm{K}_{jq}\right], \tag{D.15}$$
$$i \in \{0,1\},\ j \in \{a,b,c\},\ q \in \{1,2,\ldots,N_j\}\ .$$

Because of the linear form of the Fokker-Planck equations, of the TCL boundary conditions, and of the particular FVM scheme, the PDE system can be approximated by a linear ODE system,

$$\dot{F}(t) = AF(t)\ . \tag{D.16}$$

Matrix A is guaranteed to conserve probability i.e., has the property that columns sum to 0. However, A is not guaranteed to be a proper transition rate matrix, and it can have a number of negative non-diagonal elements. Since the finite dimensional approximation of the PDE system can be seen as a Markov chain representation of the TCL SHS [10, 23], having matrix A in the form of a transition matrix is a desirable property. FVMs do not in general guarantee the positivity property [11], however the FVM scheme proposed in [21] specifically preserves a number of relevant structural properties, among which positivity. This FVM scheme is based on an alternative formulation of the master equation, using the Fokker Planck equation (D.11) recast as

$$\phi(x,t) \equiv -\frac{d\mu(x,t)}{dx} \tag{D.17}$$
$$\frac{\partial \rho(x,t)}{\partial t} = \frac{1}{D}\frac{\partial}{\partial x}\left(e^{-D\mu(x,t)}\frac{\partial}{\partial x}\left(e^{D\mu(x,t)}\rho(x,t)\right)\right) + s(x,t)\ . \tag{D.18}$$

The method in [21] is valid also for multidimensional spatial domains. We found numerically that, to obtain a good dynamic approximation, the structure preserving

FVM requires denser grids than more typical schemes. The Markov chain structure is relevant for the error model description in Section 3.3.

Distribution model with Switching-Rate

The Switching-Rate actuation can be introduced in the PDE description (D.8), wherefrom it will propagate into the state-space description (D.16). We first address the case without the locking mechanism. The new terms that are included in the PDE dynamics are marked with braces,

$$\frac{\partial f^{0b}}{\partial t} = -\frac{\partial}{\partial x}\Big((ax+b)f^{0b}\Big) \underbrace{-\lambda_1(x)f^{0b} + \lambda_0(x)f^{1b}} + \frac{\sigma^2}{2}\frac{\partial^2 f^{0b}}{\partial x^2} \tag{D.19a}$$

$$\frac{\partial f^{1b}}{\partial t} = -\frac{\partial}{\partial x}\Big((ax+b+c)f^{1b}\Big) + \underbrace{\lambda_1(x)f^{0b} - \lambda_0(x)f^{1b}} + \frac{\sigma^2}{2}\frac{\partial^2 f^{1b}}{\partial x^2}\ , \tag{D.19b}$$

where

$$\lambda_1(x) = \begin{cases} u_1,\ x \in \mathcal{S}_1 \\ 0,\ x \notin \mathcal{S}_1 \end{cases} \quad \lambda_0(x) = \begin{cases} u_0,\ x \in \mathcal{S}_0 \\ 0,\ x \notin \mathcal{S}_0\ . \end{cases} \tag{D.19c}$$

The terms $u_1 f^{0b}$ and $u_0 f^{1b}$ give a fitting dynamic for the exchange of probability from one discrete mode another due to the design of the external switching, see the infinitesimal contribution given in (D.6). The discontinuity in the $\lambda_i(x)$ functions, and thus the discontinuity in the PDE coefficients, may raise concerns. The effect of the discontinuity in the coefficients, combined with the smoothing effect of the diffusion term, is that the solution remains continuous but is non-differentiable at points $T_{\min} + \Delta T_1$ and $T_{\max} - \Delta T_1$, similar to the behavior at $T_{\min}$ and $T_{\max}$. The rigorous formulation is then to split the solutions f^{ib} into subcomponents b_1, b_2 and b_3, and connect these with boundary conditions using flow functions h, that is

$$\begin{aligned} f^{ib_1}(T_{\min} + \Delta T_1, t) &= f^{ib_2}(T_{\min} + \Delta T_1, t), \\ f^{ib_2}(T_{\max} - \Delta T_2, t) &= f^{ib_3}(T_{\max} - \Delta T_2, t) \end{aligned} \tag{D.20a}$$

$$\begin{aligned} h^{ib_1}(T_{\min} + \Delta T_1, t) &= h^{ib_2}(T_{\min} + \Delta T_1, t), \\ h^{ib_2}(T_{\max} - \Delta T_2, t) &= h^{ib_3}(T_{\max} - \Delta T_2, t)\ . \end{aligned} \tag{D.20b}$$

The FVM can again be applied to reduce the PDE dynamics to a finite dimensional form. The resulting system has the following form,

$$\dot{F}(t) = AF(t) + u_0(t)B_0F(t) + u_1(t)B_1F(t). \tag{D.21}$$

The locking mechanism is now included. The modeling principle is to explicitly track the part of the pdf that becomes locked for the external actuation. Two density functions are introduced to correspond to the locked condition for mode "off" and for mode "on", $L^0 : (T_{\text{minmin}}, T_{\max}) \times [0, M) \times [0, \infty) \to \mathbb{R}_+$ and $L^1 : (T_{\min}, T_{\text{maxmax}}) \times [0, M) \times [0, \infty) \to \mathbb{R}_+$,

$$L^i(x, y, t) = \lim_{\substack{dx \searrow 0 \\ dy \searrow 0}} \frac{1}{dxdy} \Pr\left[\ T(t) \in (x, x+dx] \wedge \tau(t) \in (y, y+dy]\ \wedge m(t) = i\ \right]. \tag{D.22}$$

The part of $f^i(x,t)$ which remains responsive to the actuation is evaluated by subtracting the probability of being locked, and the following updates are made to (D.19a) and (D.19b),

$$\lambda_1(x)f^{0b} \to \lambda_1(x)\left(f^{0b} - \overbrace{\int_0^M L^0(x,y,t)dy}^{\text{amount of locked } f^{0b}}\right) \tag{D.23a}$$

$$\lambda_0(x)f^{1b} \to \lambda_0(x)\left(f^{1b} - \overbrace{\int_0^M L^1(x,y,t)dy}^{\text{amount of locked } f^{1b}}\right) . \tag{D.23b}$$

The dynamics of L^i are given by normal Fokker-Planck equations in the two-dimensional state space (T,τ) with the underlying process driven by (D.1b) and (D.4), with no external switching contributions. The dynamics are thus,

$$\frac{\partial L^i}{\partial t}(x,y,t) + \frac{\partial}{\partial x}\Big((ax+b+ic)L^i(x,y,t)\Big) + \frac{\partial}{\partial y}L^i(x,y,t) = \frac{\sigma^2}{2}\frac{\partial^2}{\partial x^2}L^i(x,y,t) , \tag{D.24}$$

with boundary conditions,

$$h^{L0}(T_{\text{minmin}},y,t) = 0,\ h^{L1}(T_{\text{maxmax}},y,t) = 0 \tag{D.25a}$$

$$L^1(T_{\text{min}},y,t) = 0,\ L^0(T_{\text{max}},y,t) = 0 \tag{D.25b}$$

$$L^i(x,0,t) = \lambda_{\bar{i}}(x,t)\big(f^{\bar{i}b}(x,t) - \int_0^M L^{\bar{i}}(x,y,t)dy\big) \tag{D.25c}$$

Equations (D.25a) represent impenetrable walls conditions where the probability flow h is zero, and (D.25b) represent absorbing boundaries due to the thermostat action. Finally, (D.25c) accounts for the incoming probability of a new switching event and the zero reset of the timer state. This is a boundary condition that has discontinuities in the x-space and in time, see (D.19c) and the fact that $u_i(t)$ is due to the nature of broadcast communication a piecewise constant function. Again, discontinuities can be a problem for the current mathematical description. A solution can be to modify the TCL unit behavior to an ideal version where a smooth approximate of the $\lambda_i(x,t)$ is used. However, such modifications do not change any of the practical considerations and have little impact on the results of the computational algorithms, including the FVM procedure. The main difference introduced by the modeling of the locking mechanism is that a two dimensional FVM scheme needs to be used for the state L^i. The final form of the finite-dimensional dynamic is,

$$\dot{X}(t) = A^X X(t) + u_0(t)B_0^X X(t) + u_1(t)B_1^X X(t) ,\ X = (F\ L^0\ L^1) , \tag{D.26}$$

where $L^0 \in \mathbb{R}^{(N_a+N_b)M_d}$, $L^1 \in \mathbb{R}^{(N_b+N_c)M_d}$, $X \in \mathbb{R}^{N(M_d+1)}$, and M_d is the number of grid cells with size Δy used to discretize the timer-state domain $[0,M]$. A coordinate

change can be used to create a Markov chain formulation, by separating the unlocked from the locked states,

$$X' = \left(F^0 - \Delta y \sum_{l=1}^{M_d} \overbrace{L^0_{(l-1)N_{a+b}+1:lN_{a+b}}}^{\text{off, locked, } \tau\in[(l-1)\Delta y, l\Delta y)}, F^1 - \Delta y \sum_{l=1}^{M_d} \overbrace{L^1_{(l-1)N_{b+c}+1:lN_{b+c}}}^{\text{on, locked, } \tau\in[(l-1)\Delta y, l\Delta y)}, L^0, L^1\right)$$
$$= T_X X \tag{D.27}$$

This completes the Switching-Rate model.

Remarks

Locking effects after a thermostatic switch are not considered. The reason why this is not necessary is due to the temperature safe-zones feature. After a thermostatic switch, the unit is prevented from switching again until it is some distance ΔT away from the thermostat boundary. This temperature distance can be chosen such that its effects are practically equivalent to a timer condition.

The expected power consumption output of a TCL unit can be obtained by calculating the total probability of a unit being "on", and scaling it with the power rating parameter W,

$$z(t) = CF(t), \tag{D.28}$$

with $C = W\Delta x \begin{bmatrix} 0_{1\times(N_a+N_b)} & 1_{1\times(N_b+N_c)} \end{bmatrix}$.

The Fokker-Planck approach to modeling the distribution dynamics can also be used when considering other elements in the TCL unit model, such as nonlinear terms or jump noises. Another remark is that coefficients and parameters characterizing the dynamical behaviors can take different values in mode "on" compared to mode "off", for example the entire drift field, the diffusion coefficients, and temperature safe zones ΔT, and the timer setting M.

The fact that the actuation takes a bilinear form in (D.21) and (D.26) can be seen as intrinsic to distribution modeling approach. It also appears in the case of a thermostat set-point actuation [3], and in the case of the Switching Fraction. This is because the actuation does not represent an external input to the system, but rather an internal transformation that is defined in relation to the current state.

Populations

As mentioned, when considering a large group of units with identical parameters, probabilities simply change meaning to fractions. This means that models (D.21) and (D.26) can be initialized with values for F (or X) reflecting the distribution of temperature and mode (and timer) states values across the population, and will naturally propagate these distributions over time and under inputs.

Small heterogeneities of the TCL population should not cause severe modeling errors, but large heterogeneities will cause a significant departure from the homogeneous case. However, exact modeling of heterogeneous population is impractical since it suffers from "curse of dimensionality" (the state-space is extended with an extra dimension for each parameter). Therefore, heterogeneity is not explicitly accounted for

in the distribution model. Instead, this work makes use of the fact that the switching actuation has a certain amount of robustness to model variations due to its percentage formulation, and furthermore, measurements and online estimation can be used to periodically update the distribution state in real-time operation. In the numerical simulations, moderate levels of heterogeneity are considered for the TCL population. For a more pronounced dispersion of parameters, a clustering strategy [35] should be applied first.

3 Model-based Control Algorithms

This section presents two model-based control algorithms that can be used to manipulate the aggregated power consumption of the TCL population via the Switching-Rate actuation. The control objective is to have the power output track an input reference. State estimation is also addressed, by describing an error model that can be used with a linear Kalman filter. The error model uses results from [10]. Finally, observations are made about the measurement channels.

3.1 Control system

Whether considering or not the switch-lock effect, the TCL population model has a continuous-time, bilinear, homogeneous input form,

$$\dot{F}(t) = \big(A + \sum_i u_i(t) B_i\big) F(t), \tag{D.29a}$$

$$\dot{X}(t) = \big(A^X + \sum_i u_i(t) B_i^X\big) X(t)\ , \tag{D.29b}$$

with $u_i \in [0, u_{\max}]$. The aggregated power consumption is a linear combination of the states,

$$z_a(t) = nCF(t), \tag{D.30}$$

where n is the number of units in the population.

The free dynamics of the system without the switch-lock effect are given by matrix A, which has stable eigen values, except one which is exactly zero. This is due to the FVM procedure producing a dynamic matrix that conserves the probability invariant of the system state, by having columns that sum to 0. This fact can be used to reduce the system dimension by one state. Given an initial state $F(0)$ s.t. the sum of its elements is f (in particular $f = \frac{1}{\Delta x}$), the sum of $F(t)$ will remain f. Therefore, one of the states can be written as the difference between f and the sum of all others.

$$F(t) = \begin{bmatrix} \bar{F}(t) \\ F_N(t) \end{bmatrix},\ \bar{F} \in \mathbb{R}^{N-1}, F_N \in \mathbb{R} \tag{D.31a}$$

$$\begin{bmatrix} \dot{\bar{F}} \\ \dot{F}_N \end{bmatrix} = \left(\begin{bmatrix} A_{11} & A_{12} \\ A_{21} & a_{22} \end{bmatrix} + \sum_i u_i \begin{bmatrix} B_{i,11} & B_{i,12} \\ B_{i,21} & b_{i,22} \end{bmatrix} \right) \begin{bmatrix} \bar{F} \\ F_N \end{bmatrix} \tag{D.31b}$$

$$F_N = f - 1_{N-1}^T \bar{F} \tag{D.31c}$$

$$\dot{\bar{F}} = A_{11}\bar{F} + A_{12}(f - 1_{N-1}^T \bar{F}) + \sum_i u_i \bar{B}_{i,11} \bar{F} = \left(\bar{A} + \sum_i u_i \bar{B}_i \right) \bar{F} + \bar{a} \tag{D.31d}$$

In (D.31b) matrix $B_{i,12} = 0$ for the switching actuation, in (D.31d) $\bar{A} = A_{11} - A_{12}1_{N-1}^T \in \mathbb{R}^{(N-1)\times(N-1)}$, and $\bar{a} = A_{12}f$. The dynamic matrix of the transformed system, $\bar{A}$, is Hurwitz. Furthermore, a change of variables can move the equilibrium state of the affine system (D.31d) to 0, resulting in linear, stable free dynamic at the expense of an added affine input term,

$$\bar{F}_0 = \bar{F} + \bar{A}^{-1}\bar{a} \tag{D.32a}$$

$$\dot{\bar{F}}_0 = \left(\bar{A} + \sum_i u_i \bar{B}_i\right)\bar{F}_0 + \sum_i u_i \overbrace{\bar{B}_i \bar{A}^{-1}\bar{a}}^{\bar{b}_i} \tag{D.32b}$$

In summary, we started with matrix A which has a one-dimensional null-space, identified the equilibrium state in the null-space by the "sums to f" constraint given by the initial state, and then shifted the equilibrium to zero using a change of variable. Notice also that the equilibrium distribution can be easily calculated as

$$\bar{F}_e = \left[-\bar{A}^{-1}\bar{a}, \quad f + 1_{N-1}^T\left(\bar{A}^{-1}\bar{a}\right)\right] . \tag{D.33}$$

The same process of changing from a marginally stable to a fully stable dynamic description can be applied to the augmented systems that include locking states. The control and estimation algorithms presented here do not require strict stability, and in the following we will continue to work with the homogeneous forms (D.29).

3.2 Reference tracking

This section presents two control algorithms for tracking an external power reference. By necessity (the geographically distributed nature of the control structure), all control algorithms operate in discrete-time. TCL units maintain the switching rates u constant until the next broadcast event (piecewise constant actuation). The first algorithm uses switch-off and switch-on actions one at a time, while the second algorithm uses an energy storage heuristic and simultaneous switch-off and switch-on actions. The algorithms use the distribution model and measurements of the total power consumption at every step, perform calculations or optimizations over short time horizons, and require an estimate for the initial state (which is expected to be close to equilibrium in the absence of actuation). The algorithms can benefit from - but *do not* require - frequently updated state information. The control structure is shown in Fig. D.7.

The main elements of the first control strategy are sketched in Alg. 2. This is a predictive scheme with a single time-step lookahead. First, a prediction is made about the power output in the absence of control. If this is bigger than the reference, the switch-off action is selected for activation. In the opposite case, the switch-on action is selected. In this way, basic knowledge of the system is embedded in the algorithm. The main step then consists of calculating the precise input value that would bring the internal model of the controller to the desired reference. A input-output linearization technique [19] is used, together with the simplified assumption

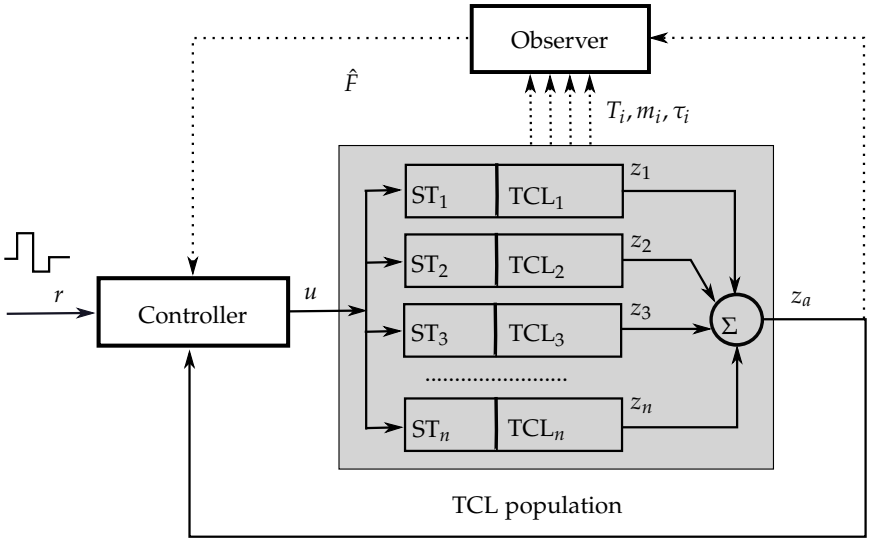

Fig. D.7: Controller structure. The dotted lines indicate signals with low update frequency.

that the output velocity remains constant in the control sample time Δt,

$$z_a(k+1) = z_a(k) + \dot{z}_a(k)\Delta t \tag{D.34a}$$

$$\dot{z}_a(k) = nCAF(k) + u_i(k)nCB_iF(k) \tag{D.34b}$$

$$u_i(k) = \frac{-nCAF(k) + v}{nCB_iF(k)} \tag{D.34c}$$

$$z_a(k+1) = z_a(k) + v\Delta t \tag{D.34d}$$

$$v = \frac{r(k+1) - z_a(k)}{\Delta t}\,. \tag{D.34e}$$

For robustness to heterogeneity and other prediction errors, the actuation is wrapped in an error integration structure (PI), preferably with anti-windup. Algorithm 2 is suitable for both the simple and the augmented models, since the computation load is light.

While arguably practical, Alg. 2 manages the power flexibility of the TCL population in a simplistic manner. This is because, in most cases, there exists more than one actuation option for bringing the output of the system to $r(k+1)$. By having a lookahead horizon of just one step, and using a preset strategy for choosing between the actuation options, Alg. 2 is not able to track challenging references. A challenging reference that is of particular importance is a step-down to zero.

The second control algorithm is an example of an heuristic that can, under certain conditions, maintain a zero power consumption over a time horizon of reasonable length. This control uses a slightly modified version of the switching action. Since the TCL unit temperature sensor is already required to distinguish between three domains in the thermostat band (b_1,b_2,b_3), we can easily consider an actuation variant with four input channels: u_{0b_1}, u_{0b_2}, u_{1b_2} and u_{1b_3}. This means that it is possible to

Algorithm 2 Step k

$e = K_i e + z_a(k) - r(k)$
$e_p = nCA_d F(k) - r(k+1) + e$
if $e_p > 0$ **then**
  $u_0(k) = \text{CONTROL}(B_0)$
else if $e_p < 0$ **then**
  $u_1(k) = \text{CONTROL}(B_1)$
end if

---

function CONTROL(B)
  $v = \big(r(k+1) - z_a(k)\big)/\Delta t$
  $u = \big(-nCAF(k) + v\big)/\big(nCBF(k)\big)$
  $u =$LIMIT(u,0,$u_{\max}$)
  $F(k+1) = e^{(A+uB)\Delta t}F(k)$
  return u
end function

use one switch-off rate for the on-units in the temperature range $\mathcal{S}_{b_1}$ and another for the on-units in the temperature range $\mathcal{S}_{b_2}$, and similarly, two different switch-on rates for the off-units in the $\mathcal{S}_{b_2}$ and $\mathcal{S}_{b_3}$ ranges.

The strategy is composed of three phases, sketched in Fig. D.8. Each phase of the strategy is controlled by a different algorithm. In the first phase, the units are pushed away from the right (hot) thermostat band using the switch-on action u_{1b3}. In order to keep the power consumption close to a normal level, this action must be compensated by switching-off units from the left (cold) side of the thermostat using the u_{0b1}. The combined effect is equivalent to a narrowing of the thermostat band to the $\mathcal{S}_{b_2}$ interval. In this operation mode, the duty-cycle of a unit will be only slightly higher than the normal value, and the aggregated power output of the population can remain close to the baseline value. The second phase corresponds to the zero power consumption period. The on- and off-distributions are now collected in the midband range $\mathcal{S}_{b_2}$. It is therefore possible to switch-off all units using input u_{0b_2}. Power consumption will remain zero as the collected off-distribution is slowly moving right (heating) across the $\mathcal{S}_{b_1}$ domain and up until the $T_{\max}$ threshold of the thermostat is reached. The third stage is recovery. The population needs to be controlled to slowly return to the equilibrium distribution, all the while maintaining a power consumption level close to the baseline. We do not solve the recovery problem in this work, but simply apply Alg. 2 to return power consumption to the baseline level (the distribution state does not return to equilibrium).

Algorithm 3 details this second control strategy. The storage phase consists of a multi-objective optimization over a single control sample time. We want to switch-on as many units as possible using u_{1b3}, and compensate by the switching-off action u_{0b1} in order to keep the power consumption close to a baseline reference. To avoid large fluctuations within the control sample time Δt, the reference tracking objective is formulated using a series of n intra-period time points. The multi-objective optimization was implemented using `fgoalattain()` MATLAB function, based on the goal

attainment method [15]. While the optimization approach has the potential of becoming computationally heavy, it is sufficient to use the basic, unaugmented distribution model for both TCL populations with and without minimum on/off time constraints. This is because the input actions are well separated between different temperature zones and thus also separated in time, and the locking effect is inherently respected. With this observation, Alg. 3 remains computationally feasible.

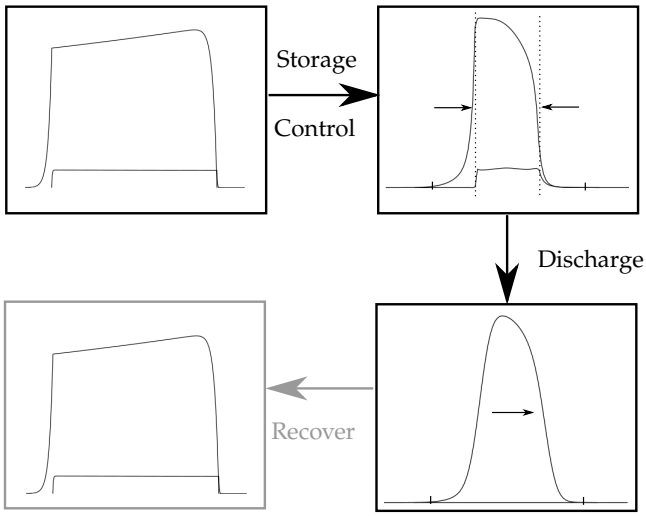

Fig. D.8: Second control algorithm

3.3 State estimation algorithm

From the point of view of estimation, models (D.29) are linear time-varying systems. As such, a Kalman filtering technique can be readily applied as long as error models are set in place. The objective of this section is to discuss the error between the distribution state coming from the modeling process and the empirical distribution of the TCL population (the plant).

The estimation algorithm uses discrete dynamic models. If we assume piecewise-continuous inputs, the discrete-time equivalents of (D.29) are

$$F(k+1) = e^{(A+\sum_i u_i(k)B_i)\Delta t}F(k), \tag{D.35a}$$

$$X(k+1) = e^{\left(A^X+\sum_i u_i(k)B_i^X\right)\Delta t}X(k)\ . \tag{D.35b}$$

Reviewing the construction process of these models, there are three categories of errors. First, the omissions and inaccuracies coming in the SHS unit model will propagate to the Fokker-Planck description and therefore also in the population model. For the most part however, these types of errors should be either small or addressable by adjusting the SHS unit model, and are not considered in the following. Another type of errors is introduced by the transformation of the PDE system into a finite dimensional approximation. Again, for the most part, these errors can be kept small

Algorithm 3 Step k

if phase(k+1) == "Storage" **then**
  $e = K_i e + z_a(k) - r(k)$
  $[\ u_{0b_1}(k),\ u_{1b3}(k)] = \textsc{Optim}(r(k+1) - e)$
else if phase(k+1) == "Discharge" **then**
  $u_{0b_1}(k) = u_{\max}$, $u_{0b_2}(k) = u_{\max}$
else if phase(k+1) == "Recovery" **then**
  use Algorithm 2 ▷ Partial recovery
end if

---

function OPTIM(r)
  $n = 5$
  ir = LINSPACE($z_a(k)$,r,$n+1$)
  lb = [0,0], ub =[$u_{\max}$, $u_{\max}$]
  u = MIN-MULTI-OBJECTIVE(@objectives, lb, ub)
  return u
end function
function OBJECTIVES(u)
  $A_{dn} = e^{(A+u(1)B_{0b1}+u(2)B_{1b3})\Delta t/n}$
  $F_p = F(k)$, obj(1) $= 0$
  for $j = 1$ to n **do**
    $F_p = A_{dn}F_p$
    obj(1) $=$ obj(1) $+ \left(CF_p - \text{ir}(j)\right)^2$
  end for
  obj(2) $= -u(2)$ ▷ or equiv. $-u(1)$
  return obj
end function

by employing a proper spatial discretization technique over a reasonably dense grids. The third type of errors is related to the aggregation procedure.

The aggregation procedure makes the leap from the discretized Fokker-Planck unit model to the population model. There are two main assumption during this process. First, it is assumed that the population is infinite in size, such that probability quantities are in effect equivalent to population fractions. The errors introduced by this assumption can be quantified using the Markov chain interpretation of the unit dynamics. This has been addressed in [10] and we now state this result. Let $P(k)$ denote either of the transition matrices $e^{(A+\sum_i u_i(k)B_i)\Delta t}$ or $e^{\left(A^X+\sum_i u_i(k)B_i^X\right)\Delta t}$, and let $p(k)$ denote either of the probability/fraction vectors $\Delta xF(k)$, $\Delta xX(k)$ of dimensions N, and $N(M_d+1)$ respectively. The conditional random variables $\Big(p_j(k+1)|p(k)\Big)$, where subscript notation j indicates one of components of the vector p, are characterized by Poisson binomial distributions, while the conditional random vector $(p(k+1)|p(k))$ is characterized by a generalized multinomial distribution. The mean, variance and

covariances are given by

$$\mathrm{E}\left[\ p_j(k+1)|p(k)\ \right] = \sum_i p_i(k)P_{ji} \tag{D.36a}$$

$$\mathrm{Var}\left[\ p_j(k+1)|p(k)\ \right] = \sum_i p_i(k)P_{ji}(1-P_{ji}) \tag{D.36b}$$

$$\mathrm{Cov}\left[\ p_j(k+1)|p_l(k)\ \right] = -\sum_i p_i(k)P_{ji}P_{li}\ . \tag{D.36c}$$

This result points to the addition of an error term $M(k)$,

$$p(k+1) = P(k)p(k) + M(k), \tag{D.37}$$

with $\mathrm{E}\left[M(k)\right] = 0$, and state-dependent covariance matrix $\mathrm{Cov}\left[M(k)\right]$ given by relations (D.36b) and (D.36c).

A further source of errors, and one of the most concerning, is population heterogeneity. Obtaining a good characterization of the errors is however a more difficult task. If the heterogeneity is not too large, an additional white noise term can be added to complete an error model,

$$p(k+1) = P(k)p(k) + M(k) + w(t)\ . \tag{D.38}$$

Having an error model makes it possible to use a linear Kalman filter to perform state estimation. Model (D.38) can easily be reformulated back in terms of the states F or X.

3.4 Measurements

The main measurement used by the control algorithm is the total power consumption signal. This is the driving signal of the control loop structure. In this work, the TCL population has been considered in isolation, but in a realistic scenario aggregate power measurements from the electrical grid (a feeder, a transformation station, or at the regional level) will include other consumption. Therefore a method would be needed to separate the contribution of the TCLs from the total consumption data. However, the control objective is not the TCL consumption per se, but rather the total consumption in an area (or portfolio). As long as the control objective can be measured, it can be used directly (without separation) to create the control error signal.

Monitoring the distribution state of the TCL requires individual unit measurements. The advantage of the distribution approach is that individual state measurements can be infrequent, partial and are used anonymously. Individual unit measurements consists of the temperature and mode (and timer) data from a limited number of units in the population, e.g. 10% or 20%. These can be processed to create a distribution measurement $\tilde{F}$, which can be characterized using the variance and covariance properties of the multivariate hypergeometric distribution. This is because, by extracting a finite number of units n_m from the TCL population with $n > n_m$ units and N possible outcomes, we are effectively performing a "draws without replacement"

random experiment.

$$\mathrm{E}[\tilde{F}] = F \tag{D.39a}$$

$$\mathrm{Var}[\tilde{F}_i] = \frac{n-n_m}{n-1}\frac{1}{n_m}F_i\frac{1-F_i\Delta x}{\Delta x} \tag{D.39b}$$

$$\mathrm{Cov}[\tilde{F}_i,\tilde{F}_j] = -\frac{n-n_m}{n-1}\frac{1}{n_m}F_iF_j \tag{D.39c}$$

Since the true underlying distribution F is not known, the right hand-side of the equations (D.39) will be evaluated using the filter estimate $\hat{F}$. To assure that the estimation algorithm does not change the system invariant, a virtual measurement is added that always gives the total probability/fraction of the distribution state as 1.

4 Numerical Simulations

This section contains numerical results on a case-study for domestic refrigerators. The ETP parameters used for the TCL unit model (D.1a) are listed in Table D.1. The actuation parameters are the minimum on/off time $M = 300s$, the temperature safe-zones are $\Delta T_1 = \Delta T_2 = 1^\circ C$, and $u_{\max} = 2$.

Table D.1: TCL unit parameters

C (J/K)	UA (W/K)	T_a ($^\circ C$)	W (W)
93920	1.432	24	100
η	σ ($^\circ C/s$)	$T_{\min}(^\circ C)$	$T_{\max}(^\circ C)$
2.8	0.0065	2	5

In all cases, a population of 10000 units is considered. In addition to the homogeneous population, two types of heterogeneities, each with three increasing levels, have been tested. The ETP parameters have been randomly distributed around the mean values from Table D.1 according to a 3σ-truncated Gaussian distribution with standard deviations of 5%, 10%, and 15%, and according to a uniform distribution with standard deviations of 10%, 20%, and 30%. The C, UA, T_a, η, W, and σ parameters have been affected, while the thermostat range, temperature safe-zones and the minimum on/off time are uniform across the population. The TCL population (plant) has been simulated using Monte Carlo techniques. Each of the 10000 SHS models is run individually with a sample rate of $0.1s$. For control, a broadcast rate $\Delta t = 60s$ has been used.

4.1 FVM results

We first give a qualitative and quantitative comparison for the dynamical matrix A obtained with different FVM techniques. In all cases, the used FVM grid is uniform, with extended domain boundaries $T_{\text{minmin}} = 1.5^\circ C$ and $T_{\text{maxmax}} = 5.5^\circ C$. Three cases are compared: a second order upwind scheme with a coarse (a) and dense (b) grid, and the structure preserving FVM on a coarse (c) and on a dense (d) grid.

Positivity refers to the Mertzel property of matrix A. Because in addition the columns each sum to 0 (conservative property), whenever matrix A is positive, it is

also a proper transition rate matrix. The duty-cycle calculation is done using the equilibrium distribution computed by (D.33) and evaluating the percentage of represented by the total area under the on-distribution. It is used as an indicator for the absolute error of the FVM schemes. The duty-cycle for the TCL unit with the parameters from Table D.1 is close to 0.105 value. Fig. D.9 shows the equilibrium distributions obtained from the four methods. It can be seen that the second order up-wind scheme (a) is not positive, and shows the spurious oscillation effects (see Godunov's order barrier theorem, [30] ch.13), but both of these effects are reduced when the grid size is reduced in scheme (b). The structure preserving schemes (c) and (d) are positive, but slower to converge, and as a result the distribution (and duty-cycle) of coarse scheme (c) has significant errors. Although accuracy criteria would suggest using schemes (d) or (b), scheme (a) has the advantage of a small computational footprint, and proves to capture the dynamical behavior suitably well for control algorithms.

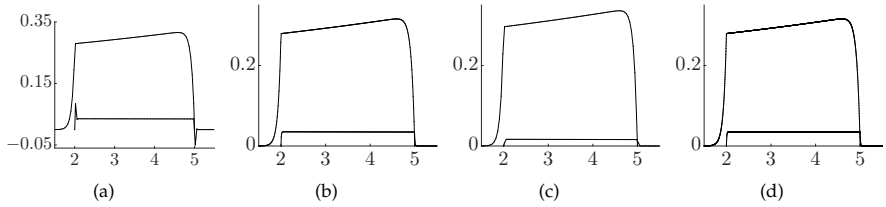

Fig. D.9: Equilibrium distributions as obtained using the second order up-wind coarse and dense schemes (a) and (b) respectively, and the structure preserving coarse and dense schemes (c) and (d) respectively. The grid parameters are given in Table D.2.

Augmented systems have a significantly higher dimensionality. The spatial discretization and overall matrix size used in the following control simulations is also given in Table D.2.

4.2 Free response simulations

Figure D.10 shows the free response from an initial state where all units are initially off and have the same temperature, its value close to the hot threshold of the thermostat.

This synchronized initial state showcases the oscillatory nature of the power response, and the differences between the homogeneous and heterogeneous populations. A main and well-known characteristic of heterogeneous populations is that

Table D.2: Dynamic matrix A, and augmented A^X

	Δx	N	Positivity	Duty-Cycle
(a)	0.0385	182	No	0.105
(b)	0.01	700	No	0.105
(c)	0.0385	182	Yes	0.04878
(d)	0.0025	2800	Yes	0.1046

	Δx	Δy	N
A^X	0.0385	30s	2002

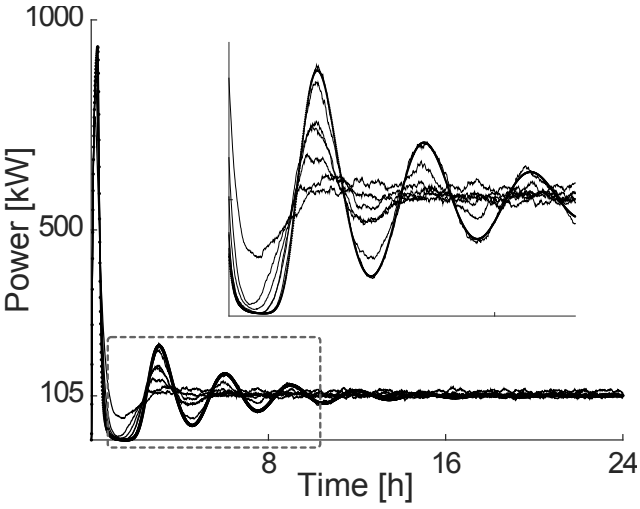

Fig. D.10: Free response of the TCL populations from a synchronized initial state. The thick line is the distribution model response, while the thin lines are the responses of TCL populations with different levels of heterogeneity.

they desynchronize and reach the equilibrium state faster. On the other hand, the model error is small for the homogeneous population and increases with heterogeneity.

4.3 Control simulations

The TCL populations are known to initially be close to equilibrium, and no additional state updates are used for the duration of a 2 hours control horizon. Measurement of the aggregate power consumption is done without error terms, see the discussion in Section 3.4.

Algorithm 2 is tested using two piecewise constant references. Reference I is a repeated sequence consisting of a moderate step-up doubling the baseline, followed by a step-down to zero, placed in between baseline values. Results are shown in Fig. D.11. The control is able to follow the step-up section, as this reference lies comfortably within the power consumption flexibility, but cannot reach the zero-level of the step-down section.

Reference II consists of a single step-down to zero. Results are shown in Fig. D.12. Once again, the control is not able to reach zero power consumption. The only way to guarantee a zero consumption is to move units away from both the "off" and "on" b_3 zones. This strategy is showcased by Alg. 3. Nevertheless, Alg. 2 is arguably a practical, efficient and *fully responsive* control scheme.

Algorithm 3 performs the storage control until the amount of units in the b_3 temperature zone (both on the "on" and on the "off" distribution) reaches a low value, and then enters the discharge phase. When the power consumption cannot be maintained close to zero anymore, the power consumption is returned to a level close to baseline using Alg. 2. Results are shown in Fig. D.13. It can be seen that different popula-

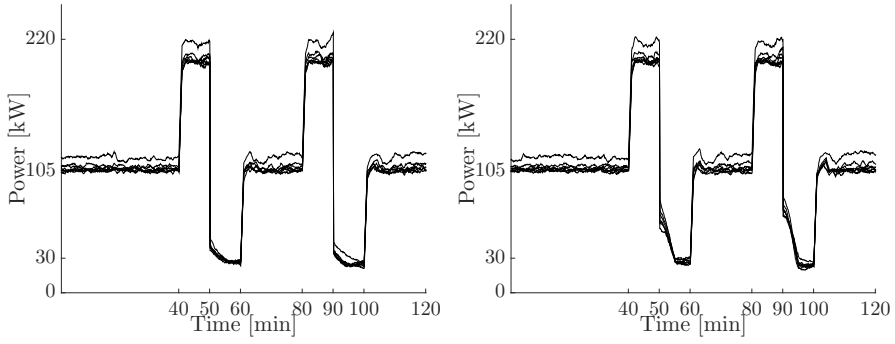

(a) Control of TCLs without minimum on/off timers (b) Control of TCLs with minimum on/off timers

Fig. D.11: Switching-Rate actuation, Alg. 2, Reference I. The plots shows overlapped results from the one homogeneous and the six heterogeneous populations. The baseline levels of each population are slightly different.

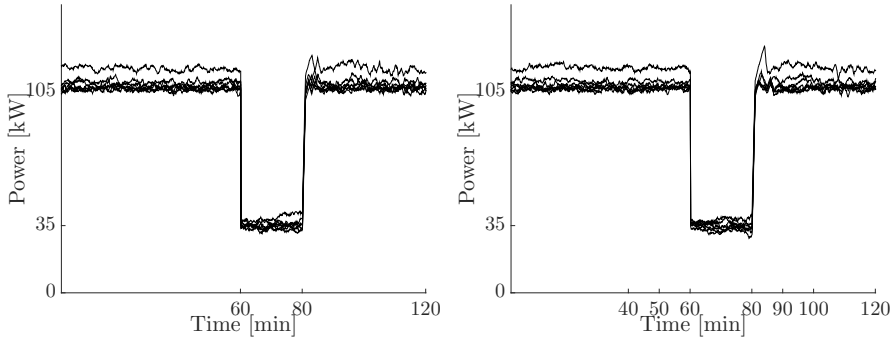

(a) Control of TCLs without minimum on/off timers (b) Control of TCLs with minimum on/off timers

Fig. D.12: Switching-Rate, Control Alg. 2, Reference II

tions take different time to charge - the charging time increasing with heterogeneity, and also that the duration of the discharge period (the zero consumption period) is different, decreasing with heterogeneity. This is because the algorithm is performing a type of state synchronization, and the heterogeneous populations have a higher natural rate of de-synchronization, as can be seen from the free response results in Section 4.2, working against the algorithm.

Both control techniques can handle some amount of heterogeneity, with the biggest errors occurring for the largest tested dispersion of the parameters (the uniform distribution with a standard parameter deviation of 30%).

4.4 State estimation

Implementing the linear Kalman requires the error model (D.37), which is build on the Markov chain interpretation of the space- and time-discretized model. As such,

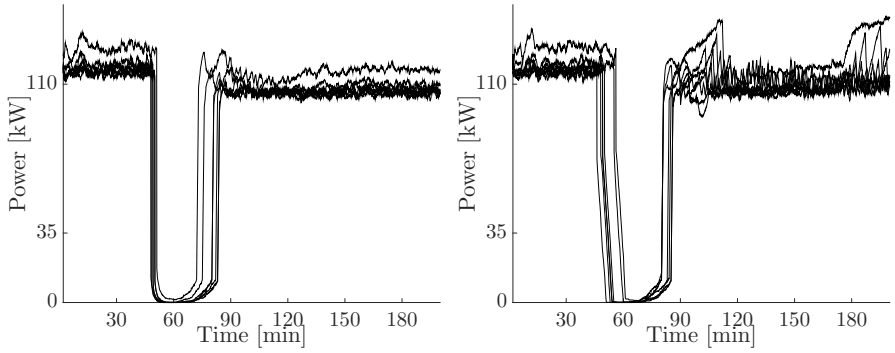

(a) Control of TCLs without minimum on/off timers (b) Control of TCLs with minimum on/off timers

Fig. D.13: Switching Rate, Control Alg. 3

we need to use a dynamic model build with the structure preserving FVM, since the models constructed with the second-order upwind technique produce dynamic matrices with negative entries. The structure preserving FVM requires a dense grid for good accuracy. At a dimension of 2800×2800, scheme (d) is still under-performing as the duty-cycle is not correctly approximated, see Table D.2, but is suitable for estimation.

This section presents numerical results for control with estimation using the Switching-Rate case for models without locking feature (as the structure preserving FVM models with the locking feature are computationally too heavy), for the population with the highest heterogeneity. The control Alg. 2 continues to use model (a) for the one time-ahead prediction, but the estimation runs in parallel using model (d) and updates the distribution state. The estimation uses individual measurements from 1000 randomly chosen units (10% of the population) at each step. Control and estimation algorithms run with the same sample rate $\Delta t = 60s$. Power trajectories of the estimation run are compared with the simulation results from Section 4.3 (the state of internal model is not updated during the control horizon, and a PI structure is used to compensate for heterogeneity), and also with a run where the PI structure is deactivated.

The results in Fig. D.14 show that the estimation works well, and outperforms the PI algorithm. However, the estimation is computationally more heavy, as the required model has a high dimensionality.

5 Conclusion

This work has proposed a new, practical actuation strategy for enabling large scale demand response of thermostatic loads. The Switching-Rate actuation has been described, modeled and used to activate the power consumption flexibility of a population of thermostatic loads in a numerical scenario.

Several directions for future work open up as a result of the promising numerical scenario. First, it would be of interest to study the actuation in a demonstration setup, subject to the real life thermal and population dynamics, and under realistic distur-

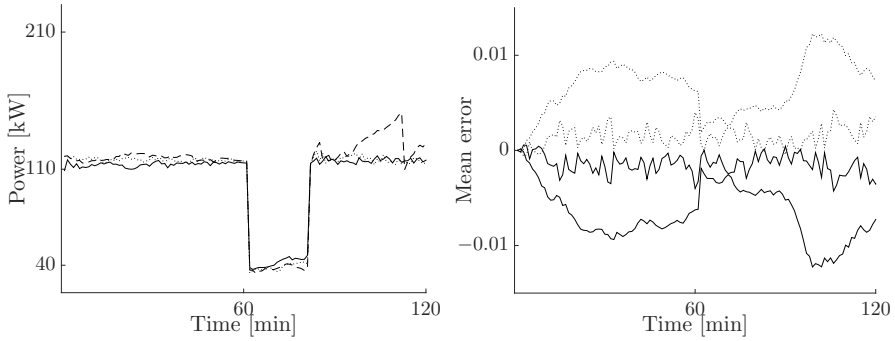

(a) Alg. 2, Reference II. Solid line shows the trajectory using state estimation, the dotted line uses PI, and the dashed line no estimation and no PI

(b) Control of TCLs with minimum on/off timers

Fig. D.14: Mean error of the state for the estimation vs PI. The full-line shows the mean error in the on-distribution, and the dotted line the off-distribution. The state error is smaller when using the estimation.

bances. Secondly, we note that more advanced issues of the problem formulation remain open. Neither Alg. 2 nor Alg. 3 return the distribution state to equilibrium. Stopping the control broadcast returns the system to a free response with oscillatory output behavior before the equilibrium state is reached. The problem of a controlled return to the equilibrium state using the switching actuation remains as yet open, although we can point towards Lyapunov techniques as a promising direction. Furthermore, it is clear that not all power references are tractable. The problem of describing tractable references, problem that depends not only on the system parameters but also on the control algorithm, has not been addressed. Finally, we point to problem of reducing the system dimensionality. In this work, the PDE dynamics have been brought to a finite dimensional, continuous-time form using FVMs as numerical techniques. General FVMs schemes however do not preserve structural properties such as positivity, while the special technique in [21] has the disadvantage of producing very large matrices not directly suitable for online algorithms. Model order reduction techniques for bilinear systems could be tested in future work.

Acknowledgment

This work has been supported by the Southern Denmark Growth Forum and the European Regional Development Fund under the project “Smart & Cool". The authors would like to extends thanks to Karl Damkjaer Hansen for his work setting up an instrumented refrigerator unit and practical insights.

References

[1] International Energy Agency. *The Power of Transformation Wind, Sun and the Economics of Flexible Power Systems*. 2014.

[2] European Wind Energy Association et al. *Large Scale Integration of Wind Energy in the European Power Supply: Analysis, Issues and Recommendations: a Report*. European Wind Energy Association, 2005.

[3] Saeid Bashash and Hosam K Fathy. Modeling and control of aggregate air conditioning loads for robust renewable power management. *Control Systems Technology, IEEE Transactions on*, 21(4):1318–1327, 2013.

[4] Jan Bendtsen and Srinivas Sridharan. Efficient desynchronization of thermostatically controlled loads. *11th IFAC International Workshop on Adaptation and Learning in Control and Signal Processing*, 2013.

[5] Manuela L Bujorianu and John Lygeros. General stochastic hybrid systems: Modelling and optimal control. In *Decision and Control, 2004. CDC. 43rd IEEE Conference on*, volume 2, pages 1872–1877. IEEE, 2004.

[6] Manuela L Bujorianu and John Lygeros. Toward a general theory of stochastic hybrid systems. In *Stochastic Hybrid Systems*, pages 3–30. Springer, 2006.

[7] Duncan S Callaway. Tapping the energy storage potential in electric loads to deliver load following and regulation, with application to wind energy. *Energy Conversion and Management*, 50(5):1389–1400, 2009.

[8] Duncan S Callaway and Ian A Hiskens. Achieving controllability of electric loads. *Proceedings of the IEEE*, 99(1):184–199, 2011.

[9] E B Dynkin. *Markov processes*. Springer, 1965.

[10] S. Esmaeil Zadeh Soudjani and A. Abate. Aggregation and control of populations of thermostatically controlled loads by formal abstractions. *Control Systems Technology, IEEE Transactions on*, PP(99):1–1, 2014.

[11] Lorenzo Farina and Sergio Rinaldi. *Positive linear systems: theory and applications*, volume 50. John Wiley & Sons, 2011.

[12] Joel H Ferziger and Milovan Perić. *Computational methods for fluid dynamics*, volume 3. Springer Berlin, 2002.

[13] Renewable Energy Policy Network for the 21st Century. Global status report, 2014.

[14] Crispin W Gardiner. *Handbook of stochastic methods: for Physics, Chemistry and the Natural Sciences*. Springer Berlin, 1985.

[15] FW Gembicki. *Vector optimization for control with performance and parameter sensitivity indices*. PhD thesis, Ph.D. Thesis, Case Western Reserve Univ., Cleveland, Ohio, 1974.

[16] Azad Ghaffari, Scott Moura, and Miroslav Krstic. Analytic modeling and integral control of heterogeneous thermostatically controlled load populations. In *Dynamic Systems and Control Conference, ASME Proceedings*, 2014.

[17] Doug Hurley, Paul Peterson, and Melissa Whited. Demand response as a power system resource, 2013.

[18] Satoru Ihara and Fred C Schweppe. Physically based modeling of cold load pickup. *Power Apparatus and Systems, IEEE Transactions on*, (9):4142–4150, 1981.

[19] Hassan K Khalil and JW Grizzle. *Nonlinear systems*, volume 3. Prentice Hall Upper Saddle River, 2002.

[20] Arman C Kizilkale and Roland P Malhame. Collective target tracking mean field control for markovian jump-driven models of electric water heating loads. In *IFAC World Congress*, 2014.

[21] Juan C Latorre, Philipp Metzner, Carsten Hartmann, and Christof Schütte. A structure-preserving numerical discretization of reversible diffusions. *Commun. Math. Sci*, 9(4):1051–1072, 2011.

[22] Roland Malhame and Chee-Yee Chong. Electric load model synthesis by diffusion approximation of a high-order hybrid-state stochastic system. *Automatic Control, IEEE Transactions on*, 30(9):854–860, 1985.

[23] J.L. Mathieu, S. Koch, and D.S. Callaway. State estimation and control of electric loads to manage real-time energy imbalance. *Power Systems, IEEE Transactions on*, 28(1):430–440, Feb 2013.

[24] RE Mortensen and KP Haggerty. A stochastic computer model for heating and cooling loads. *Power Systems, IEEE Transactions on*, 3(3):1213–1219, 1988.

[25] Peter Palensky and Dietmar Dietrich. Demand side management: Demand response, intelligent energy systems, and smart loads. *Industrial Informatics, IEEE Transactions on*, 7(3):381–388, 2011.

[26] Cristian Perfumo, Ernesto Kofman, Julio H Braslavsky, and John K Ward. Load management: Model-based control of aggregate power for populations of thermostatically controlled loads. *Energy Conversion and Management*, 55:36–48, 2012.

[27] Nikolai A Sinitsyn, Soumya Kundu, and Scott Backhaus. Safe protocols for generating power pulses with heterogeneous populations of thermostatically controlled loads. *Energy Conversion and Management*, 67:297–308, 2013.

[28] Ingo Stadler. Power grid balancing of energy systems with high renewable energy penetration by demand response. *Utilities Policy*, 16(2):90–98, 2008.

[29] Michael Stadler, Wolfram Krause, Michael Sonnenschein, and Ute Vogel. Modelling and evaluation of control schemes for enhancing load shift of electricity demand for cooling devices. *Environmental Modelling & Software*, 24(2):285–295, 2009.

[30] Eleuterio F Toro. *Riemann solvers and numerical methods for fluid dynamics*, volume 16. Springer, 1999.

[31] Jacopo Torriti, Mohamed G Hassan, and Matthew Leach. Demand response experience in europe: Policies, programmes and implementation. *Energy*, 35(4):1575–1583, 2010.

[32] Luminita C Totu, John Leth, and Rafael Wisniewski. Control for large scale demand response of thermostatic loads. In *American Control Conference (ACC)*, pages 5023–5028. IEEE, 2013.

[33] Luminita Cristiana Totu and Rafael Wisniewski. Demand response of thermostatic loads by optimized switching-fraction broadcast. In *IFAC World Congress*, 2014.

[34] Luminita Cristiana Totu, Rafal Wisniewski, and John-Josef Leth. Modeling populations of thermostatic loads with switching rate actuation. In *4th Hybrid Autonomous Systems (HAS) Workshop*, 2014.

[35] Wei Zhang, Jianming Lian, Chin-Yao Chang, and Karanjit Kalsi. Aggregated modeling and control of air conditioning loads for demand response. *IEEE Transactions on Power Systems*, 28(4):4655 – 4664, 2013.

Part III

Appendices

Notes on Duty-Cycle Calculations

The duty-cycle is defined in relation to the durations of the ON and OFF power cycles. The duty-cycle will be considered for the normal thermostat operation (without any external control). The thermostat limits are $T_{\min}$ and $T_{\max}$, and the TCL unit is performing a cooling task. If the thermal dynamics are deterministic, the durations of the ON and OFF cycles are deterministic. If the thermal dynamics are stochastic, the durations of the ON and OFF cycles are random variable.

1 Deterministic Duty-Cycle

In the deterministic case, the Themostatically Controlled Load (TCL) model with the normal thermostat operation is

$$\dot{T}(t) = \begin{cases} -aT(t) + b_0, & \text{when the power cycle is off} \\ -aT(t) + b_1, & \text{when the power cycle is on} \end{cases}, \tag{Y.1}$$

where $a = \frac{\mathrm{UA}}{C}$, $b_0 = \frac{\mathrm{UA}}{C} T_{\mathrm{amb}}$, $b_1 = \frac{\mathrm{UA}}{C} T_{\mathrm{amb}} - \frac{\eta W}{C}$, with UA, C, T_{amb}, η, and W standing in for physical coefficients, all positive. Let variable $m(t)$ denote the state of the power cycle, $0 \equiv$ OFF and $1 \equiv$ ON, then the thermostat logic can be expressed as

$$m(t) = \begin{cases} 1, & T(t) \geq T_{\max} \\ 0, & T(t) \leq T_{\min} \\ m(t^-), & \text{otherwise} \end{cases}.$$

A TCL first changes to ON state when the temperature reaches $T_{\max}$ and remains ON until the temperature reaches $T_{\min}$. To find out how much this takes according to the model, we study the solution of the Ordinary Differential Equation (ODE)

$$\dot{T}_{\mathrm{ON}}(t) = -aT_{\mathrm{ON}}(t) + b_1, \; T_{\mathrm{ON}}(0) = T_{\max}. \tag{Y.2}$$

The solution is given by the function

$$T_{\mathrm{ON}}(t) = \frac{b_1}{a} + \left(T_{\max} - \frac{b_1}{a}\right) \exp(-at). \tag{Y.3}$$

By setting $T_{\mathrm{ON}}(\tau_{\mathrm{OFF}}) = T_{\min}$, we obtain an expression for the duration of the ON cycle as

$$\tau_{\mathrm{ON}} = -\frac{1}{a} \ln \left(\frac{T_{\min} - \frac{b_1}{a}}{T_{\max} - \frac{b_1}{a}} \right). \tag{Y.4}$$

It was possible to determine a unique solution for τ_{OFF} because of the nice monotonic form of the solution $T_{\text{ON}}(t)$.

Similarly, the duration of the OFF cycle is

$$\tau_{\text{OFF}} = -\frac{1}{a}\ln\left(\frac{T_{\max} - \frac{b_0}{a}}{T_{\min} - \frac{b_0}{a}}\right). \tag{Y.5}$$

Using the numerical values for the refrigerator test case used in Papers B, C and D, it is obtained that $\tau_{\text{ON}} = 1124.17[\text{s}] = 18.74[\text{min}]$ and $\tau_{\text{OFF}} = 9615.22[\text{s}] = 160.25[\text{min}]$, leading to a duty-cycle value:

$$\text{dc} = \frac{\tau_{\text{ON}}}{\tau_{\text{ON}} + \tau_{\text{OFF}}} = 0.1047$$

2 Stochastic Case

In the stochastic case, the thermal dynamics are given by Stochastic Differential Equations (SDEs),

$$dT(t) = \begin{cases} \big(-aT(t) + b_0\big)dt + \sigma dW(t), & \text{when the power cycle is off} \\ \big(-aT(t) + b_1\big)dt + \sigma dW(t), & \text{when the power cycle is on ,} \end{cases} \tag{Y.6}$$

while the thermostat logic remains the same as in the deterministic case. The ON and OFF mode durations are equivalent to first exit times of the stochastic thermal process from a corresponding thermostat region. This exposition follows the treatment of first exit times from [1](Ch.5.2.7).

For the TCL to be OFF, its temperature must belong to the interval $[T_{\text{minmin}}, T_{\max})$. This is because as soon as the temperature reaches $T_{\max}$, the thermostat changes to mode ON. Furthermore, it has been assumed that temperatures smaller than T_{minmin} are not possible in normal operation[1].

Starting from an initial time $t = 0$ with temperature $T(0) = x \in [T_{\text{minmin}}, T_{\max})$ [2], the interest is on the first time when the temperature reaches $T_{\max}$. The time t, defines the end of the OFF duration and is a random variable. Let $G(x,t) \triangleq \Pr\big[\tau_{\text{OFF}} > t \;\big|\; T(0) = x\big]$ be the tail distribution function of the random variable $\tau_{\text{OFF}}(x)$. This means that until time t the temperature remained in the proper interval range, and thus $G(x,t) = \int_{T_{\text{minmin}}}^{T_{\max}} f(y,t,x,0)dy$, where f is the transition density function of the thermal process with the dynamic given by the "cooling" SDE, and considering that the dynamic rules include a reflecting boundary at T_{minmin} (keeping the probability in the system) and an absorbing boundary at $T_{\max}$ (taking the probability out of the system).

Because the thermal dynamics are time-homogeneous, it is possible to write $f(y,t,x,0)$ as $f(y,0,x,-t)$, and write a Backward differential equation for f as

$$\begin{aligned} \frac{\partial f(y,0,x,-t)}{\partial(-t)} &= -(ax+b_0)\frac{\partial f(y,0,x,-t)}{\partial x} - \frac{\sigma^2}{2}\frac{\partial^2 f(y,0,x,-t)}{\partial x^2} \equiv \\ \equiv \frac{\partial f(y,t,x,0)}{\partial t} &= (ax+b_0)\frac{\partial f(y,t,x,0)}{\partial x} + \frac{\sigma^2}{2}\frac{\partial^2 f(y,t,x,0)}{\partial x^2} \end{aligned} \tag{Y.7a}$$

[1] An alternative is to consider an infinite left boundary.

[2] The case $x = T_{\min}$ is of interest here, as this defines the beginning of an OFF cycle. The first exit times are best studied by not fixing the x variable to its desired valued in the beginning of the analysis $T_{\min}$

with boundary conditions corresponding to a reflecting boundary and to an absorbing boundary,

$$\frac{\partial f(y,t,x,0)}{\partial x}\Big|_{x=T_{\text{minmin}}} = 0, \quad f(y,t,T_{\max},0) = 0. \tag{Y.7b}$$

This leads to the $G(x,t)$ function satisfying the same expression,

$$\frac{\partial G(x,t)}{\partial t} = (ax+b_0)\frac{\partial G(x,t)}{\partial x} + \frac{\sigma^2}{2}\frac{\partial^2 G(x,t)}{\partial x^2} \tag{Y.8a}$$

where the boundary conditions

$$\frac{\partial G(x,t)}{\partial x}\Big|_{x=T_{\text{minmin}}} = 0\,, G(T_{\max},t) = 0. \tag{Y.8b}$$

As as a tail distribution function $G(x,t)$ (with x is a parameter, t is the variable) has also the property that $G(x,0) = 1$, and $\lim_{t\to\infty} G(x,t) = 0$ with $G(x,t) = o(1/t)$ (for the given situation), meaning $\lim_{t\to\infty} tG(x,t) = 0$.

A more simple description can be found for the moments of τ_{OFF}. Only the first two are investigated here. First,

$$\begin{aligned}\mathrm{E}\big[\tau_{\text{OFF}}(x)\big] &= \int_0^\infty td(1-G(x,t)) = -\int_0^\infty tdG(x,t) = -\int_0^\infty t\frac{\partial G(x,t)}{\partial t}dt = \\ &= -tG(x,t)\big|_0^\infty + \int_0^\infty G(x,t)dt = \int_0^\infty G(x,t)dt \triangleq M(x),\end{aligned} \tag{Y.9}$$

which leads to the following second order differential equation,

$$\begin{aligned}\int_0^\infty \frac{\partial G(x,t)}{\partial t}dt &= (ax+b_0)\frac{dM(x)}{dx} + \frac{\sigma^2}{2}\frac{d^2M(x)}{dx^2} \equiv \\ \equiv -1 &= (ax+b_0)\frac{dM(x)}{dx} + \frac{\sigma^2}{2}\frac{d^2M(x)}{dx^2}\end{aligned} \tag{Y.10a}$$

with boundary conditions

$$\frac{dM(x)}{dx}\Big|_{x=T_{\text{minmin}}} = 0,\ M(T_{\max}) = 0\,. \tag{Y.10b}$$

This form can be solved numerically (e.g. MATLAB®. `bvp4c`), and it can be obtained that $M(T_{\min}) = E\left[\tau_{\text{OFF}}(T_{\min})\right] = 159.73[\text{min}]$. It is noted that a closed form expression for M(x) in given in [1], however this includes embedded integrals that are arguably more difficult to evaluate numerically. For the second moment,

$$\begin{aligned}\mathrm{E}\big[\tau^2_{\text{OFF}}(x)\big] &= -\int_0^\infty t^2\frac{\partial G(x,t)}{\partial t}dt = -t^2G(x,t)\big|_0^\infty + \int_0^\infty 2tG(x,t)dt = \\ &= \int_0^\infty 2tG(x,t) \triangleq Q(x)\,,\end{aligned} \tag{Y.11}$$

where it was assumed that $\lim_{t\to\infty} t^2G(x,t) = 0$. The following differential equation is obtained

$$-2M(x) = (ax+b_0)\frac{dQ(x)}{dx} + \frac{\sigma^2}{2}\frac{d^2Q(x)}{dx^2}, \tag{Y.12a}$$

showing a dependence on $M(x)$, and with similar boundary conditions

$$\frac{dQ(x)}{dx}\Big|_{x=T_{\text{minmin}}} = 0,\ Q(T_{\max}) = 0\ . \tag{Y.12b}$$

A numerical solution can be obtained for $Q(x)$ and $Q(T_{\min})$, and used to calculate the standard deviation as $\text{std}\big[\tau_{\text{OFF}}(T_{\min})\big] = 33.86$ [min].

A similar analysis carried on for $\tau_{\text{ON}}(x)$ leads to the following numerical results, $E\left[\tau_{\text{ON}}(T_{\max})\right] = 18.73$ [min] and $\text{Std}\big[\tau_{\text{ON}}(T_{\max})\big] = 1.36$ [min].

It is noted that by definition/construction, the random variables τ_{OFF} and τ_{ON} are independent, however this does not allow for a straightforward evaluation of the statistic properties of the duty-cycle $\tau_{\text{ON}}/(\tau_{\text{ON}} + \tau_{\text{OFF}})$.

Some further consideration can be made directly about the duty-cycle, and are given below, however these do not lead to a closed solution.

First, it can seen that the joint density of the random variables τ_{ON} and $\tau_{\text{ON}} + \tau_{\text{OFF}}$ is given by

$$f_{\tau_{\text{ON}},\tau_{\text{ON}}+\tau_{\text{OFF}}}(x,y) = f_{\tau_{\text{ON}}}(x) f_{\tau_{\text{OFF}}}(y-x). \tag{Y.13}$$

Using the ratio distribution formula, it can be written that

$$f_{\text{dc}}(z) = \int_0^\infty u f_{\tau_{\text{ON}}}(zu) f_{\tau_{\text{OFF}}}\big(u(1-z)\big) du, \tag{Y.14}$$

and thus

$$\begin{aligned}
\text{E}\big[\text{dc}\big] = M(x_0,x_1) &= \int_0^1 \int_0^\infty zu f_{\tau_{\text{ON}}}(x_1,zu) f_{\tau_{\text{OFF}}}\big(x_0,u(1-z)\big) du dz \\
&= \int_0^\infty \int_0^\infty \frac{v_1}{v_1+v_0} f_{\tau_{\text{ON}}}(x_1,v_1) f_{\tau_{\text{OFF}}}(x_0,v_0) dv_1 dv_0 \\
&= \int_0^\infty \int_0^\infty \frac{v_1}{v_1+v_0} \partial_{v_1} G_1(x_1,v_1) \partial_{v_0} G_0(x_0,v_0) dv_1 dv_0
\end{aligned} \tag{Y.15}$$

Further manipulations based on integration by parts leads to the additional expression

$$M(x_0,x_1) = \int_0^\infty \int_0^\infty \frac{v_1 - v_0}{(v_1+v_0)^3} G_1(x_1,v_1) G_0(x_0,v_0) dv_1 dv_0. \tag{Y.16}$$

In the case of the expected value for the random duration times τ, the two expressions of $M(x)$ as a function of $G(x,t)$ could be closed by using the Backward equation on the $G(x,t)$. This is however not the case for the duty-cycle calculations, because the terms under the integral expressions $\frac{v_1}{v_1+v_0}$ and $\frac{v_1-v_0}{(v_1+v_0)^3}$ are not compatible.

Table Y.1: Duty calculation. The τ values are given in decimal minutes.

	Deterministic	$\sigma = 0.0065$		$\sigma = 0.06$	
		Mean	Std.	Mean	Std.
τ_{ON}	18.74	18.73	1.36	17.75	10.83
τ_{OFF}	160.25	159.73	33.86	54.89	45.90
$\frac{\tau_{\text{ON}}}{\tau_{\text{ON}}+\tau_{\text{OFF}}}$	0.1047	?	?	?	?

Finally, we point to the work [2, 3] for some analytical results on the stochastic duty-cycle calculations, under a reasonable model approximation.

References

[1] Crispin W Gardiner. *Handbook of stochastic methods: for Physics, Chemistry and the Natural Sciences*. Springer Berlin, 1985.

[2] AH Noureddine, AT Alouani, and A Chandrasekaran. On the maximum likelihood duty cycle of an appliance and its validation. *Power Systems, IEEE Transactions on*, 7(1):228–235, 1992.

[3] AH Noureddine, AT Alouani, and SA Patil. On the probability density function of an air conditioner duty cycle. In *American Control Conference, 1991*, pages 2089–2093. IEEE, 1991.

Notes on Domestic Refrigerators

Refrigerators are the main case-study devices used in this work, and this section presents some unit level modeling principles and elements, and a partial validation against real measurements.

Domestic refrigerators and freezers are typical household appliances, present in almost every home in the industrialized countries, as well as in large numbers everywhere else [2]. In Denmark, fridges and freezers accounted for about 820 [GWh] in energy consumption in 2012 [1], which is equivalent to a baseline (or instantaneous) consumption of 93 [MW].

1 Thermodynamic Principles

References for fundamental thermodynamic concepts such as systems, states, processes, equilibrium and quasi-equilibrium, and the main assumptions under which thermodynamical systems are generally studied, are [5] and [4].

A first principle when analyzing thermodynamic systems is that for any process, the overall energy is conserved. This principle can be expressed in the form of a balance equation, that in the most general terms can be written as,

$$\Delta E_{\text{system}} = E_{\text{in}} - E_{\text{out}}, \tag{Z.1}$$

meaning that the total energy variation of a predefined system over a time horizon $[t_0, t_1]$, $\Delta E_{\text{system}} = E_{\text{system}}(t_1) - E_{\text{system}}(t_0)$, is equal with the total energy received from the outside minus the total energy lost to the outside during this time. Furthermore, the left hand-side of the equation refers to energy as state or property of the system in a "static" form, while the right hand-side terms refer to the transfer or "dynamic" forms of energy, and is depended on the entire trajectory or path of the system during the $[t_0, t_1]$ time interval. Therefore an equivalent way of expressing the energy balance relation is as

$$\int_{t_0}^{t_1} dE_{\text{system}}(t) = E_{t_1} - E_{t_0} = \Delta E(t_0, t_1) = \underbrace{\int_{t_0}^{t_1} \mathcal{F}_{\text{in}}(t)dt}_{E_{\text{in}}} - \underbrace{\int_{t_0}^{t_1} \mathcal{F}_{\text{out}}(t)dt}_{E_{\text{out}}}, \tag{Z.2}$$

where $\mathcal{F}$ is the instantaneous energy transfer flow. While energy (both "static" and the overall transfered quantities) is measured in Joules $[J]$, the energy transfer flow is measured in Watts, $[W] = [J/s]$.

In thermodynamic studies there are three types or mechanism for energy transfer: heat transfer, work, and mass transfer. Heat is energy transfer as a result of temperature difference, work is energy transfer involving forces over distances (includes electrical effects), while mass transfer refers to the matter exchange of the system with the surroundings.

For a system without mass transfer with the exterior, the energy balance equation can be written as:

$$\begin{aligned}\Delta E_{\text{system}} &= Q_{\text{in}} + W_{\text{in}} - Q_{\text{out}} - W_{\text{out}} \\ &= \int_{t_0}^{t_1} \mathcal{Q}_{\text{in}}(t)dt + \int_{t_0}^{t_1} \mathcal{W}_{\text{in}}(t)dt - \int_{t_0}^{t_1} \mathcal{Q}_{\text{out}}(t)dt - \int_{t_0}^{t_1} \mathcal{W}_{\text{out}}(t)dt, \end{aligned} \tag{Z.3}$$

where $\mathcal{Q}$ and $\mathcal{W}$ are instantaneous heat and work flows respectively, both measured in $[W]$. The classical thermodynamic notation of these flows is $\dot{Q}$ and $\dot{W}$ and it is made use of path integrals notation such that $\int_{t_0}^{t_1} \mathcal{Q}_{\text{in}}(t)dt = \oint_{t_0}^{t_1} \dot{Q}_{\text{in}}(t)dt$ cannot be evaluated as $Q(t_1) - Q(t_0)$, since $Q(t)$ does not have a meaning, unlike energy which is a system state and fulfills $\int_{t_0}^{t_1} \dot{E}(t)dt = \int_{t_0}^{t_1} dE(t) = E(t_1) - E(t_0) = \Delta E(t_0, t_1)$.

The second law of thermodynamics states that the autonomous evolution of a system is always towards the direction of increasing entropy. A direct consequence of this is that energy cannot be transfered in the form of heat from a lower temperature system to a higher temperature system without work. Refrigerators and heat pumps are devices that use work to transfer energy in the form of heat from a low-temperature T_L source to a higher-temperature T_H sink, see Fig. Z.1.

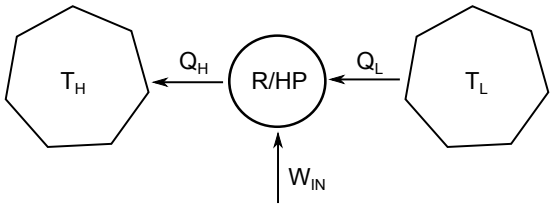

Fig. Z.1: Basic principle of a refrigerator and/or heat pump installation working between a low temperature T_L reservoir and a high temperature reservoir T_H. A (thermal) reservoir is an system that can receive and deliver very large amounts of heat without changing its temperature.

The refrigeration system itself does not store energy overall, $\Delta E_R = 0$, and thus the energy conservation principle leads to the following relations,

$$W_{\text{in}} + Q_L = Q_H \tag{Z.4a}$$

$$\dot{W}_{\text{in}} + \dot{Q}_L = \dot{Q}_H \, . \tag{Z.4b}$$

The performance or efficiency of a process is in general quantified using the ratio between the desired outcome and the required input resource. The objective of a refrigerator is to extract heat from the low-temperature heat reservoir. This leads to the definition of the COP (Coefficient Of Performance) as

$$\text{COP}_{\text{R}} = \frac{Q_L}{W_{\text{in}}} = \frac{1}{\frac{Q_H}{Q_L} - 1}. \tag{Z.5}$$

Similarly, the objective of a heat pump is to bring heat into the high-temperature reservoir, leading to a performance definition of

$$\mathrm{COP_{HP}} = \frac{Q_H}{W_{\mathrm{in}}} = \frac{1}{1 - \frac{Q_L}{Q_H}}. \tag{Z.6}$$

The energy balance equation (Z.4b) indicates that the efficiency of heat pumps is higher by using the heat extraction from lower temperature reservoir, than by transforming the work directly to heat (e.g. by Joule resistive heating).

There exists a theoretical maximum for the performance of a refrigerator/heat pump, and this is given in terms of the absolute temperatures (on the Kelvin scale) of the thermal reservoirs as,

$$\max\ \mathrm{COP_R} = \frac{1}{\frac{T_H}{T_L} - 1}, \tag{Z.7}$$

$$\max\ \mathrm{COP_{HP}} = \frac{1}{1 - \frac{T_L}{T_H}}. \tag{Z.8}$$

The COP is a practical means of evaluating the average performance of a device under specified conditions, and is a direct or indirect datasheet parameter for refrigerators. Although the theoretical maximum COP depends only on the constant T_L and T_H temperatures, a practical COP is process dependent. This means that for practical purposes an unambiguous process trajectory needs to specified, and that the datasheet COP must be understood in an average sense, both over time and over similar iterations.

2 Simple Refrigerator Model

A simple model for temperature dynamics of a refrigerator compartment can be set-up using a basic energy balance analysis and the COP factor. Additionally, the heat transfer between the low-temperature source and the high-temperature sink environment need to be considered, as shown in Fig. Z.2.

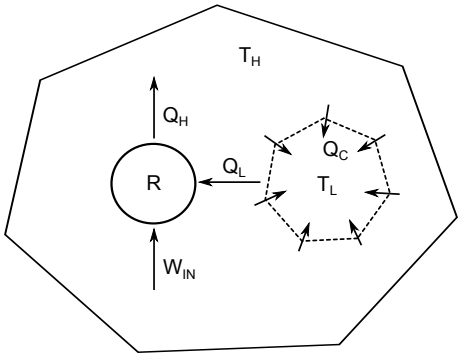

Fig. Z.2: Simple model of a household refrigerator. The low-temperature compartment loses heat to the the high-temperature room air.

Heat is naturally transfered from a warmer system to a cooler one. In the refrigerator case, the main mechanism of heat loss from the cooled compartment isolated with a shell from the external environment, is conduction. Convection effects also play a role, but are smaller and can be ignored in this approach.

The conductive heat flow though a plane layer or medium as shown in Fig. Z.3 is proportional with the temperature difference between the two sides of the medium and with the area of contact, and is inverse proportional to the thickness of the layer,

$$\dot{Q}_c = kA\frac{T_H - T_L}{\Delta x}. \tag{Z.9}$$

where k is a material dependent constant, the thermal conductivity, measured in $[W/(mK)]$.

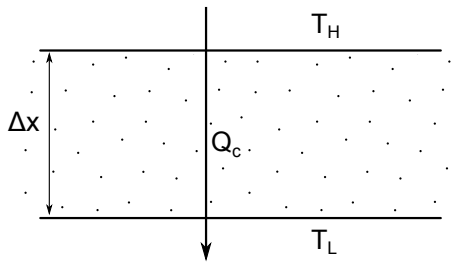

Fig. Z.3: Section through a plane contact medium with thickness Δx.

Considering a refrigerator with a single compartment and temperature zone (without freezer section), there are six such plane contact surfaces, such that

$$\dot{Q}_c = \sum_i \frac{k_i A_i}{\Delta x_i}(T_H - T_L) = \mathrm{UA} \cdot (T_H - T_L), \tag{Z.10}$$

where UA is an equivalent heat transfer coefficient, measured in $[W/K]$.

The energy balance relation can be written on the refrigerator compartment as,

$$\Delta E_R = Q_c - Q_L = Q_c - \mathrm{COP}_R \cdot W_{\mathrm{in}}, \tag{Z.11}$$

and on the outdoor/ambient room as

$$\Delta E_a = Q_H - Q_c = \underbrace{(1 + \mathrm{COP}_R)}_{\mathrm{COP_{HP}}} W_{\mathrm{in}} - Q_c. \tag{Z.12}$$

A change in the system energy will lead to a change in some of other system states e.g. volume, pressure, temperature. The amount of energy that needs to be transfered to a system such that a temperature increase of one degree is achieved is called heat capacity C, and is measured in $[J/K]$. Heat capacity is proportional with the size (mass) of system, and depends on the path/trajectory of the heat transfer process. Heat capacity measured for a constant volume process is denoted as C_V, and for a constant pressure process as C_p. Both C_V and C_p are dependent, but vary relatively slowly, with the initial temperature.

The thermal reservoir concept used in the previous section is an idealized version of a system with very large heat capacity compared to the energy transfers involved. The refrigerator compartment does not have a very large heat capacity compared to the energy transfer ΔE_R, which is dimensioned such that T_L temperature can be controlled. Since the volume of the refrigerator compartment remains constant, the following relation can be written,

$$\Delta T_L = \frac{\Delta E_R}{C_V^R}, \tag{Z.13}$$

where C_V^R is the heat capacity of the compartment at constant volume, for ΔT_L variations that are not too large. On the other hand, the outside system (room) can be considered as a thermal reservoir since it is much larger and has a heat capacity that should dominate by order of magnitudes the energy loss ΔE_a,

$$\Delta T_H = \frac{\Delta E_a}{C_V^a \gg 1} \sim 0. \tag{Z.14}$$

Thermal dynamics T_L can now be expressed using the rate form of (Z.13) and (Z.11) as,

$$\dot{T}_L = \frac{1}{C_V^R}\dot{Q}_c - \mathrm{COP}_R \cdot \dot{W}_{\mathrm{in}}, \tag{Z.15}$$

and using the convection relation (Z.10),

$$\dot{T}_L = \frac{\mathrm{UA}}{C_V^R}(T_H - T_L) - \mathrm{COP}_R \cdot \dot{W}_{\mathrm{in}}\ , \tag{Z.16}$$

where the COP_R value was considered constant.

A normal operation for a refrigerator (without freezer compartment) takes place approximately between values $T_L \in [2, 5]$. If the ambient temperature is relatively constant and e.g. $T_H = 24$, the theoretical maximum performance of the refrigeration process is COP_R value of 13.5. Actual values are significantly lower.

A similar simplified dynamic model can be obtained for the heat-pump case, where the hot-temperature sink is the insulated system, and heat is leaked to the outdoor, low-temperature environment.

3 The Vapor-Compression Cycle

The main modeling objective with the household refrigerator analysis is on its power consumption characteristics. The thermal dynamics described by (Z.16) are the basic building block in the study of the TCL problem in this thesis, and the majority of other works discussed in the introduction part, sec. 3. At the same time, one of the most rough approximation points in (Z.16) is the lack of specificity in the work term W_{in}, and the use of the COP factor in a differential/instantaneous relation, which is a stretch from its definition. To clarify the validity range of this approach, a more detailed look can be taken at the refrigeration mechanism.

The main process taking place in a refrigerator is a thermodynamic cyclic processes. During a cycle, a working fluid called refrigerant is subject to a series of thermodynamic transformations, and is returned to the initial state. The refrigeration cycle of interest for Themostatically Controlled Loads (TCLs) is the vapor-compression cycle, which consists of four components. In an ideal sense, these are:

(a) A compression process, during which the pressure of the working fluid is increased by mechanical work. In the ideal case the process take place without heat transfer. The temperature of the working fluid will necessarily increase, but the entropy state is constant.

(b) A heat loss process with the high-temperature medium (room). This is possible because the refrigerant temperature has increased above T_H in the previous step. As a result of the heat loss, the temperature of the working fluid decreases. The pressure remains constant during this process.

(c) A pressure drop process, without any heat loss and without any work transfer. As a result of the pressure drop, the temperature of the refrigerant drops significantly and the volume increases. The enthalpy state of the refrigerant remains constant during this process.

(d) A heat absorption process with a low-temperature medium T_L. This is possible because the refrigerant temperature has dropped below T_L in the previous step. As a result, the temperature of the working fluid will increase. The pressure remains constant during this process.

The working fluid enters the compression process (a) as saturated vapor (in its gas phase, but close to the boiling/condensation/vaporization temperature for the given pressure), and exits as a superheated vapor (in the gas phase, and far from the boiling/condensation/vaporization temperature for the given pressure). During the heat loss transfer process (b) the temperature drops and the refrigerant starts to condensate, passing through a vapor-liquid mixture, and ending as a saturated liquid (close to boiling/condensation/vaporization temperature for the given pressure). From the throttling/expansion process (c) the saturated liquid exist as a saturated mixture with only a small percentage vapor (because it has not received any heat to be able to fully vaporize although the pressure dropped). During process (d), the needed heat for vaporization is received and the refrigerant should enter the compression process (a) as a saturated vapor.

The processes (a)-(d) are physically realized with the following components:

(A) The compressor is an electrically powered device that uses moving mechanical parts to take a gas from a lower input pressure to a higher output pressure. The compressor task is both to draw refrigerant vapor from the evaporator and maintain the low evaporator-side pressure, and to discharge refrigerant vapor on the condenser and maintain a high condenser-side pressure. The main type compressor used for refrigeration is the reciprocating compressor. Compressors transform electric energy to mechanical (kinetic) energy, and the kinetic energy is used to transfer work to the system.

(B) The condenser is a winding tube placed on the exterior of the refrigerator. It intermediates a heat exchange between the refrigerant and the ambient air in the room.

(C) A passive flow restricting device, such as a capillary tube or valve, realizes the pressure drop process at constant enthalpy (c), also called throttling.

(D) The evaporator is a winding tube build in the interior of the refrigerator compartment to mediate the heat exchange with the refrigerant.

Because compressors are damaged if a significant liquid refrigerant creeps and accumulates in the compressor chamber, refrigerators are designed with an internal heat exchanger to mediate heat transfer between the refrigerant at the end of the condenser tube and the refrigerant at the end of the evaporator tube. In this way, at the end of the condenser tube the refrigerant is not in the form of saturated liquid but has become subcooled by some degrees ΔT_{sub}, while at the end of the evaporator tube the refrigerant is not in the form of saturated vapor but has become superheated by some degrees ΔT_{sup}. Furthermore, some of the cycle processes depart in some measure from the ideal conditions. The compression process in particular cannot be realized close to the ideal case, as friction effects lead to an increase in entropy and heat transfer process occur as well, sometimes by design.

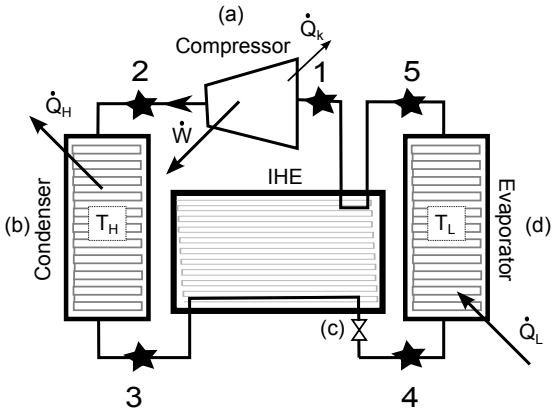

Fig. Z.4: Schematic of the refrigeration cycle.

The compressor plays the main direct role in the power consumption of a refrigeration. At the same time, the performance of the heat exchange between the refrigerant and ambient, air via the condenser, and the performance of the heat exchange between the refrigerant and the cooled compartment, via the evaporator, have an important contribution to the overall performance of the refrigeration process. Modeling the individual components of the refrigeration cycle separately will lead to a better prediction of the power consumption characteristics. Such an approach is taken in [3, 6]. A short overview of this approach is given next and preliminary results on an adapted example.

The refrigeration cycle is ON. Given the temperature at evaporator inlet as the temperature inside the cooled compartment T_L, assumed constant over a relatively

short period of time dt, the refrigeration cycle stabilize to a certain equilibrium state which determines the absorption rate by the evaporator $\dot{Q}_L$, the power used by the compressor $\dot{W}$, and other operational parameters. This equilibrium model is coupled with the compartment thermal dynamics as obtained from the energy balance, where $\dot{Q}_L$ is now given directly instead of using the COP relation. Time is advanced with dt in the thermal dynamics, and a new T_L is determined. This overall modeling approach is shown in Fig. Z.5.

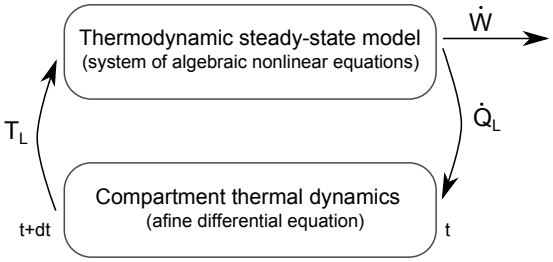

Fig. Z.5: Modeling approach for combining a quasi-steady-state (or equilibrium) model of the refrigeration cycle with the temperature dynamics of the cooled compartment.

The refrigeration cycle equilibrium model is given by the following system of nonlinear algebraic equations, see [3],

$$\dot{m}_r = \eta_v V_k N / \nu_1 \tag{Z.17a}$$
$$\dot{W} = \dot{m}_r (h_{2,s} - h_1)/\eta_g \tag{Z.17b}$$
$$h_2 = h_1 + (\dot{W} - \dot{Q}_k)/\dot{m}_r \tag{Z.17c}$$
$$\dot{Q}_k = \mathrm{UA}_k (T_{2,s} - T_H) \tag{Z.17d}$$
$$h_4 = h_3 + h_5 - h_1 \tag{Z.17e}$$
$$T_1 = T_5 + \epsilon_x (T_3 - T_5) \tag{Z.17f}$$
$$\dot{Q}_L = \dot{m}_a c_{p,a} (T_L - T_{\mathrm{sat}}(p_e))(1 - e^{-\mathrm{UA}_e/(m_a c_{p,a})}) \tag{Z.17g}$$
$$h_5 = h_4 + \dot{Q}_L/\dot{m}_r \tag{Z.17h}$$
$$\dot{Q}_H = \mathrm{UA}_c (T_{\mathrm{sat}}(p_c) - T_a) \tag{Z.17i}$$
$$h_3 = h_2 - \dot{Q}_H/\dot{m}_r \tag{Z.17j}$$
$$p_c = P_{\mathrm{sat}}(T_3 + \Delta T_{\mathrm{sub}}) \tag{Z.17k}$$
$$p_e = P_{\mathrm{sat}}(T_5 - \Delta T_{\mathrm{sup}}), \tag{Z.17l}$$

where the variables are p_e, p_c, T_1, T_3, T_5, $\dot{m}_r$, $\dot{W}$, $\dot{Q}_k$, $\dot{Q}_L$, $\dot{Q}_H$, h_2, h_4. The following expressions are variable dependent expressions,

$$\eta_v = \eta_v(p_c/p_e) \tag{Z.18a}$$
$$\eta_g = \eta_g(p_c/p_e) \tag{Z.18b}$$
$$\nu_1 = \nu_r(T_1, p_e) \tag{Z.18c}$$
$$T_{2,s} = T_1(p_c/p_e)^{(k_T-1)/k_T} \tag{Z.18d}$$
$$h_{2,s} = h_r(T_{2,s}, p_c) \tag{Z.18e}$$
$$h_1 = h_r(T_1, p_e) \tag{Z.18f}$$
$$h_3 = h_r(T_3, p_c) \tag{Z.18g}$$
$$h_5 = h_r(T_5, p_e), \tag{Z.18h}$$

while T_H, $\dot{m}_a$, $c_{p,a}$, N, V_k, UA_k, k_T, ΔT_{sub}, ΔT_{sup}, UA_e, ϵ_X, and UA_c are parameters. These equations correspond to simplified models of the refrigerator cycle components, and are not reviewed in this appendix, but reference is once again made to [3]. It is also noted that the subsequent work [6] contains further extensions not used here. The overall notation is however shortly summarized next: $\dot{m}_r$ is the mass flow rate of refrigerant in the cycle, [kg/s]; $\dot{W}$ is the power used by the compressor, [W]; the h-values are specific enthalpies at different points in the cycle, [J/kg]; p_c and p_e are the condenser and evaporator pressures, [Pa]; $\dot{Q}_k$ is the heat loss rate of the compressor, [W]; T denotes temperatures at different points in the cycles, [K]; $\dot{Q}_L$ and $\dot{Q}_H$ are, as before, the heat rates to the low- and high-temperature mediums respectively, [W]; η_V and η_g are dimensionless volumetric and isentropic compressor efficiencies and can be extracted from datasheet specifications as functions of the operational compression rate p_c/p_e, $\nu = q/\rho$ is specific volume, [m^3/kg]; $T_{2,s}$ and $h_{2,s}$ are the temperature and enthalpy at the end of the ideal isentropic compression process, notation ν_r and h_r has been used to denote property functions of the refrigerant, k_T is the polytropic coefficient of the refrigerant, $\dot{m}_a$ is the air mass flow rate, [kg/s]; across the evaporator, $c_{p,a}$ is the pressure constant specific heat capacity of air, [J/(kgK)]; N is the compressor speed (compression cycles per unit of time), $[Hz]$; V_k is the compressor intake volume, [m^3], UA are overall heat transfer coefficients, [W/K]; ϵ_X is the dimensionless effectiveness of the internal heat exchanger; and ΔT_{sub}, ΔT_{sup} are as already introduced the subcool and supheat temperature variations, $[K]$.

The compartment model is given by

$$\dot{T}_L = \frac{\mathrm{UA}}{C_V^R}(T_H - T_L) - \dot{Q}_L\,, \tag{Z.19}$$

with the observation that when compressor is off $\dot{Q}_L = 0$, and that a white noise component can be added.

4 Qualitative Comparison

Both thermodynamic models (Z.16) and (Z.17, Z.19) can be combined with the thermostat logic, to give temperature and power trajectories. It is noted that the first model, if enriched with a white noise component, becomes the TCL model as used in the main body of this work. Additionally, measured trajectories from laboratory set-up of a single compartment household refrigerator are also presented.

Figure Z.6 presents simulated trajectories using the first model. Figure Z.7 presents simulated trajectories using the second model. The equilibrium model of the refrigeration cycle is simulated using parameter values adapted from [3]. The R134a refrigerant fluid properties were used. It can be seen that the difference in the power consumption pattern is minimal, however, compared with the first model where the power consumption was modeled as a constant, the second model captures a slight dynamic, as the power-on cycle shows an angled profile. It is mentioned that the parameters are not in general coordinated between the models, and this leads to different duty-cycles between the two cases.

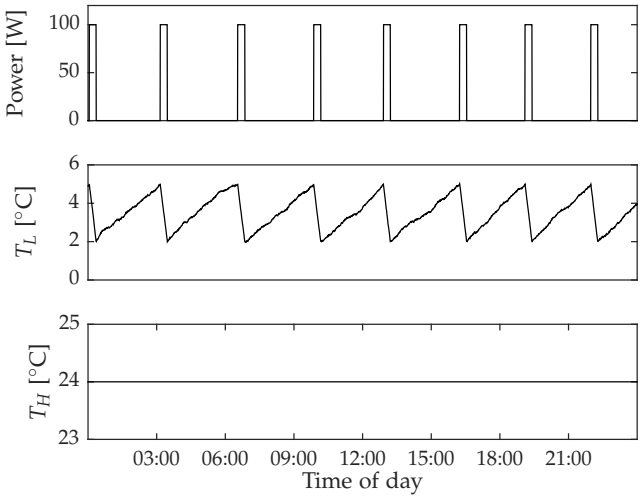

Fig. Z.6: Simulated trajectory using the energy balance model (Z.16), with a low white noise component.

A measurement session is shown next, from single-compartment ScanDomestic refrigerator, model SKS150, with a capacity of 124 [l]. The refrigeration fluid is R600a. The refrigerator is instrumented with one internal and one external temperature sensor. Power measurements are also available. The refrigerator is operating "on empty", without added thermal mass in the compartment, and in a controlled laboratory setup with no user interaction (no door openings). The thermostat operation of the unit can be adjusted via a knob button with seven settings. The refrigerator is shown in Fig. Z.8.

The measured trajectory from Fig. Z.9 qualitatively resembles that of the simulated cases. The inside temperature trajectory T_L follows the expected zig-zag pattern. The measurement of the ambient temperature T_H shows a low frequency variation, matching an intradaily expected pattern with slightly higher values around midday, and a high frequency variation matching the duty-cycle operation of the refrigerator. This is because the external temperature sensor is in relative close proximity to the condenser coil. However, in absolute values, the variation of the ambient temperature is small for this measurement, about 1 [°C], such that the constant T_H assumption from the previous models can be considered as reasonable.

The power consumption trajectory exhibits the downward angled profile predicted

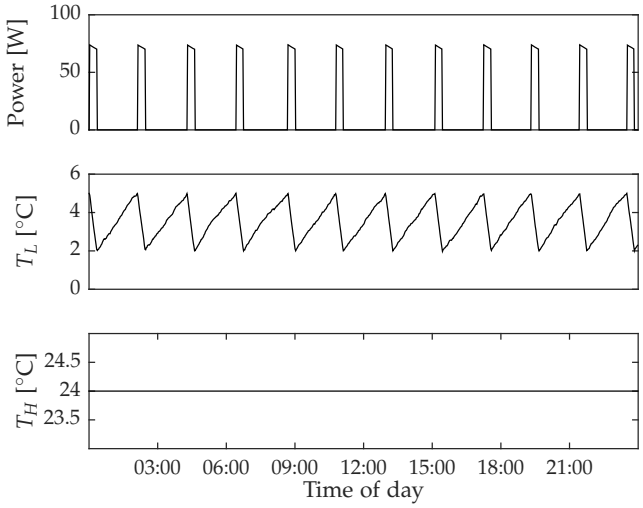

Fig. Z.7: Simulated trajectory using the refrigeration cycle equilibrium model (Z.17,Z.19).

Fig. Z.8: A ScanDomestic refrigerator, model 150. Images are from the producer's website.

by the second model, and in addition, shows peaks at the start of the on-cycle. Fig. D.1 from Paper D shows a high-frequency measurement of the power consumption, revealing more characteristics. The high power peak is consistent for each cycle, and is due to the start of the compressor motor. This peak is one of the main motivation for introducing the Switching-Rate actuation.

This concludes the qualitative comparison of the TCL models.

References

[1] Elmodelbolig statistics. `http://statistic.electric-demand.dk/`.

[2] Erik Bjork. Energy efficiency improvements in household refrigeration cooling systems. 2012.

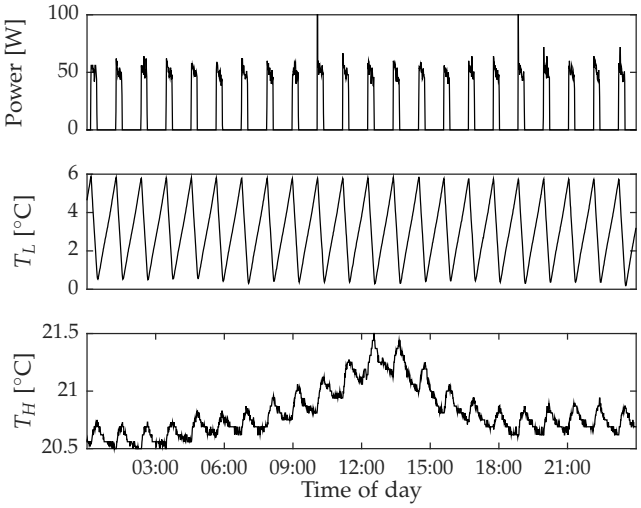

Fig. Z.9: Measured trajectories for a ScanDomestic refrigerator with a single compartment.

[3] Bruno N Borges, Christian JL Hermes, Joaquim M Gonçalves, and Cláudio Melo. Transient simulation of household refrigerators: a semi-empirical quasi-steady approach. *Applied Energy*, 88(3):748–754, 2011.

[4] Herbert B Callen. *Thermodynamics and an Introduction to Themostatistics*. John Wiley & Sons, 1985.

[5] Yunus A Cengel and Robert Turner. *Fundamentals of Thermal-Fluid Sciences*. McGraw-Hill Higher Education, 2001.

[6] Cezar OR Negrão and Christian JL Hermes. Energy and cost savings in household refrigerating appliances: A simulation-based design approach. *Applied Energy*, 88(9):3051–3060, 2011.